Phosphorus transport in a hotter and drier climate: in-channel release of legacy phosphorus during summer low flow conditions

Christine L. Dolph[1], Jacques C, Finlay[1], Brent Dalzell[2,3], Gary W. Feyereisen[2,3,4]

[1]Department of Ecology, Evolution and Behavior, University of Minnesota, 140 Gortner, 1479 Gortner Ave, St. Paul, Minnesota, 55108
[2]USDA-ARS Soil and Water Management Research Unit, St. Paul, Minnesota, 55108
[3]Department of Soil, Water, and Climate, University of Minnesota, 438 Borlaug Hall, 1991 Upper Buford Circle, St. Paul, Minnesota, 55108
[4]Department of Bioproducts and Biosystems Engineering, University of Minnesota, 1390 Eckles Ave., St. Paul, Minnesota, 55108

Correspondence to: Christine L. Dolph (dolph008@umn.edu)

Abstract. "Legacy phosphorus" is the historical accumulation of phosphorus (P) in soils and sediments due to past human inputs. River networks represent a potential sink and/or source of legacy P, with many in-channel processes potentially governing the storage and mobilization of P over time. The objective of this study was to evaluate the potential contribution of in-channel release of legacy P to bioavailable P transport in streams during summer low flow conditions across a land use gradient in Minnesota, USA. We addressed this objective through synthesis of: 1) water quality and stream flow (Q) data collected for 143 gaged watersheds across the state of Minnesota between 2007-2021 (22,750 total samples); 2) water quality data from 33 additional ditch, stream and river sites in Minnesota sampled under low flow conditions in summer of 2014; and 3) water quality data collected from tile drainage outlets for 10 monitored farm fields between 2011-2021. We used geospatial data and a random forest modeling approach to identify possible drivers of bioavailable P concentrations during summer low flows for gaged watersheds. Between one third to one half of the gaged watersheds we studied exhibited SRP concentrations during low flows in late summer above previously identified thresholds for eutrophication of 0.02 - 0.04 mg/L. For many of these watersheds, stream SRP concentrations in late summer were above those observed in tile drainage outlets. Elevated SRP concentrations during late summer low flows weakened concentration-discharge relationships that would otherwise appear to indicate more strongly mobilizing SRP-Q responses across other seasons and flow conditions. While wastewater discharge likely contributed to elevated P concentrations for watersheds with high densities of treatment plants, many watersheds did not have substantial wastewater impacts. The most important variables for predicting bioavailable P concentrations during late summer low flow conditions in a random forest model were land use in riparian areas (particularly crop cover), soil characteristics including soil erodibility, soil permeability, and soil clay content, agricultural intensity (reflected via higher pesticide use, higher phosphorus uptake by crops, and higher fertilizer application rates), watershed precipitation and stream temperature. These findings suggest that, for stream and river sites heavily impacted by past and current P inputs associated with agriculture and urbanization, biogeochemical processes mediated by climate and geology can result in the release of legacy P from in-channel stores during late summer low flow conditions. As summers become hotter and, at times, drier -- predicted changes in this region -- conditions for the release of legacy P stored in stream and river channels will likely become more prolonged and/or more acute, increasing eutrophication risk.

40 **Short Summary**

"Legacy Phosphorus" is the accumulation of phosphorus (P) in soils and sediments due to past inputs from fertilizer, manure, urban runoff, and wastewater. The release of this P from where it is stored in the landscape can cause poor water quality. Here, we examined whether legacy P is being released from stream and river channels in summer across a large number of watersheds, and we examined what factors (such as climate, land use and soil types) might be

45 driving that release.

1 Introduction

Phosphorus (P) inputs arising from urbanization and industrial/intensive agriculture have resulted in widespread eutrophication of freshwater and marine environments. Excessive inputs of P along with nitrogen (N) have resulted in costly and sometimes dangerous conditions for human society, including increased prevalence of harmful algal blooms, contamination of drinking water supplies, decreased recreational opportunities, loss of critical marine fisheries, and negative impacts to biodiversity (Bennett et al., 2001). This problem is particularly acute in the Midwestern Cornbelt of the United States, which represents a global hotspot for P fertilization (Haque, 2021).

Most progress in reduction of P release to the environment has come from the implementation of improved wastewater infrastructure (Keiser and Shapiro, 2019). However diffuse (nonpoint) sources of P such as those arising from agricultural and urban landscapes have yet to be substantially curtailed and remain largely unregulated. In addition to ongoing P inputs to the environment, water quality is also impacted by the existing supply of "legacy P" in the landscape (Goyette et al., 2018). Legacy P is the historical accumulation of P in soils and sediments due to past land use practices, such as agricultural fertilization, the spreading of manure, and wastewater discharge.

Efforts are underway to understand sources of legacy P in the terrestrial environment including agricultural soils and riparian buffers (e.g., Osterholz et al., 2020). Lentic water bodies (lakes, impoundments and wetlands) are well known for their potential to remobilize stored P and become sources instead of sinks for downstream P, especially at high rates of nutrient inputs (e.g., Vilmin et al., 2022). The river network itself represents another potential sink and/or source of legacy P; with many dynamic in-channel processes potentially governing the storage and mobilization of P over time. For example, benthic redox conditions, in-stream primary productivity, microbial respiration, and sediment adsorption-desorption can all modulate whether P is retained in stream sediments, temporarily immobilized as organic P, or released to the water column as bioavailable P (Records et al., 2016).

We previously observed that concentrations of bioavailable P (i.e., soluble reactive phosphorus, SRP) in agriculturally-dominated streams and rivers of Minnesota were often elevated during low flow conditions in late summer (Dolph et al., 2019). However, questions remained about whether the elevated SRP we observed in late summer was sourced predominantly from tile drainage (i.e., and therefore indicative of legacy and/or current P sources stored in farm soils), from point sources such as wastewater treatment plants, or possibly from legacy sources in the river network itself. Tile drainage is extensive across the agricultural Midwest (Valayamkunnath et al., 2020) and has been found to contribute substantially to and even dominate soluble P export in agricultural watersheds (King et al., 2015; Smith et al., 2015). P concentrations in tile waters have been found to be highest during summer compared to other seasons (King et al., 2015), and therefore represent a possible driver of elevated SRP in streams and rivers receiving tile drainage at this time of year. Comparatively high SRP concentrations during low flows can also be indicative of the dominance of point discharges; these concentrations are often diluted under wetter conditions (Dupas et al., 2023). Alternatively, however, there is some indication that groundwater and/or in-channel processes may drive the release of bioavailable P in river channels at some times of year, such as summer (Schilling et al., 2020; Vissers et al., 2023).

A number of recent papers have examined potential legacy P dynamics in streams and rivers; these studies have typically been deployed at the reach scale (i.e., stream reaches of a few hundred meters or less), or for individual small to medium-sized watersheds (e.g., Bieroza and Heathwaite, 2015; Casquin et al., 2020; Kreling et al., 2023; Siebers et al., 2023; Vissers et al., 2023; Dupas et al., 2023; Rode et al., 2023). These in-depth studies are important and highly useful, as the microscale dynamics governing P mobility in river channels can be complex. However, few studies have examined the potential contribution of in-channel legacy P at larger regional scales, or across a large number of watersheds.

The objective of this analysis was to determine the potential contribution of in-channel legacy P sources to SRP transport under summer low flow conditions across a relatively broad spatial scale (i.e., the state of Minnesota). We hypothesized that in-stream processes contribute to elevated concentrations of bioavailable P during summer in streams with strong agricultural and/or urban influence, in addition to the contribution of tile drainage systems and point source discharges. We addressed this hypothesis through synthesis of three water quality datasets: 1) water quality and stream flow data collected for 143 gaged watersheds across the state of Minnesota between 2007-2021 (22,750 total samples); 2) water quality data from 33 additional ditch, stream and river sites in Minnesota sampled under low flow condition in summer of 2014; and 3) water quality data collected from tile drainage outlets for 10 monitored farm fields between 2011-2021. We also used geospatial data and a machine learning approach to identify possible drivers of elevated SRP concentrations during summer low flows for gaged streams and rivers.

Watersheds across the state of Minnesota span a land use gradient from those dominated by intensive agriculture typical of the Upper Midwest region, to a major metropolitan area, to areas of heavy forest and wetland cover with comparatively fewer historic P inputs. This gradient provides a useful contrast that can potentially be applied to identify differential behavior of streams and rivers strongly impacted by legacy P.

2 Methods

2.1 Study area

The study area for this research spans the entire state of Minnesota, USA, encompassing approximately 225,163 km^2 within the Upper Midwestern region of the United States (Fig. 1). The state includes parts of four major drainage basins: the Upper Mississippi River Basin in the central, south and southeastern portions of the state, the Red River Basin in the northwest, the Great Lakes Basin in the northeast and the Upper Missouri River in the far southwest corner. Gradients in land use, soils, and precipitation vary from north to south and east to west (Fig. 1). The majority of the southern and north-western parts of the state are dominated by industrial row crop agriculture, predominantly corn and soybeans, with a high density of concentrated animal feeding operations (CAFOs) particularly in the south. By contrast, the north and northeastern parts of the state are dominated by forest and wetland cover. The state is also home to a major metropolitan area, encompassing the Twin Cities of Minneapolis and St. Paul and the surrounding seven counties (population of 3.69 million, 2020 US census) characterized by urban and suburban landscapes. Precipitation varies from driest in the northwest (annual average rainfall ~550 mm, 1991-2020) to wettest in the southeast (annual average rainfall ~950 mm, 1991-2020; Johnson et al., 2022). Mean annual temperatures are higher in the south (annual average temperature ~ 7°C, 1991-2020) and lower in the north (annual average temperatures ~ 2-

3°C, 1991-2020). The entire state is characterized by a cold climate, with average winter temperatures well below freezing and with considerable snowfall historically expected most years. Most soils are formed from glacial and peri-glacial deposits. Soil textures range from sandy soils in the central part of the state, clay loam and silty clay loam soils in the south-central and southwest, and outwash till over karst bedrock in the southeast. Many of the soils in the western part of the state are calcareous with high pH. Water quality in the state is characterized by widespread impairments in the agriculturally and urban dominated regions, with the most ubiquitous impairments attributed to turbidity, total phosphorus, fecal coliform, impaired biota, and low dissolved oxygen (MPCA, 2022). Water quality in the northeastern part of the state is comparatively good, with lower levels of nutrient enrichment, although impairments for mercury contamination arising from coal burning and subsequent atmospheric deposition are widespread.

2.2 Overview of study data

For this study, we utilized three independent datasets (Fig. 1):

1) SRP concentration and discharge data (total n=22,750 flow-matched water chemistry samples) collected for 143 gaged stream and river watersheds monitored by the state of Minnesota's Watershed Pollutant Load Monitoring Network[1] between 2007-2021. These data were used to evaluate SRP transport behavior and understand drivers of late summer SRP.

2) SRP concentration and discharge data available for 10 tiled farm fields across the state, collected between 2011-2021 by the Discovery Farms Minnesota program[2]. These data were used to estimate seasonal SRP concentrations for tile outlets as a point of comparison with riverine SRP concentrations.

3) SRP grab samples collected during low flow conditions in late summer of 2014 for an additional set of ditch, stream and river sites. (n=33; Dolph et al., 2017a[3]). These data were used to provide additional information about SRP concentrations in smaller order systems that were underrepresented among gaged watersheds.

All data analysis was performed in R (R Core Team, 2023). Study data and R scripts used for data analysis are available at https://github.com/cldolph/instream_legacyP.
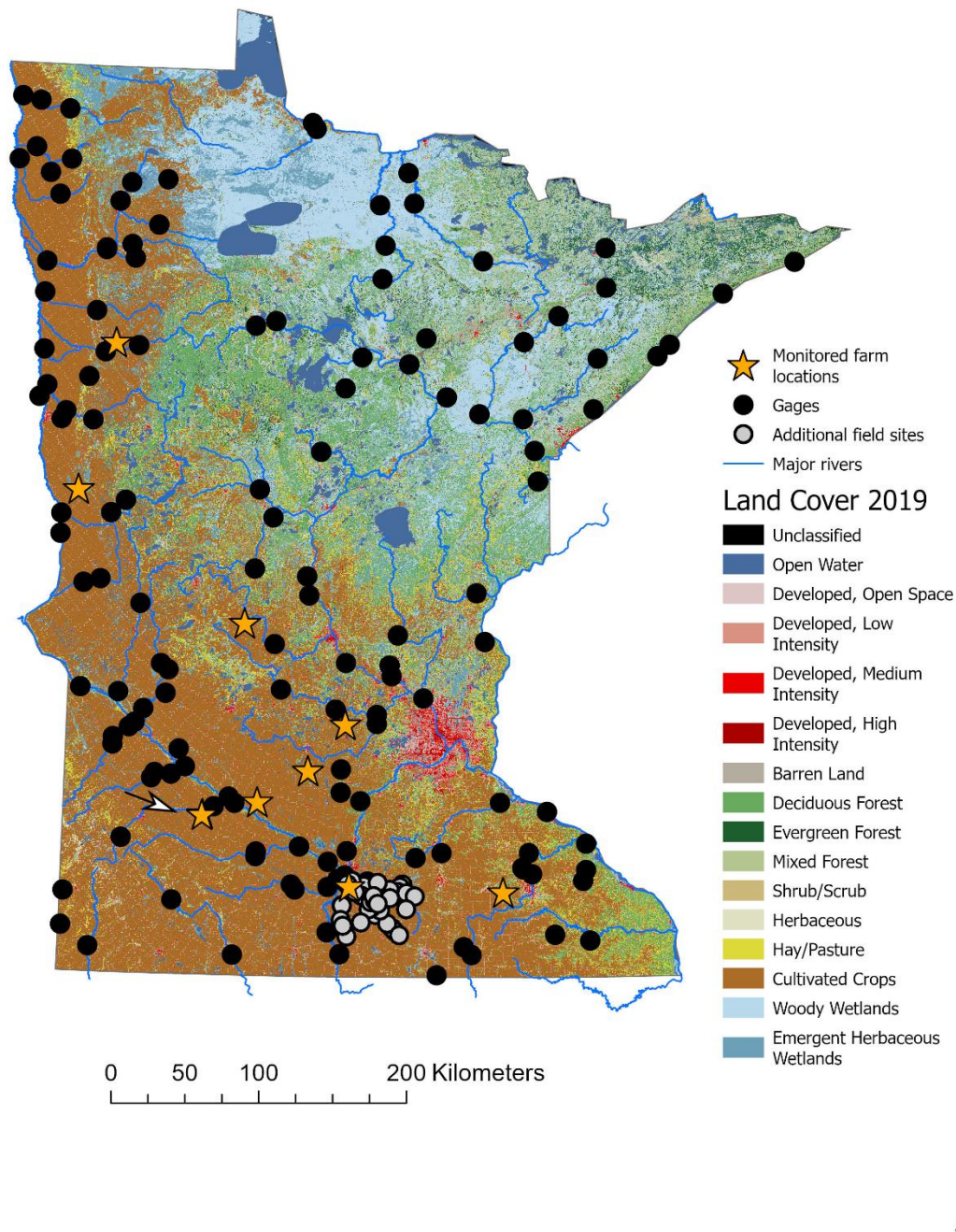
---

[1] https://public.tableau.com/app/profile/mpca.data.services/viz/WatershedPollutantLoadMonitoringNetworkWPLMNDataViewer/ProgramOverview

[2] https://discoveryfarmsmn.org/

[3] https://conservancy.umn.edu/handle/11299/189907

Figure 1: Locations of 1) 143 gaged stream and river watersheds intensively sampled for SRP and flow (total n=22,750 samples) at the watershed outlet during 2007-2021 (black dots; n=143). Data from these sites were used to evaluate SRP transport behavior and understand drivers of late summer SRP; 2) Farm fields with tile outlet water quality available (collected between 2011-2021; orange stars; n=10) used to estimate seasonal SRP concentrations for tile outlets, as a point of comparison with riverine SRP concentrations; 3) ditch, stream and river sites sampled during summer low flow conditions in 2014 (gray dots; n=33). Data from these sites were used to quantify late summer SRP concentrations in smaller order systems. Note that two farm fields (known as RW1N and RW1S) are located in close proximity, and so appear as one location on the map; this location is noted with a white arrow.

2.3 Water quality data from stream and river gages

We used paired SRP and daily discharge data from 143 gaged stream and river watersheds (Fig. 1) monitored by Minnesota's Watershed Pollutant Load Monitoring Network (WPLMN; note that the WPLMN also refers to SRP as "dissolved orthophosphate"). The total number of samples across all gaged watersheds was 22,750. Periodic water samples and continuous flow data were collected by the Minnesota Pollution Control Agency (MPCA) throughout the year at major watershed sites (watershed areas greater than ~4000 km^2) and during the period of ice-out through 31 October at smaller subwatershed sites (MPCA, 2015). Water quality sampling efforts were conducted ~biweekly with more intensive sampling focused on snowmelt and storm events, resulting in observations distributed across the range of flows observed at each site (average # of samples per year = 25 for subwatersheds and 35 for major watersheds; MPCA, 2015). The 143 gaged sites we selected for this study had >20 water chemistry samples collected across the sampling period (2007–2021). Median number of water quality samples per site across the whole time period was 120 (min=21, max=478). To determine detection limits, we inspected the data for repeated minimum concentrations and assigned detection limits equal to those minimum concentrations.

Watershed areas for gaged stream and river sites were assembled from multiple sources including existing watershed delineations (n=11 watersheds) available from USGS (2012) and previously delineated watersheds (n=65 watersheds) from Dolph et al., (2019), or delineated anew as part of the current study (n=68 watersheds). For newly delineated watersheds, we used gage locations provided by Minnesota Department of Natural Resources and Minnesota Pollution Control Agency (2023) as pourpoints, and existing flow direction and flow accumulation rasters available from the NHDv2Plus dataset (USEPA, 2019) to delineate watersheds using the Spatial Analyst toolbox in ArcGIS Pro (ESRI, 2022). Watersheds were inspected visually and manually corrected for inaccuracies in delineation. Across all gaged sites, watershed area ranged from 20 km^2 – 29,145 km^2 (mean = 1,996 km^2)

2.4 Farm tile outlets

We used SRP concentration and discharge data from tile outlets draining 10 farm fields across the state, measured between 2011-2021 (Fig. 1). These tile outlets are monitored by the Discovery Farms Minnesota (DFM) program[4]. The DFM is a farmer-led water quality research and educational program with the goal of collecting water quality information under real-world conditions to support the development of better farm management decisions. During the time of data collection, all monitored farm fields were planted in corn and soybean row crops grown in rotation. Two sites (WR1 and ST1) included dairy operations, and two sites (BE1 and DO1) included swine finishing, in addition to row crops. Swine finishing is the final stage of pig farming where young pigs are fed until they reach market weight.

The drainage areas for monitored farm fields ranged from 10-160 acres (mean = 97 acres). Farm field soil textures ranged from poorly drained silty clay loam, to well drained loam. Three of the farms (MC1, RE1, and WR1) each had one surface inlet to the tile drainage system. All other inlets were subsurface. One farm (NO1W), had monitoring data

---

[4] https://discoveryfarmsmn.org/

available for two separate fields (NO1W-N and NO1W-S). Water quality and flow data collection is described in detail by MDA (2021). Briefly, tile outlets were monitored continuously for flow (15 min interval) via area velocity sensors installed in the tile drains that measured both stage and velocity. Water quality samples were collected by ISCO 6712 automatic samplers on an equal-flow increment (EFI) composite basis, whenever tile outlets were flowing.

190 Water quality samples were composited every 125mL. Following a runoff event, water quality samples were collected and promptly transported to a state contract lab and measured for dissolved orthophosphorus (i.e., SRP) along with other water quality constituents. From continuous flow and composited sample SRP concentrations, we calculated a daily flow-weighted SRP concentration (daily C) as follows: 1) multiply composite concentrations by paired continuous flow measures to estimate continuous (15 min) loads; 2) sum composite sample loads into daily loads; 3)

195 divide daily load by summed daily flow to compute a daily flow-weighted concentration in mg/L. Seasonal SRP concentrations were calculated by taking the mean of daily SRP concentrations for each tile outlet during each season (Early winter: Nov-Dec; Late winter: Jan-Mar; Spring: Apr-May; Early summer: Jun-Jul; Late summer: Aug-Sept; Fall: Oct).

2.5 Additional field sites

200 Among gaged stream and river watersheds, small order systems (especially first through third order ditches and streams) are under-represented relative to their prevalence across the landscape. To get a better understanding of SRP concentrations in smaller order systems, we also examined late summer low flow SRP concentrations collected from 33 agriculturally-dominated ditches, streams and mid-sized rivers in the Le Sueur River Basin, Minnesota (Fig. 1). Data for these sites is part of a larger publicly available field dataset[5] for the region and described in detail by Dolph

205 et al. (2019). Briefly, SRP concentrations were determined for grab water samples collected from 33 sites during low flow conditions in August of 2014. Flow conditions at the time of sampling were characterized by flow at the gaged outlet of the major HUC8-scale watershed in which samples were collected (i.e., the Le Sueur River Basin), based on daily discharge data available from MNDR[6]. Although flow at watershed outlets is not precisely representative of flow conditions further upstream in the basin, we have shown previously that discharge conditions across study sites scaled

210 reasonably well with drainage area (Dolph et al., 2017b). We sampled on August 14, 17, 20, and 26 of 2014, during which flow conditions at the watershed outlet ranged between 19-25th percentile of all daily flows available for this watershed. Sites were categorized as ditches, perennial streams and rivers, or intermittent streams and rivers according to their designation in the NHDPlusv2 (USEPA, 2019).

2.6 Low flow conditions

215 Part of our aim in this study was to identify whether in-channel dynamics, such as instream release of legacy P, may affect stream and river SRP concentrations and transport behavior. Thus, we sought to identify low flow conditions where we assumed in-channel processes were likely to dominate P dynamics. We identified 'low flow' conditions as those falling within the lowest 25% of all daily discharge conditions measured for each watershed during the period

---

[5] https://doi.org/10.13020/D6FH44
[6] https://www.dnr.state.mn.us/waters/csg/index.html

of record for that gage. We defined seasons as follows: Early winter (Nov-Dec); Late winter (Jan-Mar); Spring (Apr-May); Early summer (Jun-Jul); Late summer: (Aug-Sept); Fall (Oct). We defined these seasons in approximate relation to the agricultural growing seasons in our study region, with spring corresponding to when crops are planted, summer corresponding to when crops are growing rapidly, fall corresponding to when dominant crops (corn, soybeans) are harvested, and winter corresponding to when crops are dormant. We divided winter into early winter when snow is accumulating and generally not melting, and late winter, which is associated with snowmelt. We divided summer into early summer when conditions are generally wetter and crops are experiencing rapid growth, and late summer when climate conditions are generally drier and warm season crops mature rapidly.

We calculated mean SRP during low flow conditions for each gaged watershed in each season, for gages that had a minimum of three SRP samples collected during low flow conditions in that season. Note that not all gaged watersheds had three or more SRP samples collected during low flows in each season (Table A4); thus, the number of gaged watersheds with mean low flow SRP values available for analysis was different during each season (this parallels the availability of low flow conditions across seasons, with low flows being most common during late summer compared to other seasons).

We hypothesized that low flow SRP concentrations could be substantially affected by one or all of the following: tile outlet concentrations, wastewater treatment plant discharges, or riverine legacy P stores. To help discern these influences, we compared low flow riverine SRP concentrations to tile outlet concentrations. In addition, we evaluated low flow riverine SRP concentrations for gaged watersheds relative to wastewater treatment plant density (sites/km^2) in the watershed. Wastewater treatment plant density estimates were obtained from the US EPA StreamCat dataset (Hill et al., 2016; see additional details about StreamCat below), and were based on wastewater treatment plants listed in EPA's Facility Registry Services and National Pollutant Discharge Elimination System (NPDES)[7]. We also evaluated low flow riverine SRP concentrations relative to % cropland land use in gaged watersheds, to examine the assumption that agricultural land use and the associated past and current P inputs might drive the supply of riverine P. Cropland land use estimates were also obtained from StreamCat and were based on the 2019 National Land Cover Database (Dewitz, 2021).

2.7 Influence of late summer low flows on concentration-discharge relationships

We evaluated the relationship between SRP concentration (C) and discharge (Q) using the power law relationship in Eq. 1:

$C=aQ^b$ (1)

where the curve's coefficient (*a*) and exponent (*b*) are representative of the degree, direction, and rate at which SRP is transported as a function of stream flow. This equation can alternatively be expressed in log-log scale as Eq. 2:

$\log(C) = b \log(Q) + \log(a)$ (2)

---

[7] https://catalog.data.gov/dataset/epa-facility-registry-service-frs-wastewater-treatment-plants

where b is the slope of the linear log-log relation, and $\log(a)$ is the y-intercept. Normalizing Q by the geometric mean of discharge (Q_{GM}) shifts the center of mass of the log-transformed Q data to the y-intercept, allowing for comparison of rating curves among different watersheds (Warrick et al., 2015). We performed linear regression of log-transformed SRP concentrations on log-transformed normalized discharge using Eq. 3:

255    $$\log(C) = b \log(Q/Q_{GM}) + \log(a) \tag{3}$$

All regressions were performed in R (R Core Team, 2023). We evaluated the fit of the power law relationship for all gaged watersheds using the significance value p, slope b and R^2 of the linear regression.

The slope b of this relationship describes the per unit increase in concentration as discharge increases. Concentrating relationships ($b > 0$) imply higher flows are mobilizing more of a waterborne constituent, particularly through erosion
260   or greater landscape connectivity. Diluting relationships ($b < 0$) suggest that constituents are source-limited or that relatively consistent inputs are diluted by greater discharge (Godsey et al., 2009). When b is near 0, C-Q relationships may be either chemostatic (i.e., relatively constant concentrations across the range of discharge conditions), or chemodynamic (i.e., concentrations are highly variable across the range of discharge conditions but not linearly related to flow). Chemostatic behavior has been observed for mineral weathering products or for constituents with large legacy
265   sources like nitrate (Godsey et al., 2009; Basu et al., 2010; Musolff et al., 2015), whereas chemodynamic behavior may indicate that biogeochemical processes such as sorption/desorption, biotransformation or oxidation/reduction strongly affect nutrient transport behavior (e.g., Wanner et al., 1989). To distinguish between these two behaviors, we evaluated the coefficient of variation of C relative to the coefficient of variation of Q (CV_C/CV_Q). A $CV_C/CV_Q < <1$ suggests that concentrations are relatively constant compared to variability in flow, indicating chemostatic behavior.
270   By contrast, a larger CV_C/CV_Q indicates chemodynamic behavior (i.e., comparatively large variations in concentration relative to variation in flow). Thompson et al. (2011) suggested that CV_C/CV_Q values ≈ 0.3 could be used as a threshold to identify chemostatic vs chemodynamic behavior.

To determine the influence of low flow conditions in late summer on the nature of the C-Q relationships for all watersheds, we refit power law relationships to all watersheds after excluding SRP samples that were collected during
275   late summer low flow conditions. We compared regression parameters (p, slope b and R^2) before and after withholding samples collected during late summer low flow conditions, to determine if these samples had a widespread effect on C-Q relationships for SRP across gaged watersheds.

2.8 Regression analysis

2.8.1 Random Forest models

280   We used random forest modeling to identify possible predictors of SRP during low flow conditions in late summer for gaged stream and river watersheds. Random forest regression is a nonparametric ensemble learning method that utilizes predictions from multiple decision trees to improve model accuracy. Each tree is composed of branches ("nodes") representing yes–no questions where features (i.e., predictive variables) are used to split the dependent variable into two groups that minimize in-group variability and maximize between group variability. We selected a
285   random forest approach because these models require few assumptions about data structure (i.e., data need not conform

to assumptions of classical statistics such as linearity, normality, and constant variance), are robust to outliers, and generally perform as well or better than other data intensive approaches (Hagenauer et al., 2019). The use of random forest models also allows for the identification of predictors that are important to model accuracy, using measures such as condition permutation importance and post-hoc partial dependence plots (see additional details below).

2.8.2 Predictor Variables

Predictor variables for random forest (RF) models were assembled from the U.S. EPA StreamCat dataset[8]. StreamCat contains information for over 600 different environmental metrics linked to individual stream reaches in the NHDv2Plus dataset (Hill et al., 2016). These metrics summarize diverse geospatial attributes—including aspects of land cover, impervious surfaces and road density, soil type, point source and nutrient inputs, and climatic factors (temperature and precipitation), among others—at the catchment and watershed scale draining into each reach. "Catchments" (i.e., local drainage areas) include the immediate land area draining into each individual stream reach in the NHD excluding areas draining to upstream reaches; "watersheds" include the entire land area draining into each stream reach. StreamCat contains land use data for catchments and watersheds summarized from the National Land Cover Database (NLCD) for multiple years. We used land cover attributes only from the 2019 iteration of the NLCD (DeWitz, 2021). To supplement this dataset, we derived estimates of tile density (i.e., area tiled per area watershed) for each gaged watershed using estimates of tiled areas (30 m resolution) from Valayamkunnath et al. (2020). Prior to developing a random forest model, we excluded predictors from the StreamCat dataset that did not contain useful information (i.e., all rows=0). We also excluded attributes where information was missing ('NA') for >20% sites. Some of the remaining attributes still contained some missing values. Because random forest models cannot handle missing values in predictor variables, we used the *missRanger* package in R (Mayer, 2023) to impute the remaining missing values for the training and testing datasets. In total, we used 253 predictor variables in the model, after excluding variables that did not provide useful information (i.e., were all 0s or had too many missing values), that did not match the timing of our dataset (i.e., land cover data from years other than 2019), or were not especially relevant (e.g., variables describing forest fire intensity or extent). Prior to random forest modeling, we normalized (i.e., centered and scaled) numeric attributes to have a mean of zero and a standard deviation of one.

2.8.3 Model Tuning and Selection

We developed the random forest model to predict mean SRP during late summer low conditions, based on data for 127 gaged watersheds. Only 128 of the 143 total gaged watersheds in the study had >=3 SRP samples collected during late summer low flow conditions and were therefore used to calculate mean SRP values. Prior to model development, we excluded one additional site from the testing dataset (Buffalo Creek near Glencoe, MN) that had a mean SRP value for late summer that exceeded the range of SRP values in the training dataset (see Appendix Fig. S1). To develop the RF model, we used the same general approach to random forest modeling described in detail by Dolph et al. (2023). Data were split randomly into independent model training (70%, n=88) and model testing (30%, n=39) datasets. Using the training dataset and the *ranger* package in R (Wright and Ziegler, 2017), we applied tenfold cross validation to

---

[8] https://www.epa.gov/national-aquatic-resource-surveys/streamcat-dataset

320 tune model hyperparameters across a range of possible values. K-fold cross validation can assist in avoiding model over-fitting and works by partitioning training data into K equal sized "folds" (in our case 10). The model is iteratively trained on various combinations of tuning hyperparameters across K-1 folds, leaving the remaining fold to evaluate model performance for each combination. The hyperparameters selected for tuning were: mtry (i.e., number of variables randomly sampled as candidates at each split) and min_n (i.e., the minimum number of data points in a

325 node). The trees hyperparameter (i.e., number of trees) was set to 1000 across all models. We defined a grid of 20 potential combinations of hyper-parameters using the *tune_grid*() function from the *tidymodels* collection of packages in R (Kuhn and Wickham, 2020). This approach draws hyperparameter values semi-randomly from parameter space such that the various combinations cover the whole space of potential values. We selected hyperparameter values using out-of-bag (OOB) RMSE and R^2 for the associated models. Once hyperparameter values were tuned, we reran

330 the random forest model using the *randomForest* package (Liaw and Weiner, 2002), to create a *randomForest* object that was compatible with our selected measure of predictive variable importance (conditional permutation importance, see next paragraph). We evaluated overall model performance using R^2 and RMSE between predicted and observed SRP values in the independent test dataset (comprising 30% of the original dataset).

2.8.4 Variable importance

335 We used Conditional Permutation Importance (CPI) to evaluate the importance of predictors to model performance. CPI aims to capture the dependence between a predictor and the response variable, conditionally on the values of all other predictors. CPI can be used to assess how much each variable contributes to accurately predicting the response variable, given what we know from all other predictive variables. We implemented the CPI approach from the *permimp* package in R (Debeer and Stobl, 2021). In *permimp*, a threshold value, equal to 1- the *p*-value for the

340 association between predictor variables, is used to determine whether to include a predictor in the conditioning for the predictor of interest. We used the default value for the threshold parameter in permimp (0.95; Debeer and Strobl, 2021).

While the CPI method can rank predictors in terms of their importance to model accuracy, it does not convey information about the nature of the relationship between predictor variables and late summer SRP concentrations. To

345 visualize these relationships, we created partial dependence plots (PDPs) using the *partialPlot* function in R (part of the *randomForest* package, Liaw and Weiner, 2002). These plots illustrate the change in predicted SRP concentration when the values of one predictor are changed while all other predictors are kept constant at their original values (Greenwell, 2017). We generated PDPs for the top 15 predictor variables identified as most important by the measure of CPI.

350 **3 Results**

3.1 SRP concentrations at gaged watersheds during low flow

Across gaged watersheds, we expected SRP concentrations at low flow conditions to differ depending on the extent of historic and current P inputs associated with anthropogenic land use. Most gaged watersheds in our study region (90%, n=128) were substantially impacted by either agricultural or urban land use (defined here as watersheds with

355 >=50% crop cover and/or >=10% high intensity urban land use). The remaining watersheds (n=15) were characterized as 'less impacted'.

Among watersheds with substantial agricultural or urban influences, mean low flow SRP concentrations were highest in late winter, lowest in spring, and then increased progressively through early summer, late summer, fall and early winter (Table 1).

360 However, there was large variation (3–4 orders of magnitude) in low flow SRP concentrations across sites in any given season (range across all samples = 0.001–3.9 mg/L). For less impacted sites, seasonal low flow SRP concentrations were also highest on average during late winter, although the absolute concentrations were much lower than more heavily impacted sites. By contrast to more heavily impacted sites, mean low flow SRP concentrations at less impacted sites dropped in spring and stayed steady through summer, and dropped slightly again in fall. Less

365 impacted sites showed comparatively low SRP concentrations and lower variability in low flow SRP concentrations across sites or seasons (range 0.001-0.046 mg/L).

Table 1: Mean, minimum and maximum low flow SRP concentrations (mg/L) for more heavily impacted gaged watersheds (>=50% crop cover and/or >=10% high intensity urban land use) and less impacted gaged watersheds<50% crop cover and < 10% high intensity urban land use), across seasons.

Degree of anthropogenic disturbance	Season	Mean SRP	Min SRP	Max SRP
More impacted	Late Winter	0.129	0.002	3.550
	Spring	0.030	0.001	0.384
	Early Summer	0.039	0.001	0.526
	Late Summer	0.055	0.001	1.350
	Fall	0.069	0.002	1.595
	Early Winter	0.117	0.002	3.900
Less Impacted	Late Winter	0.008	0.002	0.019
	Spring	0.007	0.002	0.031
	Early Summer	0.006	0.001	0.028
	Late Summer	0.005	0.001	0.046
	Fall	0.004	0.002	0.008
	Early Winter	0.008	0.002	0.030

3.2 Influences of wastewater treatment facilities (point sources) on riverine SRP concentrations at low flow

Mean SRP concentrations at low flow for gaged watersheds were significantly related to the density of wastewater treatment plants in the watershed during early winter, late winter, late summer, and fall but not in spring or early summer (Fig. 2). Part of the discrepancy across seasons may have been caused by the fact that few watersheds with a high density of wastewater treatment plants were sampled during low flows in spring and early summer. The relationship between mean low flow SRP and wastewater treatment plant density was strongest in early winter (though still somewhat weak overall; $R^2=0.26$) and comparatively weaker in other seasons (Appendix Table A1). These relationships were largely driven by watersheds where density of wastewater treatment plants was comparatively high (>0.005 sites/km^2). When watersheds with wastewater treatment plant density > 0.005 sites/km^2 were excluded, we observed a persevering very weak significant positive relationship between wastewater treatment plant density and mean lowflow SRP during late summer and late winter ($R^2=0.06$ and 0.10, respectively), but not during any other season. (see Appendix Table A1).
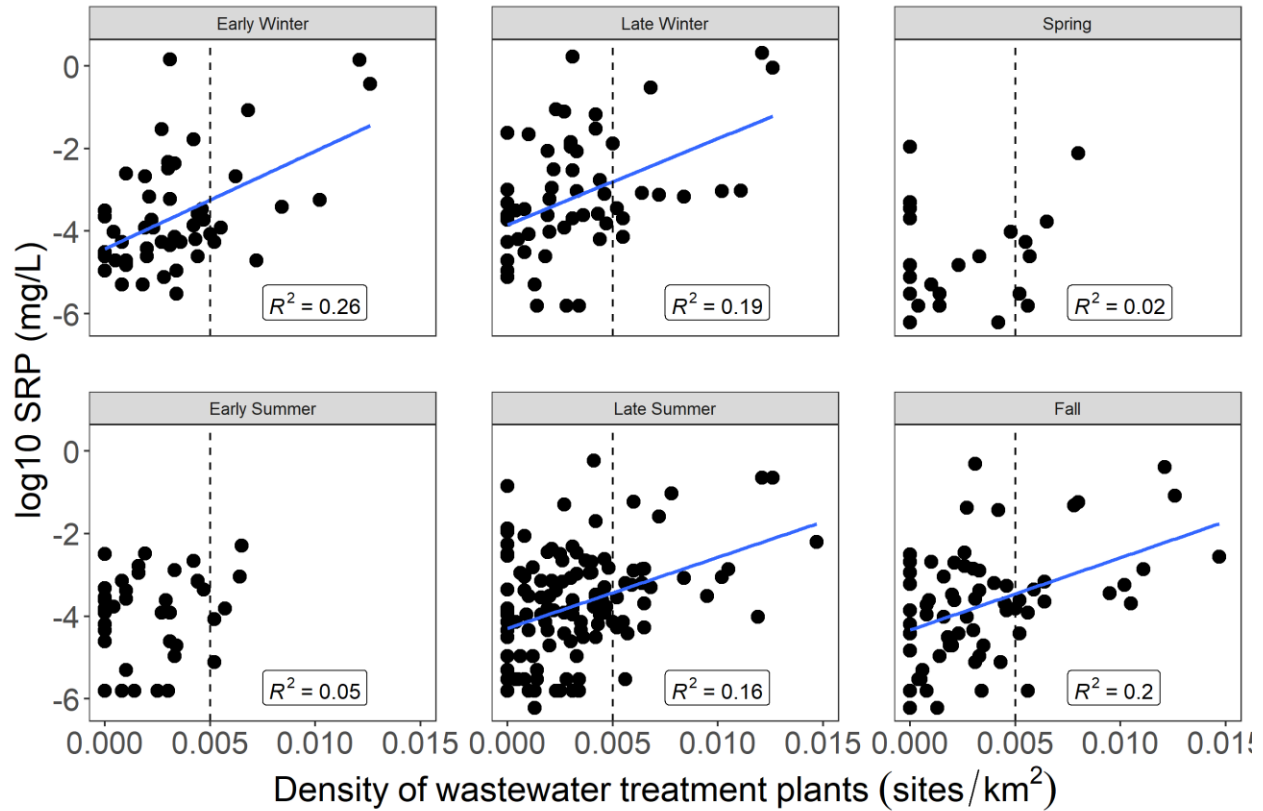
385

Figure 2: Relationship of SRP concentrations at low flows (log scale) in gaged watersheds to the density of wastewater treatment plants (sites/km^2) in the watershed, by season. Blue lines indicate statistically significant linear regressions ($p <$ 0.05). Linear regression statistics are shown in Appendix Table A1. Dashed line indicates wastewater treatment plant density of 0.005 sites/km^2. Note that not all gaged watersheds had sufficient samples collected during low flows in each

390 **season to generate mean values; thus, the number of gaged watersheds with low flow mean SRP values available was different during each season.**

3.3 Riverine SRP at low flows in relation to agricultural land use

We observed consistent and positive relationships between agricultural land use (% cropland) and mean low flow SRP

395 concentrations across gaged watersheds during all seasons, with the strongest relationships occurring during late summer and late winter (Fig. 3; Appendix Table A2). When we examined only sites without wastewater treatment plant influence, these relationships appeared even stronger, as evidenced by increased R^2 values (Fig. 4; Appendix Table A2). The strongest correlations were evident in late summer and early winter (R^2 of 0.69 and 0.86, respectively; Fig. 4). However, it should be noted that the sample size for early winter was small (n=5), which may have inflated

400 the R^2 value for this season.

15

Figure 3: Mean low flow SRP concentrations across gages (log scale), in relation to % crop cover, by season. Color scale indicates density of wastewater treatment plants in the watershed. Relationships in all seasons were significant and positive. Linear regression statistics are shown in Appendix Table A2.
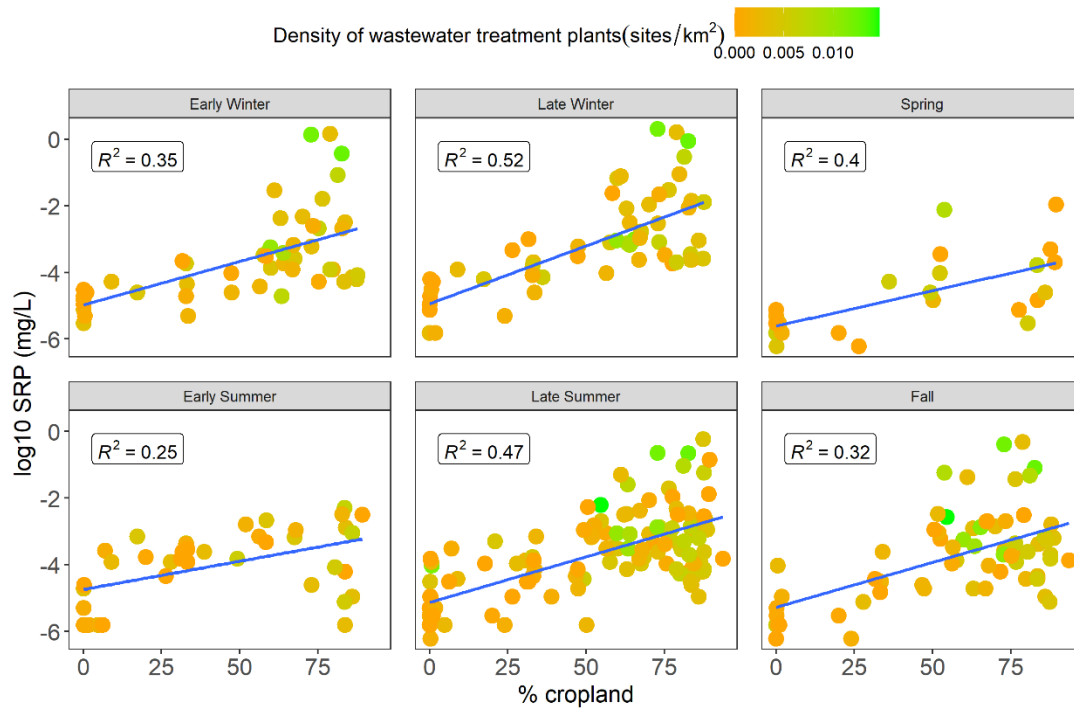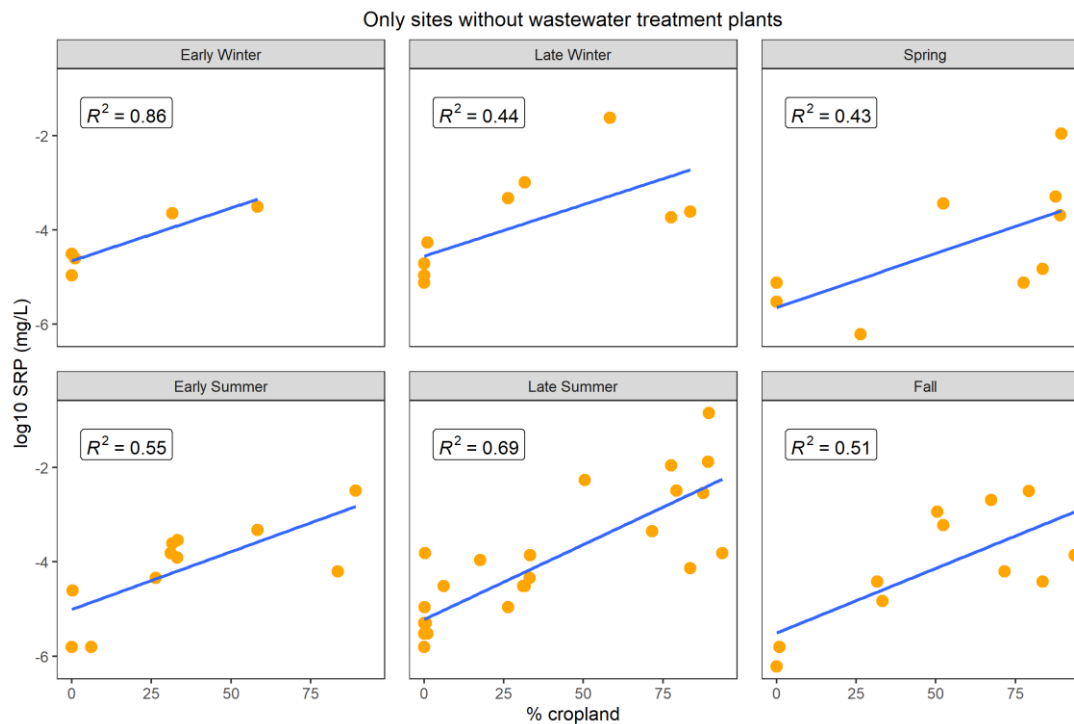

Figure 4: Mean low flow SRP concentrations across gages (log scale), in relation to % crop cover, by season, for sites with *no wastewater treatment plant influence*. Relationships in all seasons were significant and positive. Linear regression statistics are shown in Appendix Table A2.

16

3.4 SRP concentrations at tile outlets

Across tile outlets for 10 conventionally farmed fields (corn-soybean rotation), mean SRP concentration of tile drainage was highest in late winter (mean SRP = 0.131 mg/L) and lowest in early, late summer and early winter (mean
415   SRP = 0.03 mg/L; Table 2). Two sites (WR1 and ST1) included dairy operations, and two sites (BE1 and DO1) included swine finishing, in addition to row crops. The two dairy-influenced farm fields (WR1 and ST1) had notably higher tile SRP concentrations across all seasons relative to other sites. Three sites (MC1 RE1, and WR1) had one surface inlet to the tile system (all other inlets were subsurface). These sites appeared to have higher mean SRP concentrations in late winter (coinciding with snowmelt) and early summer (in the case of WR1), but of the surface
420   inlet sites only WR1 (the dairy farm site) had higher mean SRP concentrations in late summer.

**Table 2: Mean flow-weighted daily SRP concentrations (mg/L) from farm tile outlets, by season. Tile outlet data were collected from 10 farms between 2011-2021. Note that one farm field (NOW1) had two tile outlets (NOW1-N and NOW1-S) that drained different areas of the same field. Early winter: Nov-Dec; Late winter: Jan-Mar; Spring: Apr-May; Early summer: Jun-Jul; Late summer: Aug-Sept; Fall: Oct. [a]Farms included dairy operations. [b]Farms included a surface inlet to
425   tile drainage system. [c]Farms included swine finishing.**

Site	Early Winter	Late Winter	Spring	Early Summer	Late Summer	Fall	Annual mean
BE1[c]	0.064	0.053	0.031	0.017	0.023	0.132	0.036
DO1[c]	0.012	0.029	0.036	0.015	0.018	0.010	0.023
MC1[b]	0.019	0.139	0.023	0.012	0.022	0.024	0.037
NO1W-N	0.008	0.011	0.018	0.015	0.016	0.008	0.014
NO1W-S	0.017	0.025	0.024	0.012	0.018	0.015	0.018
RE1[b]	0.014	0.070	0.045	0.075	0.022	0.043	0.049
RW1N	0.023	0.231	0.025	0.014	0.011	0.033	0.061
RW1S	0.011	0.278	0.059	0.019	0.017	0.045	0.069
ST1[a]	0.053	0.164	0.091	0.062	0.073	0.048	0.084
WI1	0.011	0.008	0.009	0.008	0.005	0.010	0.008
WR1[a,b]	0.055	0.307	0.156	0.119	0.157	0.105	0.151
All sites	**0.029**	**0.131**	**0.051**	**0.036**	**0.033**	**0.035**	**0.052**

3.5 Riverine SRP at low flows compared to tile concentrations

We evaluated SRP during low flow conditions for each gaged watershed in each season (Table A3), and compared these riverine SRP values to SRP concentrations in monitored tile outlets. Note that not all gaged watersheds had sufficient samples collected during low flows in each season to generate mean values (Table A4); thus, the number of gaged watersheds with low flow mean SRP values available was different during each season. Comparisons for late winter, spring and late summer are shown in Fig. 5 (only a subset of seasons are shown for improved clarity in data visualization; similar figures for early winter, early summer and fall are shown in Appendix Fig. A2).

In early winter, 36% of gaged watersheds (n=18/50 sites for which low flow data was available) exhibited SRP concentrations at low flows that were higher than mean tile SRP concentration. Six of these watersheds were characterized by comparatively high wastewater treatment plant density (defined as >0.005 sites/km^2). In late winter when tile SRP concentrations were highest, 23% of gaged watersheds (n=13/57) exhibited SRP concentrations at low flows that were higher than mean tile concentrations. A minority of these sites (3/13) had considerable wastewater treatment plant influence (wastewater treatment plant density > 0.005 sites/km^2). In spring, SRP concentrations during low flow conditions were uniformly low across nearly all gaged watersheds. SRP samples collected during low flow conditions were fairly uncommon, with only 23 watersheds having >=3 SRP samples collected during spring low flows. Of these, two sites (9%) had SRP concentrations at low flows that were higher than mean tile concentrations. In early summer (Jun-Jul), 28% of sites (n=11/40) had SRP concentrations at low flow that were higher than mean tile concentrations. Two of these sites had considerable wastewater treatment influence. In late summer (Aug-Sep), 39% of gaged watersheds (n=50/128) had SRP concentrations at low flow that were higher than mean tile concentrations, and 16 of these sites had considerable wastewater treatment influence. In fall (Oct), 35% of gaged watersheds (n=24/68) sites had SRP concentrations at low flow that were higher than mean tile concentrations; eight of these sites had comparatively higher wastewater treatment plant density.

430

435

440

445

450
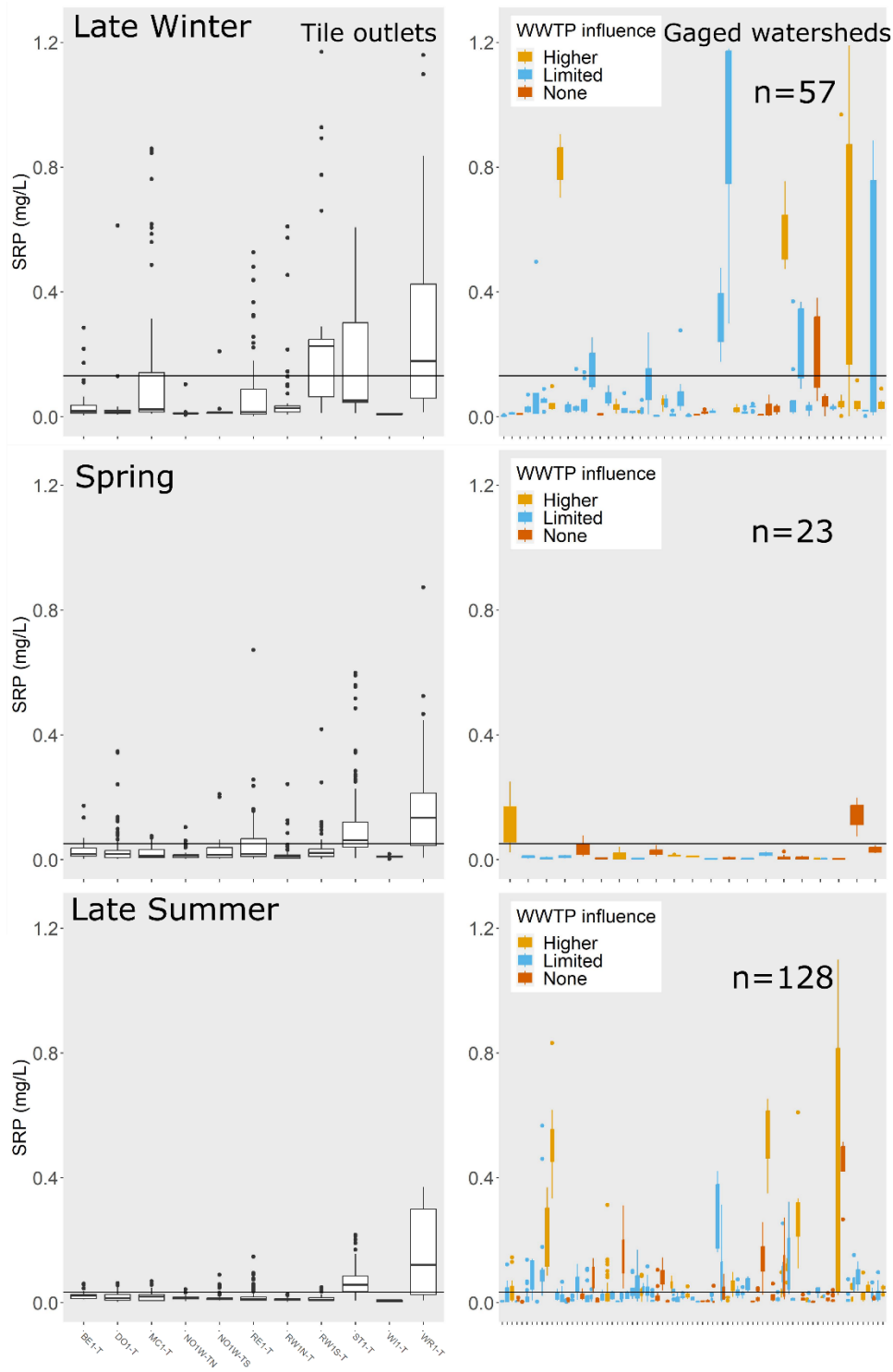
Figure 5: SRP concentrations (mg/L) for tile outlets and during low flow conditions for gaged watersheds, by season. Only a subset of seasons is shown for improved clarity in data visualization; similar figures for remaining seasons are shown in Appendix Fig. A2. The horizontal line in each plot is the mean SRP concentration among tile outlets for that season. For gaged watersheds, color of boxplots indicates degree of influence from wastewater treatment plants: light orange: wastewater treatment plant density >0.005 sites/km^2; blue = wastewater treatment plant density <0.005 sites/km^2 but greater than zero; dark orange: no wastewater treatment plant sites in watershed. The number of gages for which low flow data was available in each season is printed on the plot. To improve data visibility, the y-axis for SRP was limited to a maximum of 1.25 mg/L, which eliminated a small number of outliers from the plots for tile outlets (n=34 out of 11,079 records) and gaged watersheds (n=16 out of 2,696 low flow records).

**3.6 Low flow SRP concentrations from additional field sites**

Among gaged stream and river sites, small order systems (especially first through third order ditches and streams) were under-represented relative to their prevalence across the landscape. These smaller order systems are also less likely to have substantial point source discharges. To get a better understanding of SRP conditions in smaller order

500

systems, we examined SRP concentrations collected from 33 agriculturally dominated ditches, streams and mid-sized rivers in southern Minnesota during low flow conditions in August of 2014 (Dolph et al., 2017). During this sampling event, SRP concentrations at most sites were higher than mean SRP concentrations from farm tile outlets (Fig. 6). Mean SRP concentrations in late summer were highest in ditches (0.19 mg/L) and intermittent streams (0.19-0.30 mg/L).
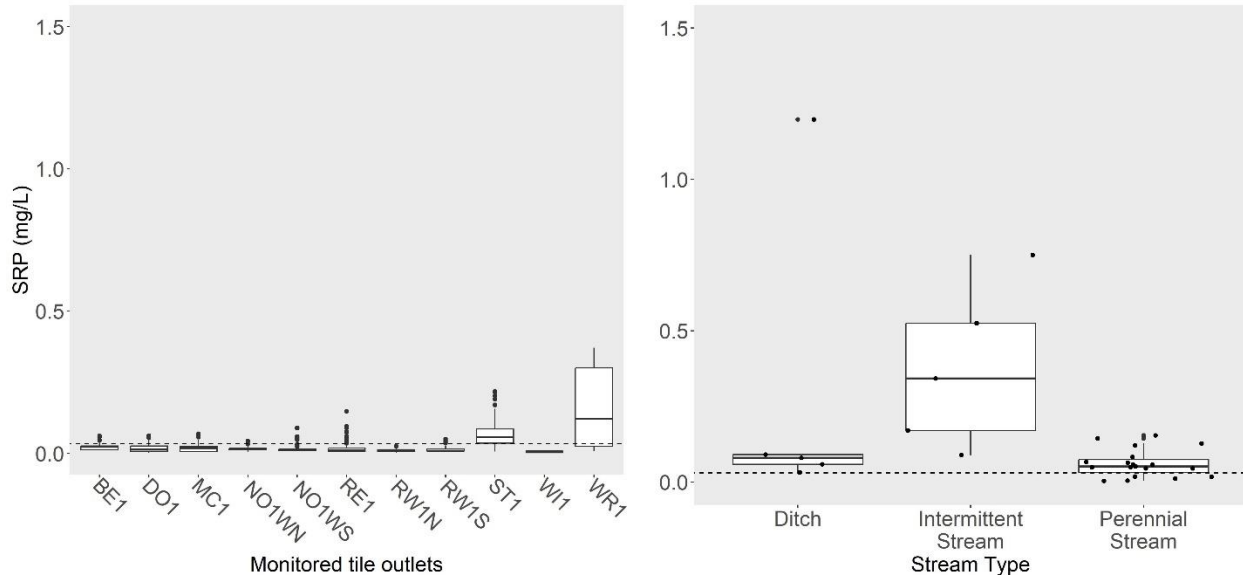
Figure 6: SRP concentrations (mg/L) among tile outlets (left panel) compared to sampled ditches (n=5), intermittent streams and rivers (n=6), and perennial streams/rivers (n=22) (right panel) during late summer low flow conditions. Dashed line shows mean SRP concentration for tile outlets in late summer.

3.7 *C-Q* relationships at stream and river gages

When *C-Q* relationships were evaluated using all flow data for each gage, the majority of gaged watersheds (72%, n=103) showed mobilizing behavior for SRP in relation to stream flow (i.e., significant positive slopes for the *C-Q* power law relationship and $CV_C/CV_Q > 0.3$; Fig. A3). Mobilizing behavior for bioavailable P ranged from very weak ($R^2=0.01$) to comparatively strong ($R^2=0.68$). Watersheds with positive SRP-Q relationships were located predominantly in the agriculturally dominated regions of the state (the southern and western parts of the state corresponding to the southern part of the Upper Mississippi River Basin, the Minnesota River Basin, the Driftless areas in the southeast, and the Red River Basin; Fig. 7). Chemodynamic behavior (non-significant slopes for the *C-Q* power law relationship and $CV_C/CV_Q > 0.3$ was observed for 24% (n=34) of sites, most located in the central and northeastern parts of the state dominated by forest and wetland cover (Fig. 7). A small number of sites (n=4, 3%) showed diluting behavior for SRP, as defined by significant negative slopes for the *C-Q* power law relationship and $CV_C/CV_Q > 0.3$. Two of these sites showed considerable wastewater treatment plant influences (wastewater treatment plant density > 0.005 sites/km[2;] Table A3). Three sites (2%) showed chemostatic behavior for SRP transport, as defined by a $CV_C/CV_Q <= 0.3$.
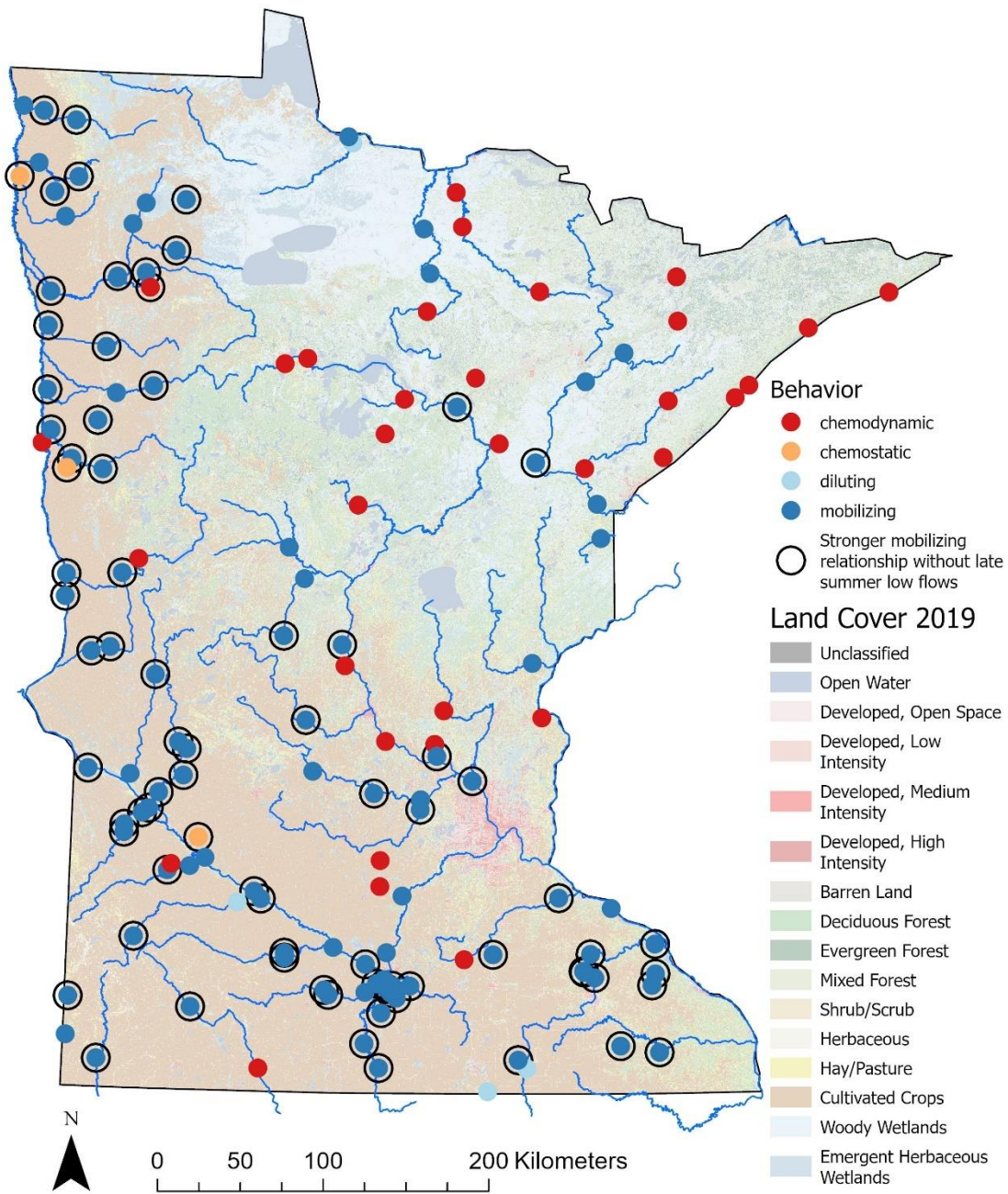
530   **Transport behavior of SRP in relation to flow (Q) for gaged watersheds (n=143). Dots indicate gage locations. Color of dots indicates transport behavior diagnosed by slope *b* of the *C-Q* power law relationship and *CV~C~/CV~Q~*. Mobilizing = black dots (n=103); Chemodynamic = light orange dots (n=34); Diluting = purple dots (n=4); Chemostatic = dark orange (n=3). Sites with a stronger mobilizing relationship (i.e., an increase in slope *b*) when late summer low flows were excluded are shown as open circles (n=78). Land cover is based on the 2019 National Land Cover Database.**

535 When low flow samples from late summer were removed, 54% of gaged watersheds (n=78) exhibited an increase in the slope of the mobilizing relationship between SRP and Q (Fig. 7; Appendix Table A5). For these sites, slopes of the *C-Q* relationships increased by 23%, on average, after late summer low flow samples were excluded (range in percent slope increase was 0.1%-273%). In other words, mobilizing behavior for SRP was stronger when these late summer low flow conditions were excluded. Examples of this phenomenon for four different gaged watersheds are

540 shown in Fig. 8, where the slope of the C-Q relationship is steeper when late summer low flow samples were excluded, and comparatively flatter when they are included. Watersheds where late summer low flows modulated (flattened) the slope of the C-Q relationship for SRP were again located predominantly in the agriculturally dominated regions of the state (Fig. 7).
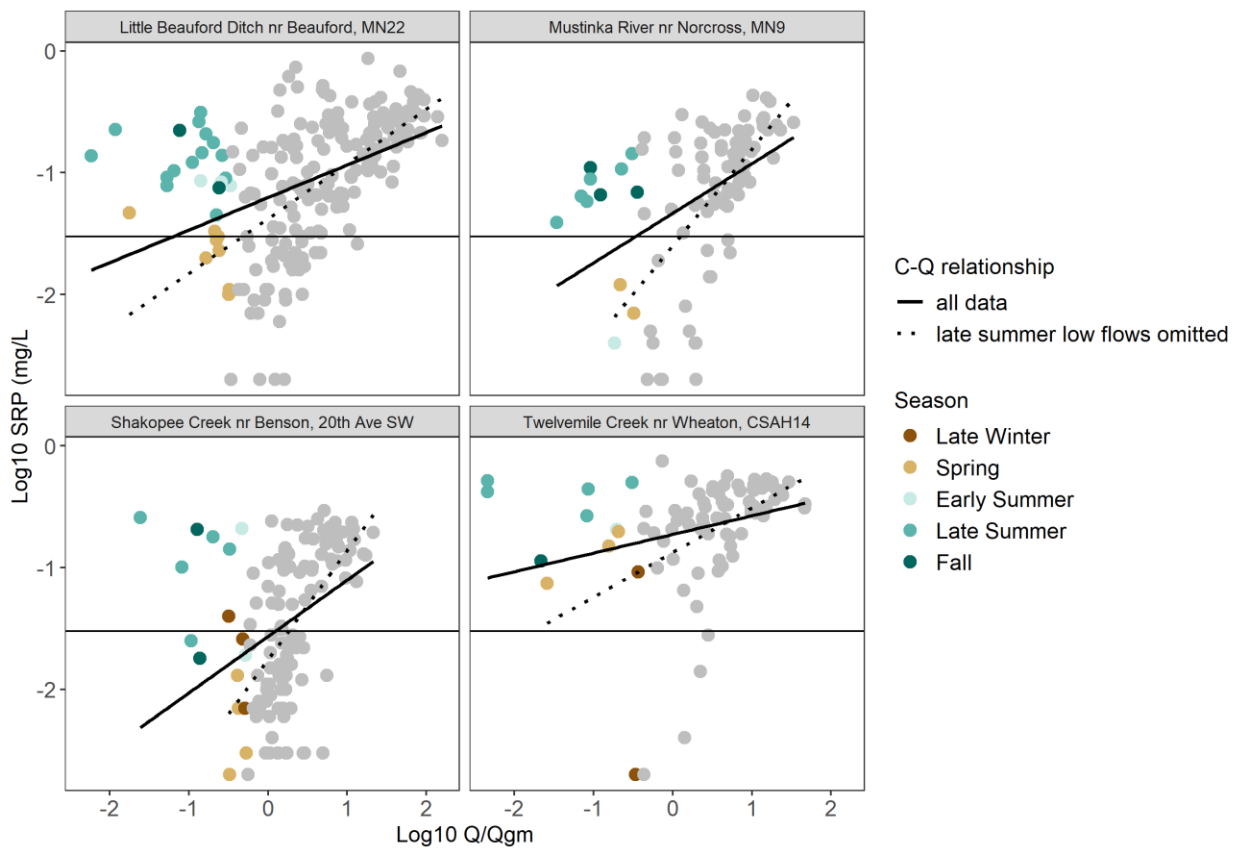
545

Figure 8: Example watersheds where low flows in late summer modulate the slope of the *C-Q* relationship for SRP. Low flow samples are shown as colored points where color indicates the season in which they were collected. All other samples are shown in gray. When all data are included, the slope of the overall *C-Q* relationship is reduced (solid line) compared to slopes for analyses with late summer low flow samples omitted (dashed line), indicating stronger mobilizing behavior.

550

3.8 Regression analysis to identify drivers of elevated SRP concentrations in late summer

The final selected hyperparameters for the random forest model based on model tuning with tenfold cross validation for this dataset were mtry = 7, trees = 1000, min_n = 6. Evaluation of predicted vs. actual late summer SRP for the independent test dataset indicated a model RMSE of 0.10, and an R^2 of 0.41 (Fig. A4). On average, the random forest

555 model underestimated actual mean SRP concentrations during late summer low flows compared to actual measured

values among test sites (mean of estimated - true values = -0.005). However, this negative bias was driven by poor predictive model performance for three sites with exceptionally high mean SRP concentrations of 0.293, 0.525, and 0.526 mg/L (Figure A4). For the remaining test sites (all with mean SRP <0.2 mg/L), predictive bias (mean of estimate - true values =0.02) was actually positive. For most sites, in other words, the random forest model over-estimated mean late summer SRP concentrations compared to measured values.

The top 15 predictors to model performance are shown in Fig. 9. Importance values for all predictors are shown in Table A6. Partial dependence plots for these top predictors (Fig. 10) showed that higher SRP during late summer low flow conditions was associated with: higher cropland land use in riparian areas, various soil characteristics (higher soil erodibility, lower soil permeability, higher soil clay content), greater agricultural intensity (higher pesticide use, higher phosphorus uptake by crops, higher fertilizer application rates), more urban land use in riparian areas, lower woody wetland, and mixed forest in riparian areas, lower grassland land use in watersheds, lower surplus precipitation in the watershed (precipitation minus evaporation) and higher stream temperatures. Table 3 summarizes possible mechanisms linking these attributes to riverine SRP concentrations.
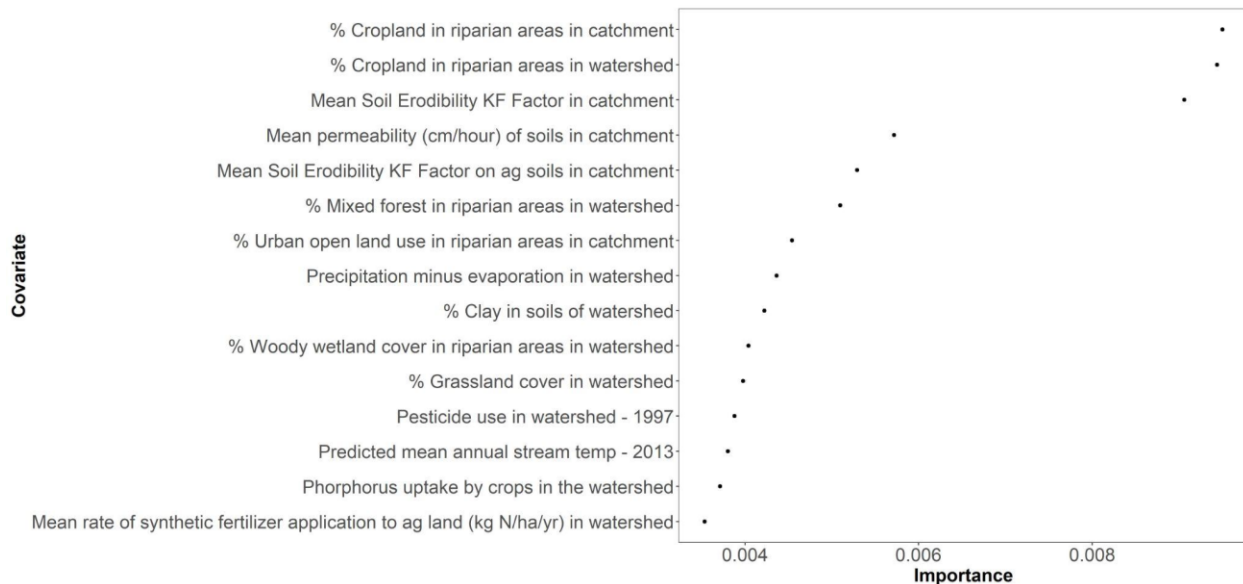
Figure 9: Conditional Permutation Importance (CPI) values for the top 15 predictors in the random forest model for late summer SRP during low flows and stream and river gages. CPI is a measure that can be used to assess how much each variable 'adds' to accurately predicting the response variable, given what we know from all other covariates. Importance values for all attributes are given in Table A6.

23
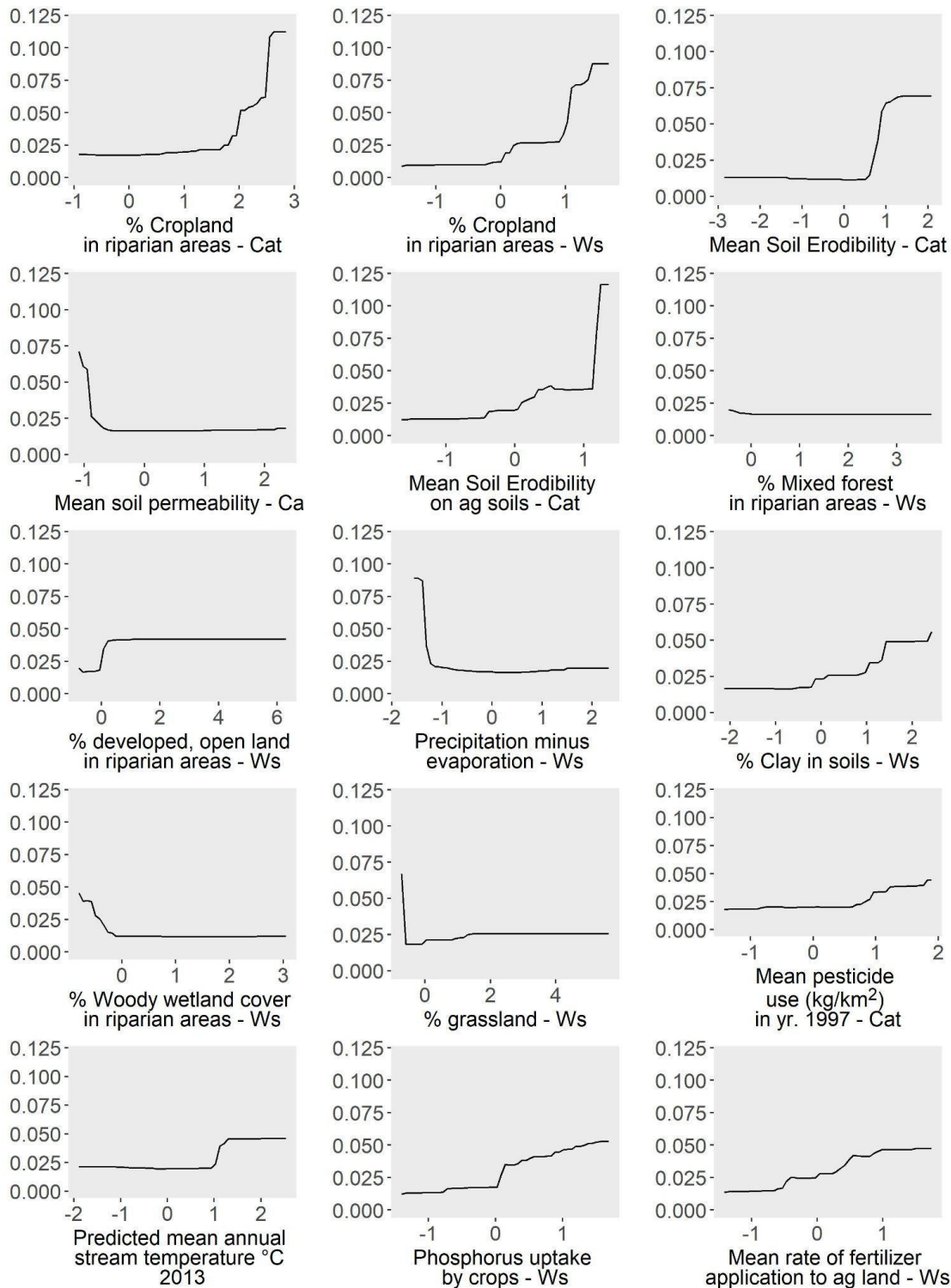
Figure 10: Partial dependence (y axis = change in predicted SRP value) for each of the 15 most important predictors to model performance. Partial dependence shows the change in the response variable (late summer low flow SRP) when each predictor of interest is varied while all other predictors stay constant. "Ws"=predictors summarized at watershed scale, "Ca"=predictors summarized at catchment scale. All predictor variables are from the U.S. EPA StreamCat dataset (Hill et al., 2016).

575

580

Table 3: Possible mechanisms linking random forest model predictor variables to late summer SRP concentrations during low flow conditions, for the top 15 attributes identified as most important to the performance of the random forest model. All attributes are from the U.S. EPA StreamCat dataset.

Attribute	Relationship	General mechanism category	Potential specific mechanism(s) linked to elevated late summer SRP
Percent of local NHD catchment classified as crop land use (NLCD 2019) within a 100-m buffer of NHD streams	Increasing SRP with increasing crop cover grown in proximity to river network	Direct inputs and/or legacy P supply	Indicator of current and historic P inputs from ag land use, especially in local riparian areas
Percent of watershed classified as crop land use (NLCD 2019) within a 100-m buffer of NHD streams	Increasing SRP with increasing crop cover grown in proximity to river network	Direct inputs and/or legacy P supply	Indicator of current and historic P inputs from ag land use, especially in local and upstream riparian areas
Mean soil erodibility factor (kffact, via STATSGO) within local NHD catchment; represents a relative index of susceptibility of bare, cultivated soil to particle detachment and transport by rainfall	Increasing SRP with increasing soil erodibility	Direct inputs and/or legacy P supply	Inputs of soil-associated P into river networks, either current or historic
Mean permeability (cm/hour) of soils (STATSGO) within local NHD catchment	Higher SRP at very low soil permeability	Mediates biogeochemical processes in near channel environment	Low permeability impedes oxygen exchange to the hyporheic zone, facilitating redox-mediated P release
Percent of watershed classified as mixed forest land cover (NLCD 2019) within a 100-m buffer of NHD streams	Higher SRP with low mixed forest cover in riparian areas	Direct inputs and/or legacy P and/or mediates biogeochemical processes	Fewer current or historic inputs of P to river networks with forested riparian areas; potential for forested riparian areas to trap P; shading of river channel alters stream productivity/stream metabolism
Percent of local NHD catchment classified as developed, open space land use (NLCD 2019) within a 100-m buffer of NHD streams	Higher SRP with higher open urban land use in riparian buffer	Direct inputs and/or legacy P supply	Indicator of urban land use and associated P inputs; could also mediate biogeochemical processes by altering stream temperature or flow conditions (i.e., higher stream temps in urban areas; stormwater infrastructure contributing to low flow conditions during dry periods, etc)
Precipitation (mm) minus potential evaporation within	Higher SRP at low and high ends of	Mediates biogeochemical	Dry conditions contribute to higher stream temperatures

watershed	precipitation range	processes in near channel environment	and lower discharge, influencing biologically-mediated P release
Mean % clay content of soils within watershed	Higher SRP with greater clay content in soils	Mediates biogeochemical processes in near channel environment	Fe-containing clay sediments can adsorb P and release it via redox reactions
Percent of watershed classified as woody wetland land cover (NLCD 2019) within a 100-m buffer of NHD streams	Higher SRP with low woody wetland cover in riparian buffers	Mediates biogeochemical processes in near channel environment	Woody wetlands acting as sinks for SRP
Percent of local catchment classified as grassland/ herbaceous land cover (NLCD 2019)	Higher SRP at low grassland cover	Direct inputs and/or legacy P supply	Fewer historic and ongoing P inputs in grasslands vs ag/urban lands
Mean pesticide use (kg/km2) in yr. 1997 within watershed	Increasing SRP with increasing pesticide use	Direct inputs and/or legacy P supply	Indicator of agricultural intensity and degree of historic/current P inputs
Predicted mean annual stream temperature for 2013	Higher SRP with higher stream temperatures	Mediates biogeochemical processes in near channel environment; Proxy for direct inputs and/or legacy P supply	Indicator of temperature-mediated biological activity, or of land use differences across climate gradients associated with P inputs (e.g., more agriculture & associated legacy P supplies in warmer climates)
Phosphorus uptake by crops in the watershed	Increasing SRP with increasing P uptake	Direct inputs and/or legacy P supply	Indicator of agricultural intensity and degree of historic/current P inputs
Mean rate of synthetic nitrogen fertilizer application to agricultural land in kg N/ha/yr, within the watershed	Increasing SRP with increasing fertilizer inputs	Direct inputs and/or legacy P supply	Indicator of agricultural intensity and degree of historic/current P inputs

4 Discussion

In this study we observed that between one third to one half of the gaged watersheds in Minnesota exhibited SRP concentrations during late summer low flows that were above previously identified thresholds for eutrophication of 0.02 - 0.04 mg/L for freshwater environments (Zeng et al., 2016; Poikane et al., 2021; (34% were above a threshold of 0.04 mg/L and 53% of watersheds were above 0.02 mg/L). One avenue for future research is to investigate how the timing and duration of elevated summer SRP concentrations affect local and downstream eutrophication outcomes. On the one hand, the large majority of annual P export by load likely occurs under high flow conditions in late winter and spring (Dolph et al., 2019; Schilling et al., 2020). However, the release of highly bioavailable P during hot, dry summer periods when conditions are optimal for algal growth in lakes and rivers may also drive increased eutrophication risk, resulting in outcomes such as increased occurrence of harmful algal blooms (Paerl and Huisman, 2008). As climate change is expected to result in increased prolonged periods of drought and heat during summers in the Upper Midwest (Wilson et al., 2023), the effects of elevated bioavailable P at low flows could be extended for longer parts of the season.

We also observed that, formore than half of the gaged watersheds we studied (54%), elevated SRP concentrations during low flows in late summer dampened *C-Q* relationships which would have otherwise appeared more strongly mobilizing across other seasons and flow conditions. Strongly mobilizing relationships are indicative of landscape connectivity as a key driver for SRP export (Musloff et al., 2015), with flow accumulation and riparian areas identified as critical source areas for SRP (Casquin et al., 2020; Dupas et al., 2023). Thus, for many of the sites we studied, connectivity appears important to SRP export during winter, spring and early summer and during moderate to high flow conditions at all times of year. During late summer low flows, by contrast, other in-channel dynamics may cause riverine *C-Q* patterns to deviate from linear relationships (Meybeck and Moatar, 2012). Below we discuss possible mechanisms that may contribute to comparatively high SRP concentrations during late summer low flow conditions in streams and rivers of our study region.

4.1 Drivers of SRP during late summer low flows

Overall, our analysis shows that landscape drivers that govern diffuse P inputs and legacy P supply in the river network, as well as wastewater inputs and biogeochemical processes, are associated with high late summer SRP concentrations during low flows at many anthropogenic-ly-dominated sites. Crop cover was strongly and directly related to SRP concentrations during low flow conditions in all seasons, and crop cover in riparian areas at the local catchment and watershed scales were the top two most important variables to the performance of the random forest model used to predict late summer low flow SRP concentrations. Other top variables to model performance included aspects of agricultural intensity at the watershed or catchment scale (pesticide use, phosphorus uptake by crops, and fertilizer application), as well as urban land use in riparian areas. The importance of these variables points to historic and ongoing inputs of P arising from intensive/industrial agriculture and urban land use that have resulted in the accumulation of legacy P in riverine channels, which can potentially be released under environmental conditions such as warm temperatures, low oxygen and variable moisture. Conversely, greater mixed forest or woody wetland land use in riparian areas was associated with lower SRP concentrations during late summer low flows, perhaps because

these environments may act as sinks for bioavailable P (Ury et al., 2023). Overall, it is notable that land use in riparian areas showed up as top variables of importance to model performance, suggesting that near channel environments (and therefore potentially near channel management practices) may be important in regulating elevated SRP during late summer low flows. Lastly, both geologic and climatic variables (soil erodibility, soil permeability, clay content of soils, mean annual stream temperatures, and precipitation minus evaporation) were also identified as important in the random forest model predicting late summer low flow SRP, suggesting that environmental factors which mediate biogeochemical processes also likely play an important role in driving late summer riverine SRP concentrations.

Interestingly, SRP concentrations during late summer low flow conditions in anthropogenic-ly-dominated watersheds often exceeded tile SRP concentrations. Although tile drainage is known to represent a key input of P to river networks (Smith et al., 2015), it may be that in-channel dynamics beyond tile concentrations drive variability in SRP concentration during summer low flows. However, it is also important to note that the two tile outlets draining farms with dairy operations exhibited much higher SRP concentrations during late summer (and all times of year), compared to tile outlets draining fields characterized only by corn and soybean row crops. Thus, the prevalence of CAFOs and other animal agriculture operations is likely to strongly influence the contribution of tile drainage to riverine SRP concentrations. Three sites also had a surface inlet to their tile drainage system. These tile systems had comparatively high SRP during winter, spring or early summer (depending on the site), which can likely be explained by the additional loss of sediment and nutrients to surface inlets during snowmelt on frozen and thawing soils (Feyereisen et al., 2015). However, the two surface inlet-influenced sites without dairy operations exhibited SRP concentrations during late summer similar to other nondairy impacted sites.

Wastewater treatment plant density did not rank among the most important predictors in our random forest model performance, and a substantial portion of sites (38%) exhibited elevated SRP concentrations (above 0.02 mg/L) during late summer low flow conditions despite having limited or no wastewater treatment plant influence in their watersheds. However, the influence of wastewater on summer low flow SRP was evident in elevated SRP concentrations at sites with strong wastewater influence throughout most seasons (apart from spring, when low flow SRP concentrations were nearly universally low, presumably due to rapid in-stream uptake or abiotic immobilization). We also observed direct (though weak) correlations with low flow SRP in late summer and wastewater treatment plant density in gaged watersheds. However, a sizeable number of the streams and rivers we studied (38%)

4.2 Biogeochemical processes and riverine SRP

Previous studies have identified a number of biogeochemical processes that can affect riverine concentrations of SRP at low flows. These processes include: 1) the concentration of legacy P entering the stream via groundwater and/or streambed pore water, 2) redox-driven release of P from stream sediments, and 3) release of P resulting from mineralization of organic matter.

During low flow conditions, groundwater and/or pore water can become proportionately dominant components of flow, with stores of legacy P in these sources contributing more strongly to overall riverine SRP. These groundwater

sources can include tile drainage (Schilling et al., 2020; Rode et al., 2023), but can also include streambed pore water entering from the hyporheic zone via upwelling flow paths with P concentrations that are distinct and potentially higher than that of tile drainage (Vissers et al., 2023). Upwelling of P-rich pore water can be patchy and is likely controlled by hyper-local spatial and temporal conditions operating at the reach scale, such as the availability and extent of reducing vs oxic conditions (e.g., Vissers et al., 2023).

SRP can also be released into river channels from stream sediments. Stream sediments often have the potential to buffer stream SRP concentrations by adsorbing P (Simpson et al., 2021). However, this buffering capacity will depend on sediment and stream characteristics, including sorption affinity, stream pH, exchangeable P concentration, sediment particle sizes, and seasonal variation in temperature, light, discharge, redox, primary productivity, stream respiration and sediment inputs (Simpson et al., 2021). Seasonal release of SRP is commonly thought to occur via the reduction of Fe-, Mn- or Al- oxyhydroxide-containing sediments under anoxic conditions, releasing PO_4^{3-}. These anoxic conditions typically arise when flow velocities are low, water and sediment temperatures increase, and oxygen becomes depleted due to increased microbial activity. For example, Smolders et al. (2017), showed that high summer concentrations of bioavailable P for rivers in Belgium were likely explained by internal loading from legacy P that was released from sediments when dissolved oxygen concentrations were low and P:Fe molar ratios in sediment were large.

Lastly, Jarvie et al., (2020) showed that, in a wetland-pond system, microbial respiration and the resulting mineralization of organic matter can also represent a source of bioavailable P under low flow conditions in summer and fall. They found that SRP release was potentially related to drier and hotter conditions that could facilitate both higher rates of biomass accumulation and its subsequent breakdown via microbial processes. Presumably, this dynamic could also be at play for slow moving ditches and streams in parts of our study region, where water is sometimes nearly stagnant in summer. Under low flow conditions and warm temperatures, ditches and streams may operate in ways that are similar to wetlands or other lentic water bodies. The stream network is also populated with in-channel and riparian wetlands that may further affect ambient SRP concentrations. Felton et al. (2023) found elevated dissolved P concentrations along a longitudinal stream gradient where the channel intersected wetlands and concluded that locally elevated SRP could reflect P release from decomposition of organic matter in wetland environments; however, in that study elevated P concentrations did not persist downstream and were assumed to be rapidly assimilated or adsorbed to sediments.

Our findings provide some insight as to the relative importance of these potential in-channel processes in determining seasonally elevated SRP concentrations at low flow. The importance of climate and geologic variables in the random forest model we used to predict late summer low flow SRP suggests that characteristics of stream sediments and/or climate-mediated biotic activity may play an important role in elevated SRP concentrations in late summer. Partial dependence plots indicated that increased SRP during late summer low flows was associated with the drier conditions (lower precipitation minus evaporation in gaged watersheds) and warmer conditions (higher predicted mean stream

temperatures)[9]. This finding could be consistent with an important role for biologically mediated processes such as microbial respiration that are affected by temperature and stream discharge. Microbial activity is important both in the decomposition of organic matter (i.e., mineralization), as well as in the reduction of redoximorphic sediments (i.e., sediments containing Fe, Al, Mn, etc.), both of which can result in the release of SRP. The predicted mean stream temperature values used in this study were derived from Hill et al. (2013), and were themselves influenced by air temperature, soil permeability, agricultural and urban land use, stream slope, the influence of reservoirs, and watershed area. The positive relationship between stream temperature and late summer SRP at low flow needs further investigation but could also be related to greater influence of groundwater or to climate gradients that correspond to variation in biological activity or in land use and associated P inputs.

Soil erodibility was also identified as one of the most important variables to random forest model performance, with partial dependence plots showing higher SRP during late summer low flows corresponding with greater soil erodibility in the local catchment. Eroded soils have long been understood as a primary vector by which P enters river networks (Berhe et al., 2018). Recently, this understanding has expanded to include eroded stream bank sediments as an additional driver of downstream P transport (Margenot et al., 2023). Sediment-associated P may be temporarily stored in river channels, with desorption of P occurring under certain environmental conditions, as described above.

Partial dependence plots showed that late summer low flow SRP concentrations were highest where soil permeability of soils in local catchments was low. This finding is also consistent with release of P from stream sediments. Low soil permeability is characteristic of fine sediments (Ren and Santamarina, 2018). If broader watershed soil types are indicative of in-stream sediment, very low permeability of fine-grained stream sediments could impede oxygen exchange to the hyporheic zone, potentially creating anoxic conditions to facilitate redox-mediated P release (Mendoza-Lera and Datry, 2017).

Partial dependence plots also indicated that increased SRP during late summer low flow conditions was associated with increased clay content of soils in gaged watersheds. Clay particles are small in size, providing greater P adsorption potential (Simpson et al., 2021). Clay sediments also typically contain iron (Fe) that can bind P and can therefore provide a substrate for microbially mediated redox reactions (Pentrakova et al., 2013). Our findings are consistent with a mechanism whereby clay sediments bind considerable P under some conditions, and then release it via redox reactions during late summer when oxic conditions are low due to microbial decomposition of organic matter.

Environmental conditions in large parts of our study region are consistent with those previously reported to foster situational SRP release from sediments. Previous studies have observed release of SRP from stream sediments when SRP to Fe ratios in sediments are high and when dissolved oxygen concentrations are low (Inamdar et al., 2020; van Dael et al., 2020; Diamond et al., 2023). These conditions are characteristic of slow-moving lowland streams with large legacy P stores arising from current and historic P inputs, and may be especially common in headwater streams

---

[9] Note that stream temperature data in the U.S. EPA StreamCat dataset is derived from Hill et al. (2013) and takes into account natural factors and certain aspects of anthropogenic influence (i.e., reservoirs, urban land use and agricultural land use) but does not account for wastewater effluent.

(Diamond et al., 2023). Such conditions are widespread across our study region. Ditches, streams, and rivers in the flat to gently rolling landscapes of southern and northwestern Minnesota are characterized by relatively low gradients, high current and historic P loading from agriculture and urban land use (Boardman et al., 2019), and high rates of instream primary productivity (Dolph et al., 2017b). These conditions are likely to coincide during warm late summer conditions in high rates of microbial respiration, anoxic conditions, and P release.

Overall, our findings agree with previous studies that have identified the importance of biogeochemical processes in seasonally modulating nutrient concentrations during low flows in lowland lotic systems (e.g., Smolders et al., 2017) and in many ways parallels findings for eutrophic lakes (Søndergaard et al., 2001). Further study is needed to parse the importance of pore water, stream sediment dynamics, and mineralization to the elevated SRP concentrations we observed at various stream and river sites during late summer low flow conditions.

Limitations and future study

A major limitation of this study is that we did not have direct information about legacy P supply in stream and river channels. Efforts to quantify the P content of stream sediments, and the potential of stream sediments to adsorp/desorb SRP in different geographic and seasonal and hydrologic contexts, could provide additional valuable information about the extent to which in-channel release of legacy P is affecting downstream water quality.

It is also important to note that performance of the random forest model we used to predict late summer SRP concentrations was middling (R^2=0.41). We speculate that improved model performance will depend on reach-scale variables that may strongly determine SRP dynamics, such as channel morphology, characteristics and volume of bed sediment, and stream productivity and respiration. Future research could aim to incorporate both reach scale and broader scale variables into a more precise understanding of in channel SRP dynamics. For example, the sampling platform described by Felton et al. (2023) presents the intriguing possibility of monitoring stream conditions intensively along longitudinal gradients and could be refined to include measures of dissolved oxygen, CO_2 (as a proxy for respiration), temperature, sorption capacity, and/or to identify P inputs associated with tile and point discharges or certain aspects of channel morphology.

5 Conclusions

In this study we observed widespread elevation of SRP concentrations during late summer low flow conditions among anthropogenically dominated ditches, streams and rivers in Minnesota. These elevated SRP concentrations altered *C-Q* transport behavior for more than half (54%) of the gaged watersheds we studied, weakening what was otherwise more strongly mobilizing behavior during higher flow conditions and other times of year.

While wastewater discharge likely contributed to elevated SRP concentration at low flow for some sites, most sites exhibiting elevated SRP concentrations during late summer low flow conditions did not have substantial wastewater treatment impacts. Moreover, elevated SRP concentrations during low flow at these sites typically exceeded tile drainage SRP concentrations from corn and soy planted farm fields during late summer. We found that late summer low flow SRP concentrations were related to land use, soil characteristics, measures of agricultural intensity, and climate. Taken together, these findings suggest that climate and geologically mediated biogeochemical processes

likely result in the release of in-channel stores of legacy P during late summer low flow conditions in a substantial number of stream and river sites that have been heavily impacted by past and current P inputs associated with industrial/intensive agriculture and urbanization. As summers become hotter and drier – predicted climate changes in our region – conditions for the release of legacy P stored in stream and river channels will likely become more prolonged and/or more acute, contributing to the increased occurrence of adverse events such as harmful algal blooms. Further study is needed to determine the duration, fate and dominant mechanisms associated with riverine release of bioavailable P during late summer and other times of year.

Our findings suggest that efforts to reduce the impacts of bioavailable P to freshwaters will need to address both 1) mobilization of dissolved P from the landscape during high flow conditions and 2) in-channel environments that result in the release of accumulated legacy P from streams and rivers during summer low flows when freshwater systems are especially vulnerable to eutrophication outcomes. With regards to management, the association of land use in riparian areas with SRP during late summer low flows suggests that practices targeting near channel and riparian environments may be important in regulating elevated SRP. In Minnesota, state law implemented in 2015 has already mandated vegetative 50-foot riparian buffers along the state's water bodies to protect water quality (Riparian Protection and Water Quality Practices Act, 2015[10]). Our findings suggest that perhaps, specific vegetative conditions within these riparian buffers – for example whether mixed forest or woody wetlands are present – could additionally enhance legacy P retention and mitigate release. Further study is needed to examine the way these habitat types interact with legacy P over time and under different conditions.

Controlling ongoing P inputs will also be instrumental to reducing riverine P loading. For example, in Minnesota, additional phosphorus regulations added to National Pollutant Discharge Elimination System (NPDES) permits since the year 2000 have resulted in substantial reductions of P loading arising from wastewater facilities[11]. Policies and management approaches to substantially reduce inputs of fertilizer, manure and wastewater, as well their losses via surface, tile and other groundwater pathways, remain critical to achieving societal water quality goals.

Code availability
All R scripts used for data analysis are available from https://github.com/cldolph/instream_legacyP

Data availability
All input data used in this paper are available from https://github.com/cldolph/instream_legacyP

Author contribution
CD, BD, GF and JF conceived study design, identified available datasets, and identified research questions. CD performed data analysis and developed R scripts. CD prepared the manuscript with contributions from all co-authors.

Competing interests
The authors declare that they have no conflict of interest.

---

[10] https://www.revisor.mn.gov/statutes/cite/103F.48
[11] https://www.pca.state.mn.us/business-with-us/phosphorus-in-wastewater

800

References

Basu, N.B., Destouni, G., Jawitz, J.W., Thompson, S.E., Loukinova, N.V., Darracq, A., Zanardo, S., Yaeger, M., Sivapalan, M., Rinaldo, A., and Rao, P.S.C.: Nutrient loads exported from managed catchments reveal
805   emergent biogeochemical stationarity, Geophysical Research Letters, 37, https://doi.org/10.1029/2010gl045168, 2010.

Bennett, E.M., Carpenter, S.R., and Caraco, N.F.: Human Impact on Erodable Phosphorus and Eutrophication: A Global Perspective, BioScience, 51, 227. https://doi.org/10.1641/0006-3568(2001)051[0227:hioepa]2.0.co;2, 2001.

810   Berhe, A.A., Barnes, R.T., Six, J., and Marín-Spiotta, E.: Role of Soil Erosion in Biogeochemical Cycling of Essential Elements: Carbon, Nitrogen, and Phosphorus, Annual Review of Earth and Planetary Sciences, 46, 521–548. https://doi.org/10.1146/annurev-earth-082517-010018, 2018.

Bieroza, M.Z. and Heathwaite, A.L.: Seasonal variation in phosphorus concentration–discharge hysteresis inferred from high-frequency in situ monitoring, Journal of Hydrology, 524, 333–347,
815   https://doi.org/10.1016/j.jhydrol.2015.02.036, 2015.

Boardman, E., Danesh-Yazdi, M., Foufoula-Georgiou, E., Dolph, C.L., and Finlay, J.C.: Fertilizer, landscape features and climate regulate phosphorus retention and river export in diverse Midwestern watersheds, Biogeochemistry, 146, 293–309, https://doi.org/10.1007/s10533-019-00623-z, 2019.

Casquin, A., Gu, S., Dupas, R., Petitjean, P., Gruau, G., and Durand, P.: River network alteration of C-N-P dynamics
820   in a mesoscale agricultural catchment, Science of The Total Environment, 749, 141551, https://doi.org/10.1016/j.scitotenv.2020.141551, 2020.

Debeer D, Hothorn T, and Strobl C:_permimp: Conditional Permutation Importance_, R package version 1.0-2, https://CRAN.R-project.org/package=permimp, 2021.

Dewitz, J.: National Land Cover Database (NLCD) 2019 Products [Data set], U.S. Geological Survey.
825   https://doi.org/10.5066/P9KZCM54, 2021.

Diamond, J.S., Moatar, F., Recoura-Massaquant, R., Chaumot, A., Zarnetske, J., Valette, L., and Pinay, G.: Hypoxia is common in temperate headwaters and driven by hydrological extremes, Ecological Indicators, 147, 109987. https://doi.org/10.1016/j.ecolind.2023.109987, 2023.

Dolph, C.L.; Hansen, A.T.; Kemmitt, K. L.; Janke, B.; Rorer, M.; Winikoff, S., et al.: Characterization of streams and
830   rivers in the Minnesota River Basin Critical Observatory: Water chemistry and biological field collections, 2013–2016, Retrieved from the Data Repository for the University of Minnesota, https://doi.org/10.13020/D6FH44, 2017a.

Dolph, C. L., Hansen, A. T., and Finlay, J. C.: Flow-related dynamics in suspended algal biomass and its contribution to suspended particulate matter in an agricultural river network of the Minnesota River Basin, USA,
835   Hydrobiologia, 785(1), 127–147, http://doi.org/10.1007/s10750-016-2911-7, 2017b.

Dolph, C.L., Boardman, E., Danesh-Yazdi, M., Finlay, J.C., Hansen, A.T., Baker, A.C., and Dalzell, B.: Phosphorus Transport in Intensively Managed Watersheds, Water Resources Research, 55, 9148–9172, https://doi.org/10.1029/2018wr024009, 2019.

Dolph, C.L., Cho, S.J., Finlay, J.C., Hansen, A.T., Dalzell, B.: Predicting high resolution total phosphorus
840   concentrations for soils of the Upper Mississippi River Basin using machine learning, Biogeochemistry, 163, 289–310. https://doi.org/10.1007/s10533-023-01029-8, 2023.

Dupas, R., Casquin, A., Durand, P., and Viaud, V.: Landscape spatial configuration influences phosphorus but not nitrate concentrations in agricultural headwater catchments, Hydrological Processes, 37, https://doi.org/10.1002/hyp.14816, 2023.

845 ESRI: ArcGIS Pro version 3.0.3. Redlands, CA: Environmental Systems Research Institute, 2022.

Felton, R., Dalzell, B.J., Baker, J., Flynn, K.D., and Porter, S.A.: Novel, Ultralight Platform for Mapping Water Quality Parameters in Low-Order Streams, ACS ES&T Water 3, 3305–3314, https://doi.org/10.1021/acsestwater.3c00280, 2023.

Feyereisen, G.W., Francesconi, W., Smith, D.R., Papiernik, S.K., Krueger, E.S., and Wente, C.D.: Effect of Replacing
850 Surface Inlets with Blind or Gravel Inlets on Sediment and Phosphorus Subsurface Drainage Losses, Journal of Environmental Quality, 44, 594–604, https://doi.org/10.2134/jeq2014.05.0219, 2015.

Godsey, S.E., Kirchner, J.W., and Clow, D.W.: Concentration-discharge relationships reflect chemostatic characteristics of US catchments, Hydrological Processes, 23, 1844–1864, https://doi.org/10.1002/hyp.7315, 2009.

855 Goyette, J.-O., Bennett, E.M., and Maranger, R.: Low buffering capacity and slow recovery of anthropogenic phosphorus pollution in watersheds, Nature Geoscience, 11, 921–925, https://doi.org/10.1038/s41561-018-0238-x, 2018.

Greenwell, B.M.: pdp: An R Package for Constructing Partial Dependence Plots, The R Journal, 9, 421, https://doi.org/10.32614/rj-2017-016, 2017.

860 Hagenauer, J., Omrani, H., and Helbich, M.: Assessing the performance of 38 machine learning models: the case of land consumption rates in Bavaria, Germany, International Journal of Geographical Information Science, 33, 1399–1419, https://doi.org/10.1080/13658816.2019.1579333, 2019.

Haque, S.E.: How Effective Are Existing Phosphorus Management Strategies in Mitigating Surface Water Quality Problems in the U.S.?, Sustainability, 13, 6565, https://doi.org/10.3390/su13126565, 2021.

865 Hill, R.A., Hawkins, C.P., and Carlisle, D.M.: Predicting thermal reference conditions for USA streams and rivers, Freshwater Science, 32, 39–55, https://doi.org/10.1899/12-009.1, 2013.

Hill, R.A., Weber, M.H., Leibowitz, S.G., Olsen, A.R., and Thornbrugh, D.J.: The Stream-Catchment (StreamCat) Dataset: A Database of Watershed Metrics for the Conterminous United States, Journal of the American Water Resources Association (JAWRA), 52, 120-128, https://doi.org/10.1111/1752-1688.12372, 2016.

870 Inamdar, S., Sienkiewicz, N., Lutgen, A., Jiang, G., and Kan, J.: Streambank Legacy Sediments in Surface Waters: Phosphorus Sources or Sinks?, Soil Systems, 4, 30, https://doi.org/10.3390/soilsystems4020030, 2020.

Jarvie, H.P., Pallett, D.W., Schäfer, S.M., Macrae, M.L., Bowes, M.J., Farrand, P., Warwick, A.C., King, S.M., Williams, R.J., Armstrong, L., Nicholls, D.J.E., Lord, W.D., Rylett, D., Roberts, C., and Fisher, N.: Biogeochemical and climate drivers of wetland phosphorus and nitrogen release: Implications for nutrient
875 legacies and eutrophication risk, Journal of Environmental Quality, 49, 1703–1716, https://doi.org/10.1002/jeq2.20155, 2020.

Johnson, L., Will Bartsch, George Hudak, Mae Davenport, Kris Johnson, Kristi Nixon, Jane Reed and Atlas Team: Minnesota Natural Resource Atlas: Online mapping tools and data for natural resource planning, management, and research in Minnesota, Natural Resources Research Institute, University of Minnesota
880 Duluth, https://mnatlas.org/, 2022.

Keiser, D., and Shapiro, J.: Consequences of the Clean Water Act and the Demand for Water Quality, The Quarterly Journal of Economics, Volume 134, Issue 1, February 2019, 349–396, https://doi.org/10.1093/qje/qjy019, 2019.

King, K.W., Williams, M.R., and Fausey, N.R.: Contributions of Systematic Tile Drainage to Watershed-Scale
885 Phosphorus Transport, Journal of Environmental Quality, 44, 486–494, https://doi.org/10.2134/jeq2014.04.0149, 2015.

Kreiling, R.M., Perner, P.M., Breckner, K.J., Williamson, T.N., Bartsch, L.A., Hood, J.M., Manning, N.F., and Johnson, L.T.: Watershed- and reach-scale drivers of phosphorus retention and release by streambed sediment in a western Lake Erie watershed during summer, Science of The Total Environment, 863, 160804,
890 https://doi.org/10.1016/j.scitotenv.2022.160804, 2023.

Kuhn, M., and Wickham, H.: Tidymodels: a collection of packages for modeling and machine learning using tidyverse principles. https://www.tidymodels.org, 2020.

Liaw, A., and Wiener, M.: Classification and Regression by randomForest, R News 2(3), 18—22, 2002.

Margenot, A.J., Zhou, S., McDowell, R., Hebert, T., Fox, G., Schilling, K., Richmond, S., Kovar, J.L., Wickramarathne, N., Lemke, D., Boomer, K., and Golovay, S.: Streambank erosion and phosphorus loading to surface waters: Knowns, unknowns, and implications for nutrient loss reduction research and policy, Journal of Environmental Quality, 52, 1063–1079, https://doi.org/10.1002/jeq2.20514, 2023.

Mayer, M.: _missRanger: Fast Imputation of Missing Values_. R package version 2.2.1, https://CRAN.R-project.org/package=missRanger, 2023.

MDA: MDA Discovery Farms Program field data and sample collection SOP. Minnesota Department of Agriculture, St. Paul, Minnesota. https://discoveryfarmsmn.org/wp-content/uploads/2021/07/DFM_Monitoring-SOP_v5_signed_Final.pdf , 2021.

Mendoza-Lera, C., and Datry, T.: Relating hydraulic conductivity and hyporheic zone biogeochemical processing to conserve and restore river ecosystem services, Science of The Total Environment, 579, 1815–1821, https://doi.org/10.1016/j.scitotenv.2016.11.166, 2017.

Meybeck, M., and Moatar, F.: Daily variability of river concentrations and fluxes: indicators based on the segmentation of the rating curve, Hydrological Processes, 26, 1188–1207, https://doi.org/10.1002/hyp.8211, 2012.

Minnesota Department of Natural Resources and Minnesota Pollution Control Agency: DNR/MPCA Cooperative Stream Gaging Locations, Available from: https://gisdata.mn.gov/dataset/env-wiski-coop-stream-gaging [Accessed January 30, 2023], 2023.

MPCA: Watershed Pollutant Load Monitoring Network (WPLMN) standard operating procedures and guidance: Surface water quality sampling, Minnesota Pollution Control Agency, St. Paul, Minnesota, https://www.pca.state.mn.us/sites/default/files/wq-cm1-02.pdf, 2015.

MPCA: Proposed impaired waters list. Minnesota Pollution Control Agency, St. Paul, Minnesota, https://www.pca.state.mn.us/air-water-land-climate/minnesotas-impaired-waters-list, 2022.

Musolff, A., Schmidt, C., Selle, B., and Fleckenstein, J.H.: Catchment controls on solute export, Advances in Water Resources, 86, 133–146, https://doi.org/10.1016/j.advwatres.2015.09.026, 2015.

Osterholz, W.R., Hanrahan, B.R., and King, K.W.: Legacy phosphorus concentration–discharge relationships in surface runoff and tile drainage from Ohio crop fields, Journal of Environmental Quality, 49, 675–687, https://doi.org/10.1002/jeq2.20070, 2020.

Paerl, H.W., and Huisman, J.: Blooms Like It Hot, Science, 320, 57–58, https://doi.org/10.1126/science.1155398, 2008.

Pentráková, L., Su, K., Pentrák, M., and Stucki, J.W.: A review of microbial redox interactions with structural Fe in clay minerals, Clay Minerals, 48, 543–560, https://doi.org/10.1180/claymin.2013.048.3.10, 2013.

Poikane, S., Várbíró, G., Kelly, M.G., Birk, S., and Phillips, G.: Estimating river nutrient concentrations consistent with good ecological condition: More stringent nutrient thresholds needed, Ecological Indicators, 121, 107017. https://doi.org/10.1016/j.ecolind.2020.107017, 2021.

R Core Team (2023). _R: A Language and Environment for Statistical Computing_, R Foundation for Statistical Computing, Vienna, Austria, https://www.R-project.org/

Records, R.M., Wohl, E., and Arabi, M.: Phosphorus in the river corridor, Earth-Science Reviews, 158, 65–88, https://doi.org/10.1016/j.earscirev.2016.04.010, 2016.

Ren, X.W., and Santamarina, J.C: The hydraulic conductivity of sediments: A pore size perspective, Engineering Geology, 233, 48–54, https://doi.org/10.1016/j.enggeo.2017.11.022, 2018.

Rode, M., Tittel, J., Reinstorf, F., Schubert, M., Knöller, K., Gilfedder, B., Merensky-Pöhlein, F., and Musolff, A.: Seasonal variation and release of soluble reactive phosphorus in an agricultural upland headwater in central Germany, Hydrology and Earth System Sciences, 27, 1261–1277, https://doi.org/10.5194/hess-27-1261-2023, 2023.

940 Schilling, K.E., Streeter, M.T., Vogelgesang, J., Jones, C.S., and Seeman, A.: Subsurface nutrient export from a cropped field to an agricultural stream: Implications for targeting edge-of-field practices, Agricultural Water Management, 241, 106339. https://doi.org/10.1016/j.agwat.2020.106339, 2020.

Siebers, N., Kruse, J., Jia, Y., Lennartz, B., and Koch, S.: Loss of subsurface particulate and truly dissolved phosphorus during various flow conditions along a tile drain–ditch–brook continuum, Science of The Total Environment, 866, 161439, https://doi.org/10.1016/j.scitotenv.2023.161439, 2023.

945 Simpson, Z.P., McDowell, R.W., Condron, L.M., McDaniel, M.D., Jarvie, H.P., and Abell, J.M.: Sediment phosphorus buffering in streams at baseflow: A meta-analysis, Journal of Environmental Quality. 50, 287–311, https://doi.org/10.1002/jeq2.20202, 2021.

Søndergaard, M., Jensen, P.J., and Jeppesen, E., Retention and Internal Loading of Phosphorus in Shallow, Eutrophic Lakes, The Scientific World JOURNAL, 1, 427–442, https://doi.org/10.1100/tsw.2001.72, 2001.

950 Smith, D.R., King, K.W., Johnson, L., Francesconi, W., Richards, P., Baker, D., and Sharpley, A.N.: Surface Runoff and Tile Drainage Transport of Phosphorus in the Midwestern United States, Journal of Environmental Quality, 44, 495–502, https://doi.org/10.2134/jeq2014.04.0176, 2015.

Smolders, E., Baetens, E., Verbeeck, M., Nawara, S., Diels, J., Verdievel, M., Peeters, B., De Cooman, W., and Baken, S.: Internal Loading and Redox Cycling of Sediment Iron Explain Reactive Phosphorus Concentrations in
955 Lowland Rivers, Environmental Science & Technology, 51, 2584–2592. https://doi.org/10.1021/acs.est.6b04337, 2017.

Thompson, S.E., Basu, N.B., Lascurain, J., Jr., Aubeneau, A., and Rao, P.S.C.: Relative dominance of hydrologic versus biogeochemical factors on solute export across impact gradients, Water Resources Research, 47, https://doi.org/10.1029/2010wr009605, 2011.

960 Ury, E.A., Arrumugam, P., Herbert, E.R., Badiou, P., Page, B., and Basu, N.B.: Source or sink? Meta-analysis reveals diverging controls of phosphorus retention and release in restored and constructed wetlands, Environmental Research Letters, 18, 083002, https://doi.org/10.1088/1748-9326/ace6bf , 2023.

USEPA: National Hydrography Dataset Plus Version 2, U.S. Environmental Protection Agency, Available from: https://www.epa.gov/waterdata/get-nhdplus-national-hydrography-dataset-plus-data [Accessed May 23,
965 2023], 2019.

USGS: USGS Streamgage NHDPlus Version 1 Basins 2011, U.S. Geological Survey, Available from: https://water.usgs.gov/GIS/metadata/usgswrd/XML/streamgagebasins.xml#stdorder [Accessed February 22, 2023], 2012.

Valayamkunnath, P., Barlage, M., Chen, F., Gochis, D.J., and Franz, K.J.: Mapping of 30-meter resolution tile-drained
970 croplands using a geospatial modeling approach, Scientific Data 7, https://doi.org/10.1038/s41597-020-00596-x, 2020.

van Dael, T., De Cooman, T., and Smolders, E.: In-stream oxygenation to mitigate internal loading of phosphorus in lowland streams, Journal of Hydrology, 590, 125536, https://doi.org/10.1016/j.jhydrol.2020.125536, 2020.

Vilmin, L., Bouwman, A.F., Beusen, A.H.W., van Hoek, W.J., and Mogollón, J.M.: Past anthropogenic activities
975 offset dissolved inorganic phosphorus retention in the Mississippi River basin, Biogeochemistry, 161, 157–169, https://doi.org/10.1007/s10533-022-00973-1, 2022.

Vissers, M.A., Roy, J.W., Yates, A.G., Robinson, K., Rakhimbekova, S., and Robinson, C.E.: Spatio-temporal variability of porewater phosphorus concentrations in streambed sediments of an agricultural stream, Journal of Hydrology, 617, 129133, https://doi.org/10.1016/j.jhydrol.2023.129133, 2023.

980 Wanner, O., Egli, T., Fleischmann, T., Lanz, K., Reichert, P., and Schwarzenbach, R.P.: Behavior of the insecticides disulfoton and thiometon in the Rhine River: a chemodynamic study, Environmental Science & Technology, 23, 1232–1242, https://doi.org/10.1021/es00068a007, 1989.

Warrick, J. A.: Trend analyses with river sediment rating curves. Hydrological Processes, 29, 936–949. https://doi.org/10.1002/ hyp.10198, 2015.

985 Wilson, A.B., Baker, J.M., Ainsworth, E.A., Andresen, J., Austin, J.A., Dukes, J.S., Gibbons, E., Hoppe, B.O., LeDee, O.E., Noel, J., Roop, H.A., Smith, S.A., Todey, D.P., Wolf, R., and Wood, J.D.: Ch. 24. Midwest. In: Fifth National Climate Assessment. Crimmins, A.R., C.W. Avery, D.R. Easterling, K.E. Kunkel, B.C. Stewart,

and T.K. Maycock, Eds. U.S. Global Change Research Program, Washington, DC, USA. https://doi.org/10.7930/NCA5.2023.CH24 , 2023.

990 Wright, M.N., and Ziegler, A.: ranger: A Fast Implementation of Random Forests for High Dimensional Data in C++ and R, Journal of Statistical Software, 77, https://doi.org/10.18637/jss.v077.i01, 2017.

Zeng, Q., Qin, L., Bao, L., Li, Y., and Li, X.: Critical nutrient thresholds needed to control eutrophication and synergistic interactions between phosphorus and different nitrogen sources, Environmental Science and Pollution Research, 23, 21008–21019, https://doi.org/10.1007/s11356-016-7321-x, 2016.

995
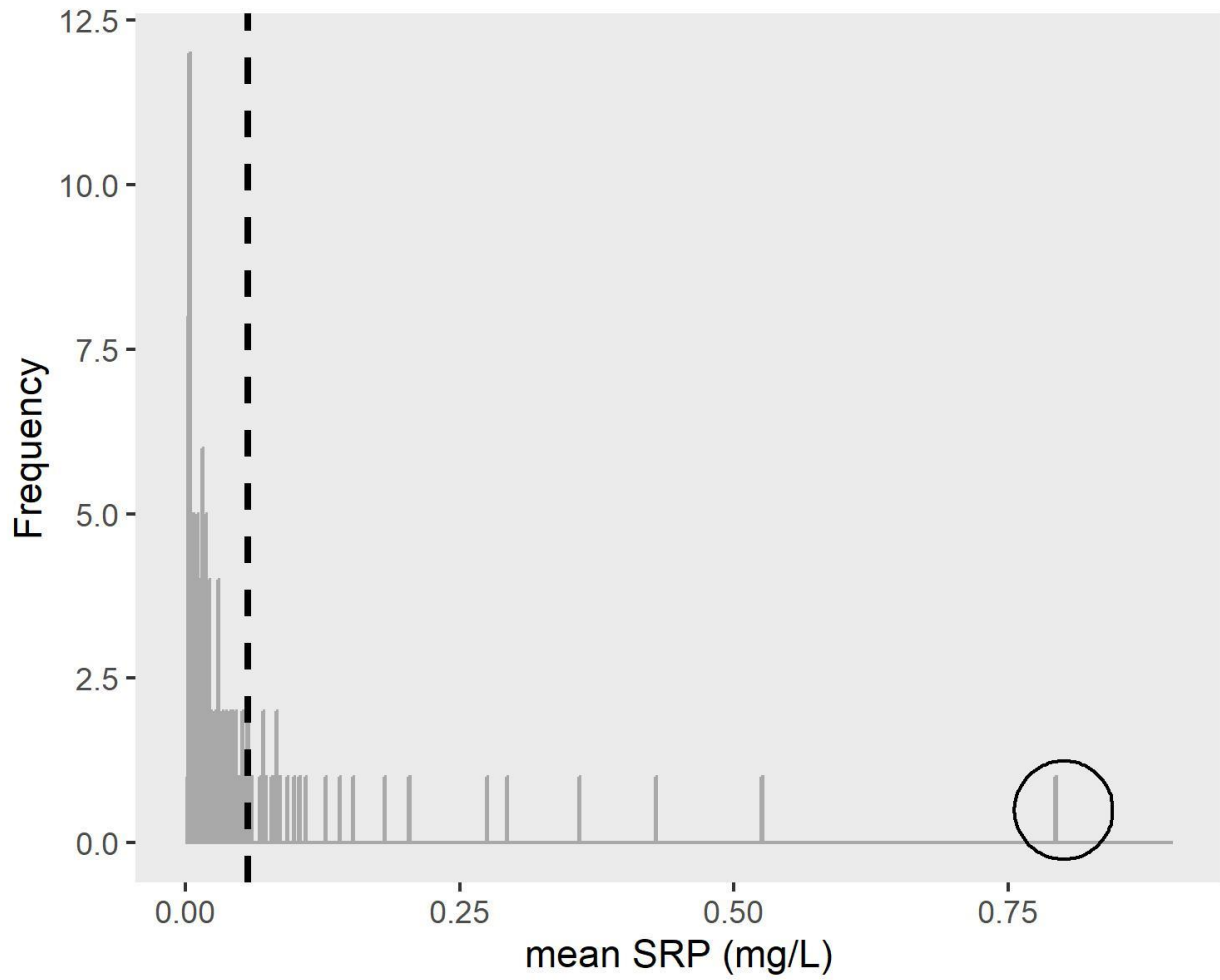
Figure A1. Distribution of mean SRP concentrations (mg/L) during late summer low flow conditions for 128 gaged watersheds with >=3 SRP samples collected during late summer low flows. Note that one outlier (circled value) was excluded prior to model development. The dashed line indicates the mean of all mean SRP values.

1000
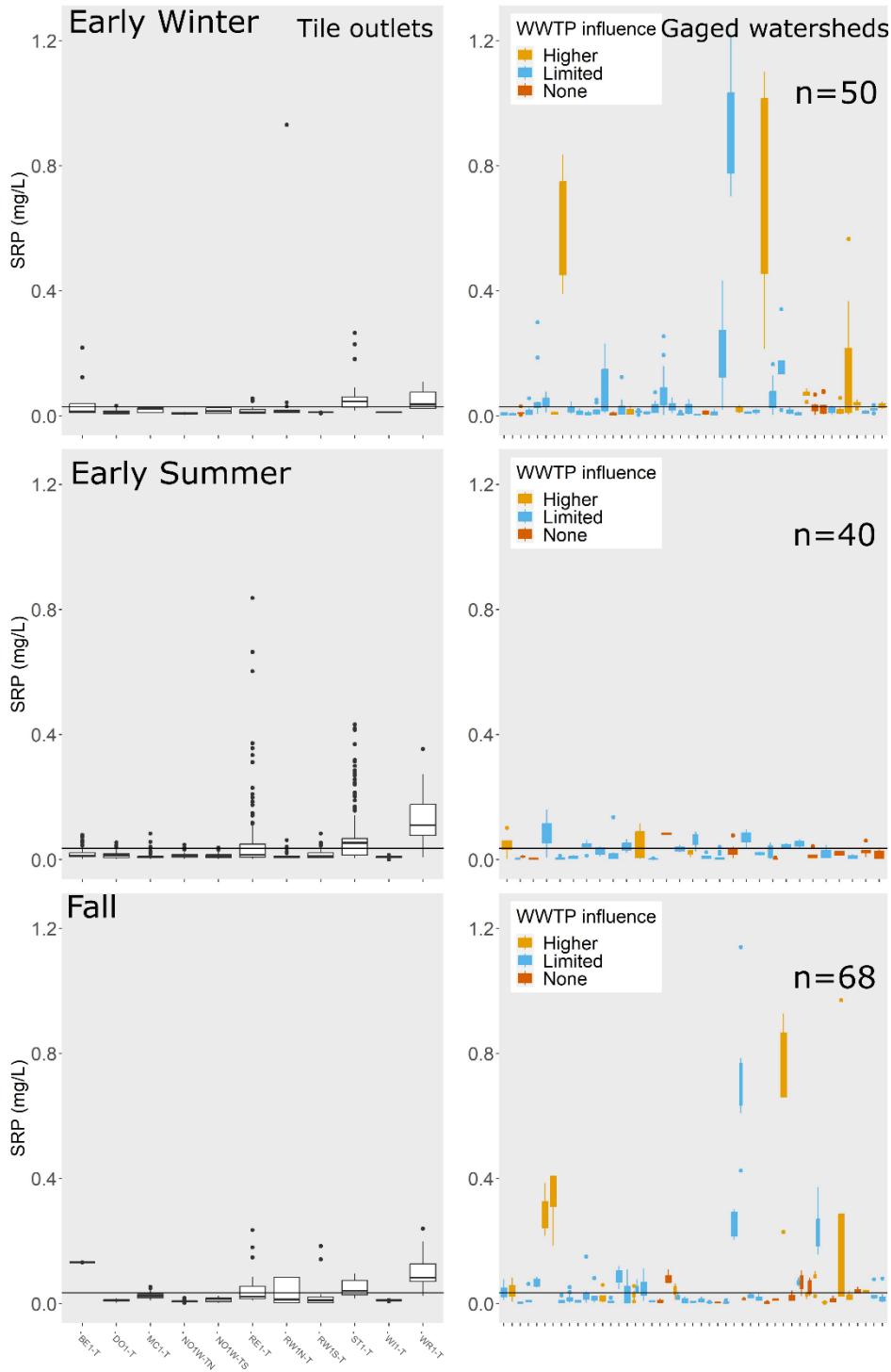
Figure A2. SRP concentrations (mg/L) for tile outlets and during low flow conditions for gaged watersheds, for early winter, early summer, and fall. See main text for similar plots for other seasons. The horizontal line in each plot is the mean SRP concentration among tile outlets for that season. The number of gages for which low flow data was available in each season is printed on the plot. For gaged watersheds, color of boxplots indicates degree of influence from wastewater treatment plants: light orange: wastewater treatment plant density >0.005 sites/km^2; blue = wastewater treatment plant density <0.005 sites/km^2 but greater than zero; dark orange: no wastewater treatment plant sites in watershed. To improve data visibility, the y-axis for SRP was limited to a maximum of 1.25 mg/L, which eliminated a small number of outliers from the plots for tile outlets (n=34 out of 11,079 records) and gaged watersheds (n=16 out of 2,696 low flow records).

1045
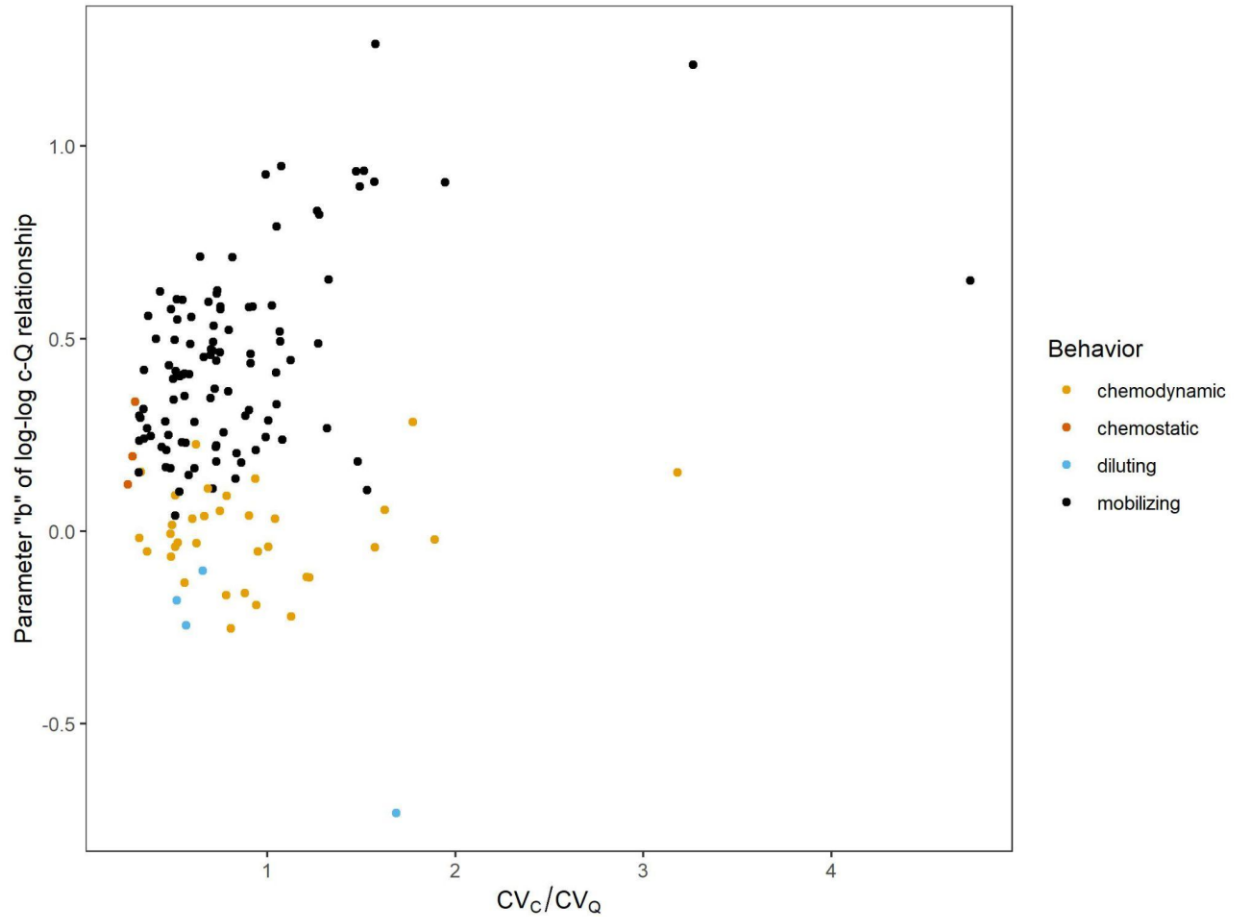
Figure A3. Parameter b (slope) of the event-scale log-log C-Q relationship for soluble reactive phosphorus (SRP, mg/L) in relation to CVC/CVQ for 143 gaged watersheds. Color indicates export behavior based on criteria defined for b and CVC/CVQ: Chemostatic: CVC/CVQ <= 0.3 (*sensu* Thompson et al., 2011); chemodynamic: CVC/CVQ > 0.3 and no significant b (p>0.05); diluting: significant b <0 ; mobilizing: significant b > 0.

1050
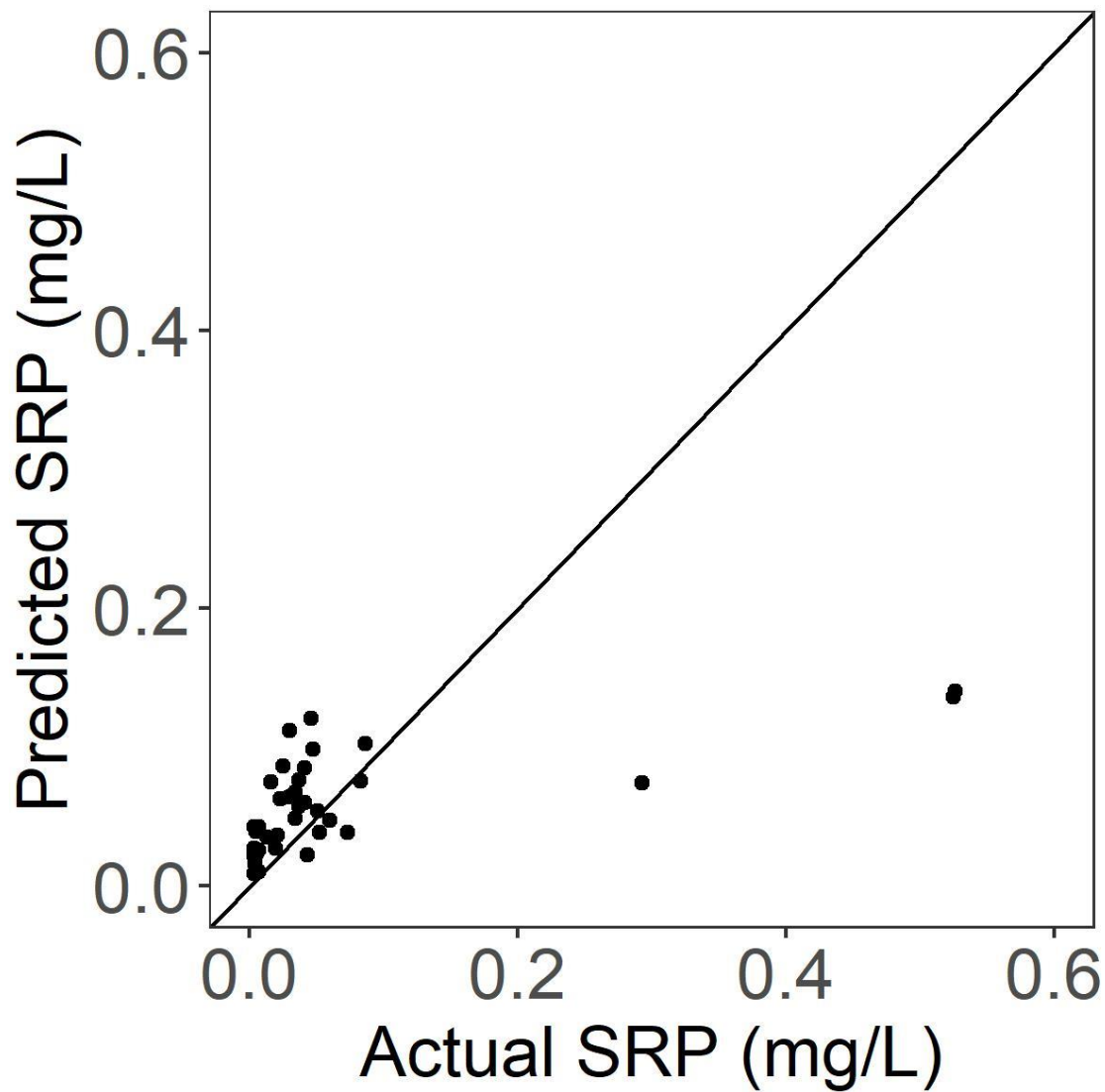
Figure A4. Actual vs predicted late summer SRP concentrations (mg/L) for gaged streams and rivers in the independent test dataset (i.e., not used to build the model). R^2=0.41, RMSE=0.010, p <0.0001. Solid line shows 1-1 relationship.

1055

Table A1. Linear regression statistics for mean SRP (log scale) during low flow conditions in relation to the density of wastewater treatment plants (sites/km^2) across gaged watersheds, by season. Linear regression were calculated with all sites, and recalculated where sites with density of wastewater treatment plants >0.005 sites/km^2 were excluded.

Season	Slope	T statistic	p	R2	n	WWTP influence
Early Winter	102.77	4.06	<0.001	0.26	50	all watersheds
Early Winter	87.12	1.61	0.12	0.06	40	gages with WWTP >0.005 sites/km2 excluded
Late Winter	90.57	3.62	<0.001	0.19	57	all watersheds
Late Winter	121.36	2.14	0.04	0.1	45	gages with WWTP >0.005 sites/km2 excluded
Spring	29.47	0.7	0.49	0.02	23	all watersheds
Spring	-55.71	-0.7	0.5	0.03	17	gages with WWTP >0.005 sites/km2 excluded
Early Summer	51.93	1.4	0.17	0.05	40	all watersheds
Early Summer	47.84	0.91	0.37	0.02	35	gages with WWTP >0.005 sites/km2 excluded
Late Summer	74.76	4.84	<0.001	0.16	128	all watersheds
Late Summer	80.66	2.44	0.02	0.06	102	gages with WWTP >0.005 sites/km2 excluded
Fall	76.03	4.07	<0.001	0.2	68	all watersheds
Fall	95.19	1.85	0.07	0.07	51	gages with WWTP >0.005 sites/km2 excluded

1065   **Table A2.** Linear regression statistics for mean SRP (log scale) during low flow conditions in relation to % crop cover across gaged watersheds, by season. Linear regression were calculated with all sites, and recalculated for sites with no wastewater treatment plant influence in their watersheds.

Season	Slope	T statistic	p	R2	n	WWTP influence
Early Winter	0.01	5.09	<0.001	0.35	50	all watersheds
Early Winter	0.01	4.25	0.02	0.86	5	no WWTP present in watershed
Late Winter	0.02	7.65	<0.001	0.52	57	all watersheds
Late Winter	0.01	2.5	0.04	0.44	10	no WWTP present in watershed
Spring	0.01	3.75	<0.001	0.4	23	all watersheds
Spring	0.01	2.27	0.06	0.43	9	no WWTP present in watershed
Early Summer	0.01	3.56	<0.001	0.25	40	all watersheds
Early Summer	0.01	3.32	0.01	0.55	11	no WWTP present in watershed
Late Summer	0.01	10.66	<0.001	0.47	128	all watersheds
Late Summer	0.01	7.39	<0.001	0.69	26	no WWTP present in watershed
Fall	0.01	5.63	<0.001	0.32	68	all watersheds
Fall	0.01	3.09	0.01	0.51	11	no WWTP present in watershed

Table A3. Mean SRP during low flow conditions (flow conditions <= lowest 25th percentile of flows on record) for each gaged watershed during each season. Note means were only calculated where gaged watersheds had >= three low flow samples collected during a season. 'NA' indicates < three low flow samples were collected during that season. 'WS Area' refers to the watershed land area draining into each gage in km^2. 'WWTP Density' is wastewater treatment plant density for each watershed in sites/km^2.

Site name	WS Area (km^2)	Human Impact	WWTP Density	Spring	Early Summer	Late Summer	Fall	Early Winter	Late Winter
Brule River nr Hovland, MN61	544.30	Less Impacted	0	NA	NA	NA	NA	NA	NA
Poplar River nr Lutsen, 0.2mi US of MN61	293.29	Less Impacted	0.003	NA	NA	0.003	0.003	0.004	0.003
Baptism River nr Beaver Bay, MN61	358.44	Less Impacted	0.003	NA	NA	0.004	NA	0.006	0.003
Beaver River nr Beaver Bay, 1.2mi us of MN61	318.73	Impacted	0.003	NA	NA	0.003	NA	NA	NA
Big Sucker Creek nr Palmers, CR258	93.48	Less Impacted	0	NA	0.003	0.003	NA	0.011	0.009
St. Louis River at Floodwood, CSAH8	4978.62	Impacted	0.004	0.002	NA	0.011	NA	NA	NA
St. Louis River nr Forbes, US53	1793.51	Impacted	0.006	0.003	NA	0.004	0.003	NA	NA
Second Creek nr Aurora, 0.6mi us of CSAH110	56.66	Impacted	0	NA	NA	0.004	0.002	NA	0.006
St. Louis River at Scanlon, MN	8893.21	Impacted	0.003	NA	0.009	0.004	NA	0.007	NA
Cloquet River nr Brimson, CSAH44	330.99	Less Impacted	0	NA	NA	0.004	NA	NA	NA
Cloquet River nr Burnett, CR694	2032.29	Less Impacted	0.001	0.005	0.005	0.003	NA	0.008	NA
Nemadji River nr Pleasant Valley, MN23	324.41	Impacted	0	NA	NA	0.005	NA	NA	NA
Mississippi River nr Bemidji, CSAH11	958.60	Impacted	0.001	NA	0.028	0.03	NA	NA	NA
Mississippi River nr Bemidji, MN	1627.93	Impacted	0.002	NA	0.003	0.003	NA	NA	NA
Leech Lake River nr Ball Club, CR139	3464.53	Impacted	0.001	0.004	0.003	0.004	NA	NA	NA
Boy River nr Boy River, CSAH53	750.13	Less Impacted	0.001	NA	NA	0.002	NA	NA	NA
Prairie River nr Taconite, MN	79.80	Impacted	0	0.006	NA	0.005	NA	NA	0.006

Mississippi River at Grand Rapids, MN	8483.32	Impacted	0.001	0.003	0.003	0.005	0.007	NA	0.003
Swan River nr Jacobson, CR438	758.11	Impacted	0.012	NA	NA	0.018	NA	NA	NA
Swan River nr Sobieski, MN238	462.60	Impacted	0.002	NA	NA	0.021	NA	NA	NA
Pine River nr Jenkins, CSAH15	743.11	Impacted	0	NA	NA	NA	NA	NA	NA
Leaf River nr Staples, CSAH29	2232.34	Impacted	0.003	NA	NA	0.022	NA	0.013	0.025
Long Prairie River at Philbrook, 313th Ave	2346.60	Impacted	0.005	NA	0.035	0.023	NA	0.024	0.022
Long Prairie River at Long Prairie, MN	1271.78	Impacted	0.005	0.014	NA	NA	NA	NA	0.016
Two Rivers nr Bowlus, 40th St	386.26	Impacted	0.008	NA	NA	NA	NA	NA	NA
Sauk River nr St. Martin, CR12	2887.54	Impacted	0.005	0.018	NA	0.059	NA	NA	NA
Clearwater River nr Clearwater, CR145	436.24	Impacted	0.002	0.008	NA	0.003	NA	NA	NA
Elk River nr Big Lake, MN	1373.83	Impacted	0.003	NA	0.027	NA	NA	NA	NA
St. Francis River nr Big Lake, 164th St	530.84	Impacted	0	NA	0.02	0.013	NA	NA	NA
Middle Fork Crow River nr Manannah, CSAH30	702.11	Impacted	0.006	0.01	0.022	0.012	NA	NA	NA
North Fork Crow River nr Cokato, CSAH4	2638.30	Impacted	0.004	NA	0.07	0.031	NA	NA	NA
North Fork Crow River nr Rockford, Farmington Ave	3444.89	Impacted	0.005	NA	NA	0.02	0.021	0.031	0.045
South Fork Crow River at Delano, Bridge Ave	3295.67	Impacted	0.004	NA	NA	0.182	0.239	0.168	0.218
Buffalo Creek nr Glencoe, CSAH1	969.28	Impacted	0.004	NA	NA	0.793	NA	NA	NA
West Branch Rum River nr Princeton, CR102	482.91	Impacted	0.006	NA	NA	NA	NA	NA	NA
Rum River at Anoka, headwater side of dam	4113.49	Impacted	0.004	NA	0.043	NA	NA	0.01	0.015

Minnesota River nr Lac qui Parle, MN	10546.93	Impacted	0.003	NA	NA	0.085	0.055	0.094	0.126
Yellow Bank River nr Odessa, CSAH40	1191.21	Impacted	0.004	NA	NA	0.03	NA	0.021	0.31
Pomme De Terre River at Appleton, MN	2227.38	Impacted	0.002	NA	NA	NA	NA	0.024	0.082
Pomme de Terre River nr Hoffman, CR76	1026.90	Impacted	0.002	NA	NA	0.013	0.01	NA	NA
Lac qui Parle River nr Lac qui Parle, CSAH31	2487.56	Impacted	0.004	NA	0.042	0.019	NA	0.028	0.063
Lac qui Parle River nr Providence, CSAH23	983.91	Impacted	0.004	NA	NA	0.023	NA	NA	NA
West Branch Lac qui Parle River at Dawson, Diagonal St	1220.43	Impacted	0.002	NA	NA	0.083	NA	NA	NA
Hawk Creek nr Maynard, MN23	1226.46	Impacted	0.003	NA	0.056	0.051	0.034	NA	NA
Hawk Creek nr Granite Falls, CR52	1321.42	Impacted	0.003	NA	0.003	0.01	0.013	0.083	0.158
Beaver Creek nr Beaver Falls, CSAH2	495.39	Impacted	0.004	NA	NA	0.053	0.041	NA	NA
Yellow Medicine River nr Granite Falls, MN	1716.39	Impacted	0.002	NA	NA	0.034	0.012	0.02	0.35
Yellow Medicine River nr Hanley Falls, CR18	1171.62	Impacted	0.001	NA	NA	0.019	0.027	NA	NA
Spring Creek nr Hanley Falls, 480th St	332.81	Impacted	0.006	NA	NA	0.293	NA	NA	NA
Chippewa River nr Clontarf, CSAH22	1731.39	Impacted	0.004	NA	NA	0.016	0.009	NA	NA
Shakopee Creek nr Benson, 20th Ave SW	786.32	Impacted	0	0.006	NA	0.141	NA	NA	0.024
Chippewa River nr Milan, MN40	4626.36	Impacted	0.002	NA	NA	0.022	0.009	0.02	0.027
East Branch Chippewa River nr Benson, CR78	1305.27	Impacted	0.001	NA	0.043	0.048	0.019	NA	NA

Redwood River nr Redwood Falls, MN	1619.96	Impacted	0.003	NA	NA	0.099	0.731	1.175	1.247
Redwood River at Russell, CR15	599.04	Impacted	0	NA	NA	0.035	0.015	NA	NA
Minnesota River at Morton, MN	23008.88	Impacted	0.003	NA	NA	0.046	0.058	0.098	0.141
Minnesota River at Judson, CSAH42	28865.06	Impacted	0.003	NA	0.01	0.027	0.028	0.04	0.08
Seven Mile Creek nr St. Peter, 0.6mi us of US169	94.16	Impacted	0	0.008	0.015	0.016	0.012	NA	0.027
Cottonwood River nr New Ulm, MN68	3374.02	Impacted	0.003	0.01	0.007	0.007	0.007	0.016	0.048
Sleepy Eye Creek nr Cobden, CR8	706.81	Impacted	0	NA	NA	0.022	0.021	NA	NA
Cottonwood River nr Leavenworth, CR8	2281.68	Impacted	0.004	NA	NA	0.013	NA	NA	NA
Blue Earth River nr Winnebago, CSAH12	3592.84	Impacted	0.004	NA	NA	0.027	0.025	NA	NA
East Branch Blue Earth River at Blue Earth, CSAH16	764.22	Impacted	0.003	NA	NA	0.071	0.062	NA	NA
Blue Earth River nr Rapidan, MN	6274.80	Impacted	0.004	NA	NA	0.015	0.006	0.015	0.028
South Fork Watonwan River nr Madelia, CSAH13	515.74	Impacted	0.004	NA	NA	0.052	NA	NA	NA
Watonwan River nr La Salle, CSAH3	875.15	Impacted	0.005	NA	NA	0.073	NA	NA	NA
Watonwan River nr Garden City, CSAH13	2205.66	Impacted	0.005	NA	NA	0.016	0.022	0.017	0.152
Maple River nr Sterling Center, CR18	801.21	Impacted	0.004	NA	NA	0.071	NA	NA	NA
Big Cobb River nr Beauford, CSAH16	787.09	Impacted	0.006	NA	0.048	0.041	0.042	NA	NA
Maple River nr Rapidan, CR35	877.79	Impacted	0.005	NA	NA	0.02	0.038	NA	NA

Little Beauford Ditch nr Beauford, MN22	22.03	Impacted	0	0.025	0.083	0.153	NA	NA	NA
Le Sueur River nr Rapidan, CR8	1156.71	Impacted	0.005	0.004	0.017	0.029	0.027	NA	NA
Le Sueur River nr Rapidan, MN	2873.06	Impacted	0.005	NA	0.006	0.014	0.012	0.014	0.032
Le Sueur River at St. Clair, CSAH28	919.12	Impacted	0.006	0.023	0.101	0.058	NA	NA	NA
High Island Creek nr Arlington, CR9	428.96	Impacted	0	0.037	NA	0.079	NA	NA	NA
High Island Creek nr Henderson, CSAH6	624.30	Impacted	0.002	NA	NA	0.019	NA	NA	NA
Snake River nr Pine City, MN	2563.68	Impacted	0.003	NA	0.02	0.012	NA	0.014	0.02
Sunrise River at Sunrise, CR88	870.50	Impacted	0.005	NA	NA	0.037	NA	NA	NA
Wells Creek nr Frontenac, US61	176.12	Impacted	0	0.032	NA	NA	0.04	NA	NA
Cannon River at Welch, MN	3477.94	Impacted	0.007	NA	NA	0.204	NA	0.009	0.044
Cannon River at Morristown, CSAH16	627.90	Impacted	0.008	0.121	NA	NA	0.29	NA	NA
Straight River nr Faribault, MN	1129.24	Impacted	0.006	NA	NA	NA	NA	0.069	NA
Whitewater River nr Beaver, CSAH30	689.62	Impacted	0.01	NA	NA	0.047	0.039	0.039	0.048
North Fork Whitewater River at Elba, Whitewater Dr	269.37	Impacted	0.011	NA	NA	NA	0.057	NA	0.049
North Fork Zumbro River nr Mazeppa, CSAH7	621.81	Impacted	0.006	NA	NA	0.057	0.026	NA	0.046
Zumbro River at Kellogg, US61	3677.89	Impacted	0.008	NA	NA	0.046	NA	0.033	0.042
South Fork Zumbro River nr Oronoco, CR121	885.55	Impacted	0.015	NA	NA	0.11	0.077	NA	NA
South Branch Middle Fork Zumbro River nr Oronoco,5th St	569.86	Impacted	0.011	NA	NA	0.057	0.025	NA	NA
Middle Fork Zumbro River nr Oronoco,5th St	534.52	Impacted	0.006	NA	NA	0.041	0.02	NA	NA
South Branch Root River at	738.36	Impacted	0.01	NA	NA	0.03	0.032	NA	NA

Lanesboro, Rochelle Ave N									
Middle Branch Root River nr Fillmore, CSAH5	506.94	Impacted	0.006	NA	NA	0.039	0.035	NA	NA
Cedar River nr Austin, MN	1030.86	Impacted	0.013	NA	NA	0.525	0.338	0.65	0.954
Turtle Creek at Austin, 43rd St	382.45	Impacted	0.008	NA	NA	0.359	0.268	NA	NA
Shell Rock River nr Gordonsville, CSAH1	496.65	Impacted	0.012	NA	NA	0.526	0.68	1.159	1.368
West Fork Des Moines River nr Avoca, CSAH6	1233.33	Impacted	0.006	NA	NA	0.014	NA	NA	NA
West Fork Des Moines River at Jackson, River St	3216.99	Impacted	0.007	NA	NA	0.037	NA	0.342	0.592
Bois de Sioux River nr Doran, MN	4713.44	Impacted	0.002	NA	0.084	0.086	NA	0.069	0.128
Mustinka River nr Norcross, MN9	486.58	Impacted	0	NA	NA	0.083	0.082	NA	NA
Twelvemile Creek nr Wheaton, CSAH14	1006.00	Impacted	0	0.141	NA	0.429	NA	NA	NA
Pelican River nr Fergus Falls, MN210	1294.46	Impacted	0.003	NA	0.02	0.019	0.006	NA	NA
Otter Tail River nr Elizabeth, MN	2974.42	Impacted	0.001	NA	NA	0.003	0.002	NA	0.005
Otter Tail River at Breckenridge, CSAH16	5116.19	Impacted	0.002	NA	NA	0.016	0.011	0.005	0.01
Red River of the North nr Kragnes, CSAH26	28555.84	Impacted	0.003	NA	NA	0.275	0.254	0.217	0.332
Buffalo River nr Georgetown, CR108	2820.97	Impacted	0.002	NA	NA	0.093	0.067	0.042	0.052
Buffalo River nr Glyndon, CSAH19	998.93	Impacted	0.004	NA	NA	0.068	NA	NA	NA
South Branch Buffalo River nr Glyndon, 28th Ave S	1314.84	Impacted	0.001	NA	NA	0.128	NA	NA	NA
Buffalo River nr Hawley, MN	837.03	Impacted	0.001	NA	NA	0.06	NA	NA	NA
Wild Rice River nr Mahnomen, CSAH25	1473.79	Impacted	0	NA	NA	0.019	NA	NA	NA

Wild Rice River at Twin Valley, MN	2405.45	Impacted	0.001	NA	NA	0.007	NA	NA	NA
Wild Rice River at Hendrum, MN	4091.49	Impacted	0.002	NA	NA	0.03	0.031	0.012	0.018
S Br. Wild Rice River at CR27 nr Felton, MN	499.54	Impacted	0.006	NA	NA	0.055	NA	NA	NA
Sandhill River nr Fertile, 450th St SW	620.95	Impacted	0.002	NA	0.052	0.029	0.018	NA	NA
Sand Hill River at Climax, MN, US-75	1209.33	Impacted	0.001	NA	NA	0.034	0.024	0.014	0.031
Red Lake River at High Landing nr Goodridge, MN	5963.65	Impacted	0	NA	0.003	0.011	NA	NA	NA
Red Lake River at Red Lake Falls, CR13	9413.51	Impacted	0	0.003	0.023	0.004	0.004	NA	NA
Red Lake River at Fisher, MN	14466.12	Impacted	0.001	NA	0.034	0.013	NA	0.009	0.017
Thief River nr Thief River Falls, MN	2515.45	Impacted	0	NA	0.027	0.011	0.012	0.026	0.05
Thief River downstream of CSAH 7, 6 mi E of Holt	1658.23	Impacted	0	0.002	0.013	0.007	NA	NA	0.036
Mud River nr Grygla, MN89	481.28	Impacted	0	NA	0.029	0.021	0.008	NA	NA
Clearwater River at Plummer, MN	1454.55	Impacted	0.002	NA	NA	0.043	0.027	NA	NA
Lost River nr Brooks, CR119	772.13	Impacted	0.003	NA	NA	0.042	0.085	NA	NA
Clearwater River at Red Lake Falls, MN	3474.65	Impacted	0.002	NA	NA	0.009	0.009	0.01	0.04
Snake River nr Big Woods, MN220	2006.98	Impacted	0.001	NA	NA	NA	0.068	0.074	0.191
Middle River at Argyle, MN	643.64	Impacted	0.002	NA	0.062	0.043	0.048	NA	NA
Snake River above Warren, MN	491.56	Impacted	0	NA	NA	NA	0.068	NA	NA
Tamarac River nr Florian, CSAH1	464.17	Impacted	0	NA	0.022	0.011	NA	NA	NA
Tamarac River nr Stephen, CSAH22	909.20	Impacted	0	NA	0.036	NA	NA	0.03	0.198
Two Rivers nr Hallock, CSAH16	2660.25	Impacted	0	NA	NA	0.016	NA	0.018	0.03

South Branch Two Rivers at Hallock, MN175	1669.83	Impacted	0.001	NA	NA	0.052	NA	NA	NA
South Branch Two Rivers at Lake Bronson, MN	1380.24	Impacted	0	NA	NA	0.104	0.053	NA	NA
Kawishiwi River nr Winton, CSAH18	3415.83	Less Impacted	0	0.004	NA	0.004	NA	0.007	0.007
Stony River nr Babbitt, Tomahawk Rd	550.10	Less Impacted	0	NA	NA	0.003	NA	NA	NA
Little Fork River nr Linden Grove, TH73	736.54	Impacted	0.003	NA	NA	0.02	0.018	NA	NA
Little Fork River at Little Fork, MN	4382.42	Less Impacted	0	NA	NA	0.004	0.004	0.009	0.015
Little Fork River nr Littlefork, MN65	3492.09	Less Impacted	0.001	NA	NA	0.007	0.005	NA	NA
Big Fork River nr Bigfork, MN6	1567.06	Less Impacted	0	NA	0.01	0.007	NA	NA	NA
Big Fork River at Big Falls, MN	3888.36	Less Impacted	0.001	NA	0.003	0.004	0.003	0.005	0.011
Big Fork River nr Craigville, MN6	2555.10	Less Impacted	0.001	NA	NA	0.004	NA	NA	NA
East Fork Rapid River nr Clementson, CSAH18	709.40	Less Impacted	0	NA	NA	0.022	NA	NA	NA
Rapid River at Clementson, MN11	2486.55	Impacted	0	NA	NA	0.004	0.003	0.01	0.014
Split Rock Creek nr Jasper, 201st St	822.62	Impacted	0.004	NA	NA	0.011	NA	0.014	0.027
Pipestone Creek nr Pipestone, CSAH13	308.55	Impacted	0.006	NA	NA	0.025	NA	NA	NA
Rock River at Luverne, CR4	1084.55	Impacted	0.005	NA	NA	0.016	NA	0.02	0.025

Table A4. Number of SRP samples collected during low flow conditions in each season for each gaged watershed. Note that mean SRP values (Table S3) were only calculated in seasons where >=3 samples had been collected during low flow conditions for that gaged watershed.

Site name	Early Winter	Late Winter	Spring	Early Summer	Late Summer	Fall
Baptism River nr Beaver Bay, MN61	4	5	NA	2	9	NA
Beaver Creek nr Beaver Falls, CSAH2	NA	1	1	1	6	5
Beaver River nr Beaver Bay, 1.2mi us of MN61	NA	NA	NA	2	4	1
Big Cobb River nr Beauford, CSAH16	NA	2	2	4	18	4
Big Fork River at Big Falls, MN	6	10	1	4	14	3
Big Fork River nr Bigfork, MN6	NA	NA	NA	4	14	NA
Big Fork River nr Craigville, MN6	NA	NA	NA	2	10	1
Big Sucker Creek nr Palmers, CR258	6	4	NA	3	4	NA
Blue Earth River nr Rapidan, MN	11	7	2	2	19	3
Blue Earth River nr Winnebago, CSAH12	NA	1	NA	NA	8	3
Bois de Sioux River nr Doran, MN	10	5	2	6	12	2
Boy River nr Boy River, CSAH53	NA	NA	1	2	5	2
Brule River nr Hovland, MN61	NA	NA	NA	NA	1	2
Buffalo Creek nr Glencoe, CSAH1	NA	1	2	1	3	1
Buffalo River nr Georgetown, CR108	8	7	NA	NA	11	4
Buffalo River nr Glyndon, CSAH19	NA	NA	NA	NA	3	2
Buffalo River nr Hawley, MN	NA	2	1	NA	4	2
Cannon River at Morristown, CSAH16	NA	1	3	NA	2	3
Cannon River at Welch, MN	8	5	1	NA	6	1
Cedar River nr Austin, MN	10	4	NA	1	9	4
Chippewa River nr Clontarf, CSAH22	NA	2	1	2	5	4
Chippewa River nr Milan, MN40	11	8	NA	NA	9	4
Clearwater River at Plummer, MN	NA	NA	2	NA	5	6

Clearwater River at Red Lake Falls, MN	14	9	2	1	16	9
Clearwater River nr Clearwater, CR145	NA	2	3	1	3	1
Cloquet River nr Brimson, CSAH44	NA	NA	1	1	7	NA
Cloquet River nr Burnett, CR694	3	2	4	4	13	2
Cottonwood River nr Leavenworth, CR8	NA	NA	2	1	6	2
Cottonwood River nr New Ulm, MN68	14	8	3	3	14	6
East Branch Blue Earth River at Blue Earth, CSAH16	NA	1	NA	1	8	3
East Branch Chippewa River nr Benson, CR78	NA	NA	NA	6	6	3
East Fork Rapid River nr Clementson, CSAH18	NA	NA	1	2	8	NA
Elk River nr Big Lake, MN	NA	1	2	5	2	1
Hawk Creek nr Granite Falls, CR52	13	7	1	3	12	5
Hawk Creek nr Maynard, MN23	NA	1	2	3	5	4
High Island Creek nr Arlington, CR9	NA	1	4	1	5	1
High Island Creek nr Henderson, CSAH6	NA	1	2	1	8	1
Kawishiwi River nr Winton, CSAH18	3	6	3	1	5	1
Lac qui Parle River nr Lac qui Parle, CSAH31	9	4	2	3	5	2
Lac qui Parle River nr Providence, CSAH23	NA	NA	NA	NA	3	2
Le Sueur River at St. Clair, CSAH28	NA	1	3	4	14	2
Le Sueur River nr Rapidan, CR8	NA	2	3	6	17	4
Le Sueur River nr Rapidan, MN	16	7	1	3	19	4
Leaf River nr Staples, CSAH29	7	9	NA	1	7	NA
Leech Lake River nr Ball Club, CR139	1	2	3	5	8	1

Little Beauford Ditch nr Beauford, MN22	NA	NA	8	3	14	2
Little Fork River at Little Fork, MN	7	9	NA	1	11	4
Little Fork River nr Linden Grove, TH73	NA	NA	NA	NA	4	3
Little Fork River nr Littlefork, MN65	NA	NA	NA	1	8	6
Long Prairie River at Long Prairie, MN	NA	3	4	1	1	2
Long Prairie River at Philbrook, 313th Ave	14	11	1	3	5	2
Lost River nr Brooks, CR119	NA	NA	NA	NA	12	3
Maple River nr Rapidan, CR35	NA	NA	NA	2	11	3
Maple River nr Sterling Center, CR18	NA	1	NA	2	15	2
Middle Branch Root River nr Fillmore, CSAH5	NA	NA	NA	NA	8	5
Middle Fork Crow River nr Manannah, CSAH30	NA	1	3	3	3	2
Middle Fork Zumbro River nr Oronoco,5th St	NA	1	NA	NA	8	5
Middle River at Argyle, MN	NA	NA	NA	3	3	4
Minnesota River at Judson, CSAH42	12	6	NA	4	14	5
Minnesota River at Morton, MN	12	5	NA	1	7	8
Minnesota River nr Lac qui Parle, MN	5	5	NA	2	3	4
Mississippi River at Grand Rapids, MN	2	5	8	8	13	4
Mississippi River nr Bemidji, CSAH11	NA	NA	NA	3	3	1
Mississippi River nr Bemidji, MN	NA	NA	1	3	4	1
Mud River nr Grygla, MN89	NA	NA	NA	8	15	3
Mustinka River nr Norcross, MN9	NA	NA	2	1	6	3
Nemadji River nr Pleasant Valley, MN23	NA	NA	NA	1	6	1

North Fork Crow River nr Cokato, CSAH4	NA	1	2	3	3	1
North Fork Crow River nr Rockford, Farmington Ave	5	7	NA	2	4	3
North Fork Whitewater River at Elba, Whitewater Dr	NA	3	2	1	2	3
North Fork Zumbro River nr Mazeppa, CSAH7	NA	3	2	NA	4	4
Otter Tail River at Breckenridge, CSAH16	10	7	NA	1	11	8
Otter Tail River nr Elizabeth, MN	NA	7	1	1	7	3
Pelican River nr Fergus Falls, MN210	NA	NA	2	4	5	3
Pine River nr Jenkins, CSAH15	NA	NA	NA	1	2	NA
Pipestone Creek nr Pipestone, CSAH13	NA	1	1	1	7	NA
Pomme De Terre River at Appleton, MN	9	7	NA	1	2	2
Pomme de Terre River nr Hoffman, CR76	NA	NA	NA	2	7	3
Poplar River nr Lutsen, 0.2mi US of MN61	3	7	1	1	7	4
Prairie River nr Taconite, MN	NA	3	3	NA	6	2
Rapid River at Clementson, MN11	8	11	1	2	13	3
Red Lake River at Fisher, MN	13	8	NA	4	17	2
Red Lake River at High Landing nr Goodridge, MN	NA	NA	2	4	6	2
Red Lake River at Red Lake Falls, CR13	NA	NA	3	4	8	5
Red River of the North nr Kragnes, CSAH26	14	8	NA	NA	7	4
Redwood River at Russell, CR15	NA	1	2	NA	7	4
Redwood River nr Redwood Falls, MN	12	7	2	1	11	6
Rock River at Luverne, CR4	7	6	1	1	4	2

Rum River at Anoka,headwater side of dam	10	14	1	6	1	NA
S Br. Wild Rice River at CR27 nr Felton, MN	NA	NA	NA	NA	4	1
Sand Hill River at Climax, MN, US-75	10	11	2	1	9	3
Sandhill River nr Fertile, 450th St SW	NA	NA	NA	3	10	4
Sauk River nr St. Martin, CR12	NA	NA	3	2	4	1
Second Creek nr Aurora, 0.6mi us of CSAH110	NA	3	2	1	9	4
Seven Mile Creek nr St. Peter, 0.6mi us of US169	NA	3	9	8	22	5
Shakopee Creek nr Benson, 20th Ave SW	NA	3	4	2	5	2
Shell Rock River nr Gordonsville, CSAH1	9	6	NA	NA	3	5
Sleepy Eye Creek nr Cobden, CR8	NA	NA	1	NA	8	3
Snake River above Warren, MN	NA	NA	2	1	1	3
Snake River nr Big Woods, MN220	13	3	NA	1	2	3
Snake River nr Pine City, MN	4	8	NA	5	7	NA
South Branch Buffalo River nr Glyndon, 28th Ave S	NA	NA	NA	1	7	2
South Branch Middle Fork Zumbro River nr Oronoco,5th St	NA	1	NA	NA	3	5
South Branch Root River at Lanesboro, Rochelle Ave N	NA	2	NA	1	7	4
South Branch Two Rivers at Hallock, MN175	NA	1	NA	1	4	2
South Branch Two Rivers at Lake Bronson, MN	NA	1	NA	2	3	4
South Fork Crow River at Delano, Bridge Ave	5	7	1	NA	6	4
South Fork Watonwan River nr Madelia, CSAH13	NA	1	NA	NA	6	1
South Fork Zumbro River nr Oronoco, CR121	NA	1	NA	NA	6	5

Split Rock Creek nr Jasper, 201st St	6	7	NA	NA	6	2
Spring Creek nr Hanley Falls, 480th St	NA	1	2	1	7	2
St. Francis River nr Big Lake, 164th St	NA	1	NA	6	5	1
St. Louis River at Floodwood, CSAH8	NA	NA	3	2	5	1
St. Louis River at Scanlon, MN	3	1	1	4	11	2
St. Louis River nr Forbes, US53	NA	NA	3	1	9	5
Stony River nr Babbitt, Tomahawk Rd	NA	1	2	1	6	1
Straight River nr Faribault, MN	5	2	NA	NA	2	NA
Sunrise River at Sunrise, CR88	2	2	NA	NA	4	NA
Swan River nr Jacobson, CR438	NA	NA	2	2	4	1
Swan River nr Sobieski, MN238	NA	NA	NA	NA	3	2
Tamarac River nr Florian, CSAH1	NA	NA	1	4	10	2
Tamarac River nr Stephen, CSAH22	11	6	NA	3	2	NA
Thief River downstream of CSAH 7, 6 mi E of Holt	NA	3	4	5	6	1
Thief River nr Thief River Falls, MN	12	12	1	3	11	3
Turtle Creek at Austin, 43rd St	NA	NA	NA	1	9	4
Twelvemile Creek nr Wheaton, CSAH14	NA	2	3	1	5	1
Two Rivers nr Bowlus, 40th St	NA	NA	NA	2	NA	NA
Two Rivers nr Hallock, CSAH16	11	9	NA	2	9	2
Watonwan River nr Garden City, CSAH13	11	8	1	1	15	3
Watonwan River nr La Salle, CSAH3	NA	1	1	NA	6	2
Wells Creek nr Frontenac, US61	NA	NA	4	1	2	3
West Branch Lac qui Parle River at Dawson, Diagonal St	NA	NA	NA	NA	4	2
West Branch Rum River nr Princeton, CR102	NA	NA	NA	NA	NA	1
West Fork Des Moines River at Jackson, River St	8	8	1	NA	5	2

West Fork Des Moines River nr Avoca, CSAH6	NA	NA	1	1	5	1
Whitewater River nr Beaver, CSAH30	7	5	2	1	5	3
Wild Rice River at Hendrum, MN	8	11	2	1	14	5
Wild Rice River at Twin Valley, MN	NA	1	NA	NA	4	1
Wild Rice River nr Mahnomen, CSAH25	NA	NA	NA	NA	5	NA
Yellow Bank River nr Odessa, CSAH40	6	5	NA	NA	4	2
Yellow Medicine River nr Granite Falls, MN	7	5	2	NA	8	7
Yellow Medicine River nr Hanley Falls, CR18	NA	1	2	NA	7	5
Zumbro River at Kellogg, US61	7	6	NA	NA	9	2
Total number of sites with >=3 samples collected during low flows	**50**	**57**	**23**	**40**	**128**	**68**

Table A5. Linear regression statistics for the log-log relationship between SRP concentrations (mg/L) and normalized flow (Q/Q_{GM}). The regressions were run twice. The first regressions (denoted with (1) in the table) included all samples collected for a given site. The second set of regressions (denoted with (2) in the table) excluded samples collected during late summer low flows. '% change in slope' indicates the change in slope between the first and second regression for each site. CV_C/CV_Q is reported using all samples collected for each site. Statistics in bold indicate statistically significant ($p < 0.05$) relationships.

Site name	Behavior	CV_C/CV_Q	Slope(1)	p(1)	R^2(1)	n(1)	Slope(2)	p(2)	R^2(2)	n(2)	% slope change
Baptism River nr Beaver Bay, MN61	chemodynamic	0.66	0.04	0.21	0.01	184	0.05	0.14	0.01	175	30.8
Beaver Creek nr Beaver Falls, CSAH2	mobilizing	0.34	**0.42**	**<0.01**	**0.36**	**113**	**0.45**	**<0.01**	**0.37**	**107**	7.7
Beaver River nr Beaver Bay, 1.2mi us of MN61	chemodynamic	0.51	0.09	0.20	0.04	48	0.07	0.42	0.02	44	-24.03
Big Cobb River nr Beauford, CSAH16	mobilizing	0.56	**0.35**	**<0.01**	**0.20**	**243**	**0.47**	**<0.01**	**0.20**	**225**	32.66
Big Fork River at Big Falls, MN	mobilizing	0.61	**0.16**	**<0.01**	**0.06**	**264**	**0.12**	**0.01**	**0.03**	**250**	-26.35

Big Fork River nr Bigfork, MN6	chemodynamic	1.01	-0.04	0.62	0.00	116	-0.01	0.91	0.00	102	-70.13
Big Fork River nr Craigville, MN6	mobilizing	0.73	**0.22**	**<0.01**	**0.07**	**112**	0.15	0.10	0.03	102	-32.38
Big Sucker Creek nr Palmers, CR258	chemodynamic	0.6	0.03	0.40	0.00	162	0.01	0.71	0.00	158	-54.47
Blue Earth River nr Rapidan, MN	mobilizing	0.74	**0.62**	**<0.01**	**0.45**	**437**	**0.64**	**<0.01**	**0.41**	**418**	1.69
Blue Earth River nr Winnebago, CSAH12	mobilizing	0.71	**0.47**	**<0.01**	**0.27**	**139**	**0.50**	**<0.01**	**0.22**	**131**	6.3
Bois de Sioux River nr Doran, MN	mobilizing	0.32	**0.23**	**<0.01**	**0.26**	**426**	**0.24**	**<0.01**	**0.25**	**414**	2.88
Boy River nr Boy River, CSAH53	chemodynamic	1.77	0.28	0.09	0.06	49	0.29	0.14	0.05	44	0.7
Brule River nr Hovland, MN61	chemodynamic	0.94	0.14	0.17	0.10	21	0.14	0.20	0.09	20	2.09
Buffalo Creek nr Glencoe, CSAH1	chemodynamic	0.95	-0.05	0.56	0.00	71	0.09	0.39	0.01	68	-260.73
Buffalo River nr Georgetown, CR108	mobilizing	0.32	**0.30**	**<0.01**	**0.25**	**438**	**0.32**	**<0.01**	**0.26**	**427**	7.98
Buffalo River nr Glyndon, CSAH19	mobilizing	0.50	**0.40**	**<0.01**	**0.28**	**73**	**0.46**	**<0.01**	**0.32**	**70**	15.25
Buffalo River nr Hawley, MN	mobilizing	0.53	**0.40**	**<0.01**	**0.27**	**97**	**0.43**	**<0.01**	**0.28**	**93**	6.76
Cannon River at Morristown, CSAH16	chemodynamic	0.81	-0.25	0.07	0.06	58	-0.20	0.18	0.03	56	-20.19
Cannon River at Welch, MN	mobilizing	1.07	**0.49**	**<0.01**	**0.09**	**119**	**0.68**	**<0.01**	**0.17**	**113**	37.33
Cedar River nr Austin, MN	diluting	0.57	**-0.25**	**<0.01**	**0.19**	**265**	**-0.22**	**<0.01**	**0.14**	**256**	-12.34
Chippewa River nr Clontarf, CSAH22	mobilizing	1.51	**0.94**	**<0.01**	**0.28**	**123**	**1.03**	**<0.01**	**0.29**	**118**	10.1
Chippewa River nr Milan, MN40	mobilizing	1.33	**0.65**	**<0.01**	**0.29**	**304**	**0.68**	**<0.01**	**0.28**	**295**	4.66
Clearwater River at Plummer, MN	mobilizing	0.73	**0.44**	**<0.01**	**0.15**	**99**	**0.55**	**<0.01**	**0.19**	**94**	24.76

Clearwater River at Red Lake Falls, MN	mobilizing	0.55	**0.41**	**<0.01**	**0.18**	396	**0.37**	**<0.01**	**0.14**	380	-10.15
Clearwater River nr Clearwater, CR145	chemodynamic	1.22	-0.12	0.44	0.01	59	-0.28	0.10	0.05	56	137.88
Cloquet River nr Brimson, CSAH44	chemodynamic	0.62	-0.03	0.75	0.00	80	-0.13	0.29	0.02	73	325.35
Cloquet River nr Burnett, CR694	chemodynamic	1.04	0.03	0.59	0.00	142	-0.02	0.77	0.00	129	-165.87
Cottonwood River nr Leavenworth, CR8	mobilizing	0.91	**0.46**	**<0.01**	**0.35**	136	**0.47**	**<0.01**	**0.27**	130	1.75
Cottonwood River nr New Ulm, MN68	mobilizing	0.73	**0.62**	**<0.01**	**0.49**	389	**0.60**	**<0.01**	**0.44**	375	-3.08
East Branch Blue Earth River at Blue Earth, CSAH16	mobilizing	0.84	**0.20**	**<0.01**	**0.06**	140	**0.29**	**<0.01**	**0.08**	132	41.42
East Branch Chippewa River nr Benson, CR78	mobilizing	0.91	**0.44**	**<0.01**	**0.13**	119	**0.69**	**<0.01**	**0.24**	113	57.36
East Fork Rapid River nr Clementson, CSAH18	diluting	0.52	**-0.18**	**<0.01**	**0.18**	93	**-0.14**	**0.01**	**0.07**	85	-24.78
Elk River nr Big Lake, MN	mobilizing	1.12	**0.44**	**0.02**	**0.09**	63	**0.50**	**0.01**	**0.11**	61	11.55
Hawk Creek nr Granite Falls, CR52	mobilizing	0.51	**0.50**	**<0.01**	**0.37**	375	**0.44**	**<0.01**	**0.31**	363	-11.18
Hawk Creek nr Maynard, MN23	chemostatic	0.3	**0.34**	**<0.01**	**0.30**	120	**0.34**	**<0.01**	**0.29**	115	2.35
High Island Creek nr Arlington, CR9	chemodynamic	0.78	0.09	0.12	0.02	100	0.14	0.07	0.03	95	54.04
High Island Creek nr Henderson, CSAH6	mobilizing	0.79	**0.36**	**<0.01**	**0.20**	96	**0.33**	**<0.01**	**0.11**	88	-10.11
Kawishiwi River nr Winton, CSAH18	chemodynamic	1.21	-0.12	0.08	0.02	143	**-0.16**	**0.02**	**0.04**	138	34.45
Lac qui Parle River nr Lac qui Parle, CSAH31	mobilizing	0.71	**0.49**	**<0.01**	**0.33**	186	**0.49**	**<0.01**	**0.31**	181	0.31
Lac qui Parle River nr Providence, CSAH23	mobilizing	0.49	**0.58**	**<0.01**	**0.40**	72	**0.70**	**<0.01**	**0.44**	69	20.68
Le Sueur River at St. Clair, CSAH28	mobilizing	0.34	**0.32**	**<0.01**	**0.21**	179	**0.38**	**<0.01**	**0.20**	165	21.25

Le Sueur River nr Rapidan, CR8	mobilizing	0.43	**0.62**	**<0.01**	**0.50**	269	**0.67**	**<0.01**	**0.45**	252	7.11
Le Sueur River nr Rapidan, MN	mobilizing	0.59	**0.56**	**<0.01**	**0.46**	478	**0.55**	**<0.01**	**0.42**	459	-0.76
Leaf River nr Staples, CSAH29	mobilizing	0.54	**0.23**	**<0.01**	**0.15**	181	**0.23**	**<0.01**	**0.14**	174	-0.59
Leech Lake River nr Ball Club, CR139	chemodynamic	1.63	0.05	0.68	0.00	77	0.05	0.76	0.00	69	-13.76
Little Beauford Ditch nr Beauford, MN22	mobilizing	0.36	**0.27**	**<0.01**	**0.18**	198	**0.42**	**<0.01**	**0.32**	184	57.82
Little Fork River at Little Fork, MN	chemodynamic	0.49	0.02	0.62	0.00	251	-0.04	0.27	0.01	240	-336.91
Little Fork River nr Linden Grove, TH73	chemodynamic	0.36	-0.05	0.35	0.02	50	-0.02	0.79	0.00	46	-65.46
Little Fork River nr Littlefork, MN65	chemodynamic	0.49	-0.01	0.88	0.00	113	-0.05	0.36	0.01	105	598.71
Long Prairie River at Long Prairie, MN	mobilizing	1.05	**0.41**	**<0.01**	**0.14**	60	**0.44**	**<0.01**	**0.16**	59	7.12
Long Prairie River at Philbrook, 313th Ave	mobilizing	0.71	**0.11**	**0.02**	**0.02**	279	**0.10**	**0.04**	**0.02**	274	-5.65
Lost River nr Brooks, CR119	chemodynamic	0.68	0.11	0.24	0.02	79	**0.42**	**<0.01**	**0.15**	67	273.75
Maple River nr Rapidan, CR35	mobilizing	0.37	**0.56**	**<0.01**	**0.50**	216	**0.62**	**<0.01**	**0.49**	205	11.2
Maple River nr Sterling Center, CR18	mobilizing	0.34	**0.24**	**<0.01**	**0.22**	269	**0.33**	**<0.01**	**0.26**	254	36.51
Middle Branch Root River nr Fillmore, CSAH5	mobilizing	0.72	**0.53**	**<0.01**	**0.32**	121	**0.60**	**<0.01**	**0.33**	113	12.67
Middle Fork Crow River nr Manannah, CSAH30	mobilizing	1.57	**0.91**	**<0.01**	**0.28**	70	**0.83**	**<0.01**	**0.25**	67	-8.82
Middle Fork Zumbro River nr Oronoco,5th St	mobilizing	0.75	**0.58**	**<0.01**	**0.50**	127	**0.62**	**<0.01**	**0.51**	119	6.60
Middle River at Argyle, MN	mobilizing	0.49	**0.16**	**<0.01**	**0.11**	99	**0.17**	**<0.01**	**0.10**	96	3.79
Minnesota River at Judson, CSAH42	mobilizing	0.79	**0.52**	**<0.01**	**0.21**	433	**0.53**	**<0.01**	**0.19**	419	1.36

Minnesota River at Morton, MN	mobilizing	0.77	**0.26**	**<0.01**	**0.06**	**299**	**0.28**	**<0.01**	**0.07**	**292**	9.18
Minnesota River nr Lac qui Parle, MN	mobilizing	0.9	**0.31**	**0.01**	**0.05**	**165**	**0.35**	**<0.01**	**0.06**	**162**	12.09
Mississippi River at Grand Rapids, MN	mobilizing	1.32	**0.27**	**<0.01**	**0.06**	**184**	**0.42**	**<0.01**	**0.11**	**171**	56.08
Mississippi River nr Bemidji, CSAH11	chemodynamic	1.13	-0.22	0.18	0.04	44	-0.19	0.32	0.03	41	-16.08
Mississippi River nr Bemidji, MN	chemodynamic	1.89	-0.02	0.92	0.00	42	-0.12	0.66	0.01	38	449.62
Mud River nr Grygla, MN89	mobilizing	1.01	**0.29**	**<0.01**	**0.17**	**157**	**0.40**	**<0.01**	**0.23**	**142**	40.11
Mustinka River nr Norcross, MN9	mobilizing	0.58	**0.41**	**<0.01**	**0.20**	**91**	**0.62**	**<0.01**	**0.30**	**85**	51.09
Nemadji River nr Pleasant Valley, MN23	mobilizing	0.88	**0.30**	**<0.01**	**0.31**	**68**	**0.28**	**<0.01**	**0.26**	**62**	-7.72
North Fork Crow River nr Cokato, CSAH4	mobilizing	1.49	**0.90**	**<0.01**	**0.19**	**74**	**1.02**	**<0.01**	**0.21**	**71**	14.2
North Fork Crow River nr Rockford, Farmington Ave	mobilizing	1.05	**0.33**	**<0.01**	**0.07**	**206**	**0.32**	**<0.01**	**0.06**	**202**	-4.36
North Fork Whitewater River at Elba, Whitewater Dr	mobilizing	0.99	**0.93**	**<0.01**	**0.68**	**82**	**0.94**	**<0.01**	**0.68**	**80**	1.08
North Fork Zumbro River nr Mazeppa, CSAH7	mobilizing	0.90	**0.58**	**<0.01**	**0.40**	**99**	**0.60**	**<0.01**	**0.39**	**95**	2.88
Otter Tail River at Breckenridge, CSAH16	mobilizing	3.26	**1.21**	**<0.01**	**0.22**	**231**	**1.35**	**<0.01**	**0.24**	**220**	11.46
Otter Tail River nr Elizabeth, MN	chemodynamic	3.18	0.15	0.32	0.01	70	0.21	0.23	0.02	63	41.57
Pelican River nr Fergus Falls, MN210	mobilizing	1.27	**0.49**	**0.01**	**0.09**	**77**	**0.60**	**<0.01**	**0.11**	**72**	23.70
Pine River nr Jenkins, CSAH15	chemodynamic	0.62	0.23	0.21	0.08	22	0.36	0.10	0.15	20	60.81
Pipestone Creek nr Pipestone, CSAH13	mobilizing	0.55	**0.60**	**<0.01**	**0.55**	**73**	**0.71**	**<0.01**	**0.56**	**66**	18.10

Pomme De Terre River at Appleton, MN	mobilizing	1.07	**0.95**	**<0.01**	**0.33**	**166**	**0.94**	**<0.01**	**0.33**	**164**	-0.47
Pomme de Terre River nr Hoffman, CR76	mobilizing	1.94	**0.91**	**<0.01**	**0.25**	**110**	**1.25**	**<0.01**	**0.32**	**103**	38.26
Poplar River nr Lutsen, 0.2mi US of MN61	chemodynamic	0.75	0.05	0.20	0.01	167	0.04	0.42	0.00	160	-29.4
Prairie River nr Taconite, MN	chemodynamic	0.56	-0.13	0.08	0.05	59	**-0.18**	**0.05**	**0.08**	**53**	33.85
Rapid River at Clementson, MN11	mobilizing	0.51	**0.04**	**0.05**	**0.01**	**309**	0.01	0.66	0.00	296	-74.51
Red Lake River at Fisher, MN	mobilizing	0.81	**0.71**	**<0.01**	**0.34**	**383**	**0.77**	**<0.01**	**0.35**	**366**	7.81
Red Lake River at High Landing nr Goodridge, MN	mobilizing	4.74	**0.65**	**0.01**	**0.11**	**59**	**0.90**	**<0.01**	**0.17**	**53**	37.65
Red Lake River at Red Lake Falls, CR13	mobilizing	1.47	**0.93**	**<0.01**	**0.42**	**121**	**1.00**	**<0.01**	**0.39**	**113**	6.80
Red River of the North nr Kragnes, CSAH26	chemodynamic	0.32	-0.02	0.46	0.00	376	0.00	0.89	0.00	369	-80.69
Redwood River at Russell, CR15	mobilizing	0.61	**0.28**	**<0.01**	**0.12**	**104**	**0.34**	**<0.01**	**0.13**	**97**	21.16
Redwood River nr Redwood Falls, MN	diluting	0.66	**-0.10**	**<0.01**	**0.02**	**327**	**-0.20**	**<0.01**	**0.10**	**316**	96.5
Rock River at Luverne, CR4	mobilizing	0.64	**0.71**	**<0.01**	**0.52**	**194**	**0.71**	**<0.01**	**0.51**	**190**	0.10
Rum River at Anoka,headwater side of dam	mobilizing	0.72	**0.37**	**<0.01**	**0.14**	**171**	**0.38**	**<0.01**	**0.14**	**170**	1.48
S Br. Wild Rice River at CR27 nr Felton, MN	mobilizing	0.32	**0.29**	**<0.01**	**0.29**	**48**	**0.30**	**<0.01**	**0.26**	**44**	2.91
Sand Hill River at Climax, MN, US-75	mobilizing	0.41	**0.50**	**<0.01**	**0.43**	**331**	**0.51**	**<0.01**	**0.43**	**322**	2.12
Sandhill River nr Fertile, 450th St SW	mobilizing	0.70	**0.47**	**<0.01**	**0.23**	**104**	**0.52**	**<0.01**	**0.23**	**94**	9.61
Sauk River nr St. Martin, CR12	mobilizing	1.27	**0.83**	**<0.01**	**0.30**	**60**	**1.01**	**<0.01**	**0.37**	**56**	21.66
Second Creek nr Aurora, 0.6mi us of CSAH110	mobilizing	1.48	**0.18**	**0.04**	**0.04**	**108**	0.20	0.06	0.04	99	8.43

Seven Mile Creek nr St. Peter, 0.6mi us of US169	mobilizing	0.56	**0.41**	<0.01	0.39	326	0.40	<0.01	0.33	304	-2.53
Shakopee Creek nr Benson, 20th Ave SW	mobilizing	0.75	**0.46**	<0.01	0.13	135	0.76	<0.01	0.28	130	64.74
Shell Rock River nr Gordonsville, CSAH1	diluting	1.69	**-0.73**	<0.01	0.29	192	-0.73	<0.01	0.28	189	-0.47
Sleepy Eye Creek nr Cobden, CR8	mobilizing	0.51	**0.42**	<0.01	0.44	118	0.43	<0.01	0.40	110	3.6
Snake River above Warren, MN	mobilizing	0.44	**0.22**	<0.01	0.12	78	0.21	<0.01	0.11	77	-5.76
Snake River nr Big Woods, MN220	chemostatic	0.26	**0.12**	<0.01	0.13	327	0.12	<0.01	0.13	325	0.48
Snake River nr Pine City, MN	mobilizing	0.57	**0.23**	<0.01	0.11	213	0.22	<0.01	0.10	206	-4.32
South Branch Buffalo River nr Glyndon, 28th Ave S	chemostatic	0.28	**0.20**	<0.01	0.17	105	0.29	<0.01	0.24	98	49.53
South Branch Middle Fork Zumbro River nr Oronoco,5th St	mobilizing	0.59	**0.49**	<0.01	0.39	103	0.52	<0.01	0.40	100	6.68
South Branch Root River at Lanesboro, Rochelle Ave N	mobilizing	1.05	**0.79**	<0.01	0.47	127	0.80	<0.01	0.45	120	1.00
South Branch Two Rivers at Hallock, MN175	mobilizing	0.46	**0.21**	<0.01	0.11	104	0.28	<0.01	0.14	100	33.96
South Branch Two Rivers at Lake Bronson, MN	mobilizing	0.46	**0.17**	0.01	0.07	89	0.17	0.02	0.06	86	1.82
South Fork Crow River at Delano, Bridge Ave	mobilizing	0.53	**0.10**	0.05	0.02	212	0.12	0.03	0.02	206	16.77
South Fork Watonwan River nr Madelia, CSAH13	mobilizing	0.94	**0.21**	<0.01	0.08	123	0.31	<0.01	0.13	117	46.6
South Fork Zumbro River nr Oronoco, CR121	mobilizing	0.86	**0.18**	<0.01	0.06	126	0.23	<0.01	0.09	120	31.70

Split Rock Creek nr Jasper, 201st St	mobilizing	0.52	**0.60**	**<0.01**	**0.50**	**171**	**0.59**	**<0.01**	**0.47**	**165**	-2.05
Spring Creek nr Hanley Falls, 480th St	chemodynamic	0.49	-0.07	0.26	0.01	106	0.02	0.77	0.00	99	-133.05
St. Francis River nr Big Lake, 164th St	chemodynamic	0.78	-0.17	0.27	0.02	61	-0.16	0.32	0.02	56	-2.19
St. Louis River at Floodwood, CSAH8	mobilizing	0.99	**0.24**	**<0.01**	**0.09**	**87**	**0.30**	**<0.01**	**0.12**	**82**	21.11
St. Louis River at Scanlon, MN	mobilizing	1.08	**0.24**	**<0.01**	**0.11**	**138**	**0.20**	**<0.01**	**0.06**	**127**	-16.9
St. Louis River nr Forbes, US53	mobilizing	0.58	**0.15**	**0.01**	**0.06**	**120**	**0.13**	**0.05**	**0.03**	**111**	-13.42
Stony River nr Babbitt, Tomahawk Rd	chemodynamic	0.9	0.04	0.70	0.00	76	-0.13	0.33	0.01	70	-419.25
Straight River nr Faribault, MN	mobilizing	0.50	**0.34**	**<0.01**	**0.28**	**111**	**0.35**	**<0.01**	**0.28**	**109**	2.89
Sunrise River at Sunrise, CR88	chemodynamic	0.51	-0.04	0.53	0.00	90	-0.02	0.81	0.00	86	-57.9
Swan River nr Jacobson, CR438	chemodynamic	0.94	-0.19	0.20	0.03	55	-0.22	0.24	0.03	51	14.27
Swan River nr Sobieski, MN238	mobilizing	1.06	**0.52**	**<0.01**	**0.26**	**62**	**0.57**	**<0.01**	**0.27**	**59**	9.49
Tamarac River nr Florian, CSAH1	mobilizing	0.73	**0.18**	**<0.01**	**0.14**	**111**	**0.26**	**<0.01**	**0.17**	**101**	41.22
Tamarac River nr Stephen, CSAH22	mobilizing	0.38	**0.25**	**<0.01**	**0.29**	**289**	**0.24**	**<0.01**	**0.27**	**287**	-2.40
Thief River downstream of CSAH 7, 6 mi E of Holt	mobilizing	1.53	**0.11**	**0.05**	**0.02**	**161**	0.06	0.34	0.01	155	-45.73
Thief River nr Thief River Falls, MN	mobilizing	0.83	**0.14**	**<0.01**	**0.05**	**421**	**0.13**	**<0.01**	**0.04**	**410**	-1.92
Turtle Creek at Austin, 43rd St	mobilizing	0.92	**0.58**	**<0.01**	**0.21**	**103**	**0.72**	**<0.01**	**0.24**	**94**	23.05
Twelvemile Creek nr Wheaton, CSAH14	mobilizing	0.32	**0.15**	**0.02**	**0.07**	**84**	**0.33**	**<0.01**	**0.20**	**79**	117.23
Two Rivers nr Bowlus, 40th St	chemodynamic	0.88	-0.16	0.47	0.03	21	-0.16	0.47	0.03	21	0

Two Rivers nr Hallock, CSAH16	mobilizing	0.46	**0.29**	**<0.01**	**0.35**	**303**	**0.27**	**<0.01**	**0.30**	**294**	-5.38
Watonwan River nr Garden City, CSAH13	mobilizing	0.66	**0.45**	**<0.01**	**0.38**	**360**	**0.42**	**<0.01**	**0.32**	**345**	-6.66
Watonwan River nr La Salle, CSAH3	mobilizing	0.44	**0.22**	**<0.01**	**0.12**	**140**	**0.30**	**<0.01**	**0.18**	**134**	38
Wells Creek nr Frontenac, US61	mobilizing	1.57	**1.26**	**<0.01**	**0.59**	**56**	**1.26**	**<0.01**	**0.58**	**54**	-0.52
West Branch Lac qui Parle River at Dawson, Diagonal St	mobilizing	0.47	**0.25**	**<0.01**	**0.12**	**64**	**0.42**	**<0.01**	**0.22**	**60**	67.62
West Branch Rum River nr Princeton, CR102	chemodynamic	0.33	0.15	0.12	0.10	25	0.15	0.12	0.10	25	0
West Fork Des Moines River at Jackson, River St	chemodynamic	1.57	-0.04	0.59	0.00	165	-0.05	0.56	0.00	160	16.04
West Fork Des Moines River nr Avoca, CSAH6	mobilizing	0.69	**0.60**	**<0.01**	**0.33**	**77**	**0.80**	**<0.01**	**0.41**	**72**	34.59
Whitewater River nr Beaver, CSAH30	mobilizing	1.28	**0.82**	**<0.01**	**0.53**	**206**	**0.83**	**<0.01**	**0.53**	**201**	0.52
Wild Rice River at Hendrum, MN	mobilizing	0.48	**0.43**	**<0.01**	**0.36**	**402**	**0.46**	**<0.01**	**0.36**	**388**	7.08
Wild Rice River at Twin Valley, MN	mobilizing	0.75	**0.58**	**<0.01**	**0.49**	**57**	**0.55**	**<0.01**	**0.39**	**53**	-3.98
Wild Rice River nr Mahnomen, CSAH25	mobilizing	0.73	**0.22**	**0.04**	**0.10**	**43**	**0.36**	**0.03**	**0.13**	**38**	60.21
Yellow Bank River nr Odessa, CSAH40	mobilizing	0.52	**0.55**	**<0.01**	**0.45**	**177**	**0.56**	**<0.01**	**0.44**	**173**	1.26
Yellow Medicine River nr Granite Falls, MN	mobilizing	0.7	**0.35**	**<0.01**	**0.25**	**257**	**0.34**	**<0.01**	**0.23**	**249**	-2.22
Yellow Medicine River nr Hanley Falls, CR18	mobilizing	0.7	**0.46**	**<0.01**	**0.34**	**119**	**0.48**	**<0.01**	**0.30**	**112**	3.82
Zumbro River at Kellogg, US61	mobilizing	1.03	**0.59**	**<0.01**	**0.38**	**229**	**0.60**	**<0.01**	**0.37**	**220**	2.57

Table A6. Conditional Permutation Importance value for predictor variables used in the random forest model.

Predictor	Importance	Description
PctCrop2019CatRp100	0.009498	% of AOI area classified as crop land use (NLCD class 82)
PctCrop2019WsRp100	0.009437	% of AOI area classified as crop land use (NLCD class 82)
KffactCat	0.009059	Mean of STATSGO Kffactor raster within AOI. The Universal Soil Loss Equation (USLE) and represents a relative index of susceptibility of bare, cultivated soil to particle detachment and transport by rainfall
PermCat	0.005716	Mean permeability (cm/hour) of soils (STATSGO) within AOI
AgKffactWs	0.005292	Mean of STATSGO Kffactor raster on agricultural land (NLCD 2006) within AOI. The Universal Soil Loss Equation (USLE) and represents a relative index of susceptibility of bare, cultivated soil to particle detachment and transport by rainfall
PctMxFst2019WsRp100	0.005098	% of AOI area classified as mixed deciduous/evergreen forest land cover (NLCD class 43)
PctUrbOp2019CatRp100	0.004543	% of AOI area classified as developed, open space land use (NLCD class 21)
Precip_Minus_EVTWs	0.004364	This dataset represents surplus precipitation (mm): precipitation minus potential evaporation described in DOI: 10.1016/j.scitotenv.2020.137661 within individual, local NHDPlusV2 catchments and upstream, contributing watersheds.
ClayWs	0.004223	Mean % clay content of soils (STATSGO) within AOI
PctWdWet2019WsRp100	0.004041	% of AOI area classified as woody wetland land cover (NLCD class 90)
PctGrs2019Ws	0.003979	% of AOI area classified as grassland/herbaceous land cover (NLCD class 71)
Pestic97Cat	0.003880	Mean pesticide use (kg/km2) in yr. 1997 within AOI.
MAST_2013	0.003805	Predicted mean annual stream temperature (Jan-Dec) for year 2008, 2009, 2013, 2014
Phos_Crop_UptakeWs	0.003715	Phosphorus uptake by crops in the watershed
FertWs	0.003536	Mean rate of synthetic nitrogen fertilizer application to agricultural land in kg N/ha/yr, within the AOI
WWTPAllDensWs	0.003328	Density (number/ km2) of all wastewater treatment plants per AOI
SiO2Cat	0.003151	Mean % of lithological silicon dioxide (SiO2) content in surface or near surface geology within AOI
PctHay2019Cat	0.003151	% of AOI area classified as hay land use (NLCD class 81)
RdCrsSlpWtdCat	0.003115	Density of roads-stream intersections (2010 Census Tiger Lines-NHD stream lines) multiplied by NHDPlusV21 slope within AOI (crossings*slope/square km)
PctImp2013CatRp100	0.003096	Mean imperviousness of anthropogenic surfaces within AOI (NLCD)
Al2O3Cat	0.003007	Mean % of lithological aluminum oxide (Al2O3) content in surface or near surface geology within AOI
PctGlacLakeFineWs	0.002988	% of AOI area classified as lithology type: glacial lake sediment, fine-textured
PctCrop2019Ws	0.002930	% of AOI area classified as crop land use (NLCD class 82)

CompStrgthCat	0.002860	Mean lithological uniaxial compressive strength (megaPascals) content in surface or near surface geology within AOI
NsurpCat	0.002853	Nitrogen Surplus (kg N / yr) per AOI - excluding biological N Fixation
K2OCat	0.002668	Mean % of lithological potassium oxide (K2O) content in surface or near surface geology within AOI
AgKffactCat	0.002657	Mean of STATSGO Kffactor raster on agricultural land (NLCD 2006) within AOI. The Universal Soil Loss Equation (USLE) and represents a relative index of susceptibility of bare, cultivated soil to particle detachment and transport by rainfall
NABD_NIDStorWs	0.002568	Volume all reservoirs (NID_STORA in NID) per unit area of AOI (cubic meters/square km)
PctMxFst2019Ws	0.002464	% of AOI area classified as mixed deciduous/evergreen forest land cover (NLCD class 43)
ElevWs	0.002449	Mean AOI elevation (m)
PctOw2019Cat	0.002403	% of AOI area classified as open water land cover (NLCD class 11)
PctDecid2019CatRp100	0.002028	% of AOI area classified as deciduous forest land cover (NLCD class 41)
OmCat	0.002027	Mean organic matter content (% by weight) of soils (STATSGO) within AOI
PctCrop2019Cat	0.001864	% of AOI area classified as crop land use (NLCD class 82)
WaterInputCat	0.001863	Water Input (km2/cm): Ratio of the total area of irrigated land to precipitation within AOI
FertCat	0.001784	Mean rate of synthetic nitrogen fertilizer application to agricultural land in kg N/ha/yr, within the AOI
PctDecid2019Cat	0.001709	% of AOI area classified as deciduous forest land cover (NLCD class 41)
NO3_2008Ws	0.001689	Annual gradient map of precipitation-weighted mean deposition for nitrate ion concentration wet deposition for 2008 in kg of NO3/ha/yr, within AOI
Phos_FertCat	0.001659	Mean rate of synthetic nitrogen fertilizer application to agricultural land in kg N/ha/yr, within the AOI
MAST_2014	0.001589	Predicted mean annual stream temperature (Jan-Dec) for year 2008, 2009, 2013, 2014
Na2OCat	0.001586	Mean % of lithological sodium oxide (Na2O) content in surface or near surface geology within AOI
WaterInputWs	0.001507	Water Input (km2/cm): Ratio of the total area of irrigated land to precipitation within AOI
RockNWs	0.001481	N from rock weathering (kg/ km2) within AOI
Pestic97Ws	0.001459	Mean pesticide use (kg/km2) in yr. 1997 within AOI.
PctUrbMd2019CatRp100	0.001402	% of AOI area classified as developed, medium-intensity land use (NLCD class 23)
MSST_2014	0.001387	Predicted mean summer stream temperature (July-Aug) for years 2008, 2009, 2013, 2014
MgOCat	0.001343	Mean % of lithological magnesium oxide (MgO) content in surface or near surface geology within AOI
MWST_2013	0.001315	Predicted mean winter stream temperature (Jan-Feb) for year 2008, 2009, 2013, 2014

PctHbWet2019Cat	0.001298	% of AOI area classified as herbaceous wetland land cover (NLCD class 95)
Fe2O3Cat	0.001270	Mean % of lithological ferric oxide (Fe_2O_3) content in surface or near surface geology within AOI
PctShrb2019Ws	0.001265	% of AOI area classified as shrub/scrub land cover (NLCD class 52)
HydrlCondCat	0.001220	Mean lithological hydraulic conductivity (micrometers per second) content in surface or near surface geology within AOI
RdDensWs	0.001211	Density of roads (2010 Census Tiger Lines) within AOI (km/square km)
Phos_ManureCat	0.001210	Mean rate of manure application to agricultural land from confined animal feeding operations in kg N/ha/yr, within AOI
PctWdWet2019Ws	0.001191	% of AOI area classified as woody wetland land cover (NLCD class 90)
RdCrsWs	0.001175	Density of roads-stream intersections (2010 Census Tiger Lines-NHD stream lines) within AOI (crossings/square km)
NPDESDensWs	0.001156	Density of permitted NPDES (National Pollutant Discharge Elimination System) sites within AOI (sites/square km)
PctImp2008Ws	0.001152	Mean imperviousness of anthropogenic surfaces within AOI (NLCD)
PctHbWet2019CatRp100	0.001149	% of AOI area classified as herbaceous wetland land cover (NLCD class 95)
MSST_2013	0.001115	Predicted mean summer stream temperature (July-Aug) for years 2008, 2009, 2013, 2014
NANIWs	0.001108	Net Anthropogenic Nitrogen within AOI: farm fertilizer + urban fertilizer + NOx deposition + CBNF + Human and Livestock food - crop N content - livestock N content
Precip8110Ws	0.001107	PRISM climate data - 30-year normal mean precipitation (mm): Annual period: 1981-2010 within AOI
MAST_2009	0.001104	Predicted mean annual stream temperature (Jan-Dec) for year 2008, 2009, 2013, 2014
SepticWs	0.000991	Density of septic systems per AOI - based on 1990 Census
Tmean8110Cat	0.000952	PRISM climate data - 30-year normal mean temperature (CÂ°): Annual period: 1981-2010 within the AOI
RunoffCat	0.000932	Mean runoff (mm) within AOI
PctHbWet2019Ws	0.000893	% of AOI area classified as herbaceous wetland land cover (NLCD class 95)
SandCat	0.000878	Mean % sand content of soils (STATSGO) within AOI
SuperfundDensWs	0.000855	Density of Superfund sites within AOI (sites/square km)
PctGlacTilLoamCat	0.000825	% of AOI area classified as lithology type: glacial till, loamy
PctImp2013Cat	0.000805	Mean imperviousness of anthropogenic surfaces within AOI (NLCD)
NCat	0.000726	Mean % of lithological nitrogen (N) content in surface or near surface geology within AOI
BFIWs	0.000721	Base flow is the component of streamflow that can be attributed to ground-water discharge into streams. The BFI is the ratio of base flow to total flow, expressed as a percentage, within AOI
PctImp2006WsRp100	0.000699	Mean imperviousness of anthropogenic surfaces within AOI (NLCD)

ManureWs	0.000695	Mean rate of manure application to agricultural land from confined animal feeding operations in kg N/ha/yr, within AOI
TRIDensWs	0.000673	Density of TRI (Toxic Release Inventory) sites within AOI (sites/square km)
PctAlluvCoastWs	0.000662	% of AOI area classified as lithology type: alluvium and fine-textured coastal zone sediment
CaOCat	0.000651	Mean % of lithological calcium oxide (CaO) content in surface or near surface geology within AOI
SandWs	0.000650	Mean % sand content of soils (STATSGO) within AOI
PctImp2019Cat	0.000636	Mean imperviousness of anthropogenic surfaces within AOI (NLCD)
PctHbWet2019WsRp100	0.000595	% of AOI area classified as herbaceous wetland land cover (NLCD class 95)
PctColluvSedWs	0.000576	% of AOI area classified as lithology type: colluvial sediment
PctBl2019Cat	0.000569	% of AOI area classified as barren land cover (NLCD class 31)
NH4_2008Ws	0.000547	Annual gradient map of precipitation-weighted mean deposition for ammonium ion concentration wet deposition for 2008 in kg of NH4/ha/yr, within AOI
PctGrs2019Cat	0.000543	% of AOI area classified as grassland/herbaceous land cover (NLCD class 71)
PctImp2016Ws	0.000522	Mean imperviousness of anthropogenic surfaces within AOI (NLCD)
PctUrbHi2019WsRp100	0.000522	% of AOI area classified as developed, high-intensity land use (NLCD class 24)
PctImp2004CatRp100	0.000521	Mean imperviousness of anthropogenic surfaces within AOI (NLCD)
Tmax8110Ws	0.000520	PRISM climate data - 30-year normal maximum temperature (CÂ°): Annual period: 1981-2010 within the AOI
PctOw2019Ws	0.000495	% of AOI area classified as open water land cover (NLCD class 11)
KffactWs	0.000492	Mean of STATSGO Kffactor raster within AOI. The Universal Soil Loss Equation (USLE) and represents a relative index of susceptibility of bare, cultivated soil to particle detachment and transport by rainfall
RdDensCat	0.000450	Density of roads (2010 Census Tiger Lines) within AOI (km/square km)
PctImp2016WsRp100	0.000447	Mean imperviousness of anthropogenic surfaces within AOI (NLCD)
MSST_2009	0.000422	Predicted mean summer stream temperature (July-Aug) for years 2008, 2009, 2013, 2014
CBNFCat	0.000417	Mean rate of biological nitrogen fixation from the cultivation of crops in kg N/ha/yr, within AOI
WtDepWs	0.000408	Mean seasonal water table depth (cm) of soils (STATSGO) within AOI
PctImp2008Cat	0.000407	Mean imperviousness of anthropogenic surfaces within AOI (NLCD)
Phos_Crop_UptakeCat	0.000385	Phosphorus update by crops in the catchment
WWTPMinorDensWs	0.000353	Density (number/ km2) of minor wastewater treatment plants per AOI
RockNCat	0.000350	N from rock weathering (kg/ km2) within AOI

PctImp2013Ws	0.000327	Mean imperviousness of anthropogenic surfaces within AOI (NLCD)
Tmean8110Ws	0.000292	PRISM climate data - 30-year normal mean temperature (CÂ°): Annual period: 1981-2010 within the AOI
NO3_2008Cat	0.000290	Annual gradient map of precipitation-weighted mean deposition for nitrate ion concentration wet deposition for 2008 in kg of NO3/ha/yr, within AOI
PctUrbOp2019WsRp100	0.000271	% of AOI area classified as developed, open space land use (NLCD class 21)
PctImp2008WsRp100	0.000255	Mean imperviousness of anthropogenic surfaces within AOI (NLCD)
SWs	0.000224	Mean % of lithological sulfur (S) content in surface or near surface geology within AOI
PctShrb2019CatRp100	0.000215	% of AOI area classified as shrub/scrub land cover (NLCD class 52)
Tmax8110Cat	0.000193	PRISM climate data - 30-year normal maximum temperature (CÂ°): Annual period: 1981-2010 within the AOI
Phos_ManureWs	0.000193	Mean rate of manure application to agricultural land from confined animal feeding operations in kg N/ha/yr, within AOI
PctAg2006Slp10Cat	0.000163	Mean % of lithological sulfur (S) content in surface or near surface geology within AOI
Fe2O3Ws	0.000162	Mean % of lithological ferric oxide (Fe2O3) content in surface or near surface geology within AOI
WsAreaSqKm	0.000155	Mean % of lithological sulfur (S) content in surface or near surface geology within AOI
PctUrbHi2019CatRp100	0.000138	% of AOI area classified as developed, high-intensity land use (NLCD class 24)
PctUrbOp2019Cat	0.000138	% of AOI area classified as developed, open space land use (NLCD class 21)
NPDESDensWsRp100	0.000119	Density of permitted NPDES (National Pollutant Discharge Elimination System) sites within AOI (sites/square km)
DamNrmStorWs	0.000118	Volume all reservoirs (NORM_STORA in NID) per unit area of AOI (cubic meters/square km)
SiO2Ws	0.000107	Mean % of lithological silicon dioxide (SiO2) content in surface or near surface geology within AOI
SuperfundDensWsRp100	0.000097	Density of Superfund sites within AOI (sites/square km)
SCat	0.000096	Mean % of lithological sulfur (S) content in surface or near surface geology within AOI
CBNFWs	0.000092	Mean rate of biological nitrogen fixation from the cultivation of crops in kg N/ha/yr, within AOI
PctAlluvCoastCat	0.000091	% of AOI area classified as lithology type: alluvium and fine-textured coastal zone sediment
PctImp2001WsRp100	0.000074	Mean imperviousness of anthropogenic surfaces within AOI (NLCD)
PctGlacLakeCrsCat	0.000069	% of AOI area classified as lithology type: glacial outwash and glacial lake sediment, coarse-textured
PctImp2001Ws	0.000058	Mean imperviousness of anthropogenic surfaces within AOI (NLCD)
PctWdWet2019CatRp100	0.000049	% of AOI area classified as woody wetland land cover (NLCD class 90)

PctColluvSedCat	0.000046	% of AOI area classified as lithology type: colluvial sediment
PctHydricWs	0.000042	% of AOI area classified as lithology type: hydric, peat and muck
PctConif2019CatRp100	0.000038	% of AOI area classified as evergreen forest land cover (NLCD class 42)
PctGlacLakeCrsWs	0.000014	% of AOI area classified as lithology type: glacial outwash and glacial lake sediment, coarse-textured
PctGlacTilClayCat	0.000000	% of AOI area classified as lithology type: glacial till, clayey
DamNIDStorCat	0.000000	Volume all reservoirs (NID_STORA in NID) per unit area of AOI (cubic meters/square km)
MineDensCat	0.000000	Density of mines sites within AOI (mines/square km)
NABD_NrmStorCat	0.000000	Volume all reservoirs (NORM_STORA in NID) per unit area of AOI (cubic meters/square km)
PctGlacTilCrsCat	0.000000	% of AOI area classified as lithology type: glacial till, coarse-textured
PctGlacTilCrsWs	0.000000	% of AOI area classified as lithology type: glacial till, coarse-textured
PctHydricCat	0.000000	% of AOI area classified as lithology type: hydric, peat and muck
SuperfundDensCat	0.000000	Density of Superfund sites within AOI (sites/square km)
TRIDensCat	0.000000	Density of TRI (Toxic Release Inventory) sites within AOI (sites/square km)
WWTPMajorDensCat	0.000000	Density (number/ km2) of major wastewater treatment plants per AOI
DamDensCat	-0.000001	Density of georeferenced dams within AOI (dams/ square km)
ElevCat	-0.000003	Mean AOI elevation (m)
RckDepCat	-0.000010	Mean depth (cm) to bedrock of soils (STATSGO) within AOI.
NABD_DensCat	-0.000011	Density of georeferenced dams within AOI (dams/ square km)
DamNrmStorCat	-0.000043	Volume all reservoirs (NORM_STORA in NID) per unit area of AOI (cubic meters/square km)
PctWaterWs	-0.000051	% of AOI area classified as lithology type: water
NPDESDensCat	-0.000064	Density of permitted NPDES (National Pollutant Discharge Elimination System) sites within AOI (sites/square km)
PctImp2011WsRp100	-0.000079	Mean imperviousness of anthropogenic surfaces within AOI (NLCD)
PctUrbLo2019Ws	-0.000088	% of AOI area classified as developed, low-intensity land use (NLCD class 22)
ClayCat	-0.000090	Mean % clay content of soils (STATSGO) within AOI
PctHay2019WsRp100	-0.000098	% of AOI area classified as hay land use (NLCD class 81)
CatAreaSqKm	-0.000113	Mean % of lithological sulfur (S) content in surface or near surface geology within AOI
NABD_NIDStorCat	-0.000113	Volume all reservoirs (NID_STORA in NID) per unit area of AOI (cubic meters/square km)
PctUrbLo2019CatRp100	-0.000115	% of AOI area classified as developed, low-intensity land use (NLCD class 22)
PctAg2006Slp20Ws	-0.000120	Mean % of lithological sulfur (S) content in surface or near surface geology within AOI
WWTPMajorDensWs	-0.000130	Density (number/ km2) of major wastewater treatment plants per AOI

P2O5Cat	-0.000134	Mean % of lithological phosphorous oxide (P2O5) content in surface or near surface geology within AOI
PctShrb2019WsRp100	-0.000136	% of AOI area classified as shrub/scrub land cover (NLCD class 52)
PctOw2019WsRp100	-0.000158	% of AOI area classified as open water land cover (NLCD class 11)
RdCrsSlpWtdWs	-0.000164	Density of roads-stream intersections (2010 Census Tiger Lines-NHD stream lines) multiplied by NHDPlusV21 slope within AOI (crossings*slope/square km)
SepticCat	-0.000164	Density of septic systems per AOI - based on 1990 Census
PctBl2019CatRp100	-0.000189	% of AOI area classified as barren land cover (NLCD class 31)
PctHay2019CatRp100	-0.000195	% of AOI area classified as hay land use (NLCD class 81)
PctImp2006CatRp100	-0.000210	Mean imperviousness of anthropogenic surfaces within AOI (NLCD)
CompStrgthWs	-0.000219	Mean lithological uniaxial compressive strength (megaPascals) content in surface or near surface geology within AOI
PctUrbMd2019Ws	-0.000224	% of AOI area classified as developed, medium-intensity land use (NLCD class 23)
MgOWs	-0.000235	Mean % of lithological magnesium oxide (MgO) content in surface or near surface geology within AOI
PctConif2019Ws	-0.000236	% of AOI area classified as evergreen forest land cover (NLCD class 42)
SN_2008Cat	-0.000237	Annual gradient map of precipitation-weighted mean deposition for average sulfur & nitrogen wet deposition for 2008 in kg of S+N/ha/yr, within AOI
PctAg2006Slp20Cat	-0.000257	Mean % of lithological sulfur (S) content in surface or near surface geology within AOI
PctUrbLo2019WsRp100	-0.000281	% of AOI area classified as developed, low-intensity land use (NLCD class 22)
PctGlacLakeFineCat	-0.000284	% of AOI area classified as lithology type: glacial lake sediment, fine-textured
RdDensCatRp100	-0.000293	Density of roads (2010 Census Tiger Lines) within AOI (km/square km)
PctImp2013WsRp100	-0.000297	Mean imperviousness of anthropogenic surfaces within AOI (NLCD)
TRIDensWsRp100	-0.000311	Density of TRI (Toxic Release Inventory) sites within AOI (sites/square km)
MineDensWs	-0.000323	Density of mines sites within AOI (mines/square km)
PctImp2019CatRp100	-0.000369	Mean imperviousness of anthropogenic surfaces within AOI (NLCD)
CaOWs	-0.000370	Mean % of lithological calcium oxide (CaO) content in surface or near surface geology within AOI
WWTPMinorDensCat	-0.000371	Density (number/ km2) of minor wastewater treatment plants per AOI
Al2O3Ws	-0.000384	Mean % of lithological aluminum oxide (Al2O3) content in surface or near surface geology within AOI
NANICat	-0.000387	Net Anthropogenic Nitrogen within AOI: farm fertilizer + urban fertilizer + NOx deposition + CBNF + Human and Livestock food - crop N content - livestock N content
PctImp2011Cat	-0.000388	Mean imperviousness of anthropogenic surfaces within AOI (NLCD)

PctUrbHi2019Ws	-0.000391	% of AOI area classified as developed, high-intensity land use (NLCD class 24)
PctGrs2019WsRp100	-0.000395	% of AOI area classified as grassland/herbaceous land cover (NLCD class 71)
PctShrb2019Cat	-0.000403	% of AOI area classified as shrub/scrub land cover (NLCD class 52)
NH4_2008Cat	-0.000420	Annual gradient map of precipitation-weighted mean deposition for ammonium ion concentration wet deposition for 2008 in kg of NH4/ha/yr, within AOI
PctGlacTilClayWs	-0.000429	% of AOI area classified as lithology type: glacial till, clayey
PctImp2001Cat	-0.000448	Mean imperviousness of anthropogenic surfaces within AOI (NLCD)
RckDepWs	-0.000461	Mean depth (cm) to bedrock of soils (STATSGO) within AOI.
HydrlCondWs	-0.000479	Mean lithological hydraulic conductivity (micrometers per second) content in surface or near surface geology within AOI
Na2OWs	-0.000487	Mean % of lithological sodium oxide (Na2O) content in surface or near surface geology within AOI
NABD_NrmStorWs	-0.000488	Volume all reservoirs (NORM_STORA in NID) per unit area of AOI (cubic meters/square km)
PctImp2004Ws	-0.000492	Mean imperviousness of anthropogenic surfaces within AOI (NLCD)
WWTPAllDensCat	-0.000542	Density (number/ km2) of all wastewater treatment plants per AOI
PermWs	-0.000550	Mean permeability (cm/hour) of soils (STATSGO) within AOI
PctMxFst2019CatRp100	-0.000556	% of AOI area classified as mixed deciduous/evergreen forest land cover (NLCD class 43)
BFICat	-0.000560	Base flow is the component of streamflow that can be attributed to ground-water discharge into streams. The BFI is the ratio of base flow to total flow, expressed as a percentage, within AOI
PctImp2019WsRp100	-0.000576	Mean imperviousness of anthropogenic surfaces within AOI (NLCD)
NsurpWs	-0.000592	Nitrogen Surplus (kg N / yr) per AOI - excluding biological N Fixation
MineDensWsRp100	-0.000632	Density of mines sites within AOI (mines/square km)
P2O5Ws	-0.000647	Mean % of lithological phosphorous oxide (P2O5) content in surface or near surface geology within AOI
PctDecid2019WsRp100	-0.000675	% of AOI area classified as deciduous forest land cover (NLCD class 41)
PctImp2004Cat	-0.000691	Mean imperviousness of anthropogenic surfaces within AOI (NLCD)
PctImp2011Ws	-0.000768	Mean imperviousness of anthropogenic surfaces within AOI (NLCD)
PctConif2019Cat	-0.000774	% of AOI area classified as evergreen forest land cover (NLCD class 42)
PctImp2011CatRp100	-0.000784	Mean imperviousness of anthropogenic surfaces within AOI (NLCD)
NWs	-0.000812	Mean % of lithological nitrogen (N) content in surface or near surface geology within AOI
PctGlacTilLoamWs	-0.000859	% of AOI area classified as lithology type: glacial till, loamy

PctImp2008CatRp100	-0.000863	Mean imperviousness of anthropogenic surfaces within AOI (NLCD)
PctBl2019Ws	-0.000940	% of AOI area classified as barren land cover (NLCD class 31)
InorgNWetDep_2008Ws	-0.000977	Annual gradient map of precipitation-weighted mean deposition for inorganic nitrogen wet deposition from nitrate and ammonium for 2008 in kg of N/ha/yr, within AOI
Tile_density	-0.000989	Tile density in the watershed in m2/km2
PctMxFst2019Cat	-0.000993	% of AOI area classified as mixed deciduous/evergreen forest land cover (NLCD class 43)
PctImp2004WsRp100	-0.000997	Mean imperviousness of anthropogenic surfaces within AOI (NLCD)
Tmin8110Ws	-0.001004	PRISM climate data - 30-year normal minimum temperature (CÂ°): Annual period: 1981-2010 within the AOI
MAST_2008	-0.001057	Predicted mean annual stream temperature (Jan-Dec) for year 2008, 2009, 2013, 2014
DamNIDStorWs	-0.001058	Volume all reservoirs (NID_STORA in NID) per unit area of AOI (cubic meters/square km)
Phos_FertWs	-0.001065	Mean rate of synthetic nitrogen fertilizer application to agricultural land in kg N/ha/yr, within the AOI
PctConif2019WsRp100	-0.001095	% of AOI area classified as evergreen forest land cover (NLCD class 42)
PctImp2001CatRp100	-0.001121	Mean imperviousness of anthropogenic surfaces within AOI (NLCD)
RdDensWsRp100	-0.001130	Density of roads (2010 Census Tiger Lines) within AOI (km/square km)
PctUrbOp2019Ws	-0.001147	% of AOI area classified as developed, open space land use (NLCD class 21)
WtDepCat	-0.001155	Mean seasonal water table depth (cm) of soils (STATSGO) within AOI
Tmin8110Cat	-0.001190	PRISM climate data - 30-year normal minimum temperature (CÂ°): Annual period: 1981-2010 within the AOI
RunoffWs	-0.001264	Mean runoff (mm) within AOI
PctDecid2019Ws	-0.001384	% of AOI area classified as deciduous forest land cover (NLCD class 41)
PctWdWet2019Cat	-0.001398	% of AOI area classified as woody wetland land cover (NLCD class 90)
PctImp2016CatRp100	-0.001416	Mean imperviousness of anthropogenic surfaces within AOI (NLCD)
SN_2008Ws	-0.001443	Annual gradient map of precipitation-weighted mean deposition for average sulfur & nitrogen wet deposition for 2008 in kg of S+N/ha/yr, within AOI
RdCrsCat	-0.001469	Density of roads-stream intersections (2010 Census Tiger Lines-NHD stream lines) within AOI (crossings/square km)
PctOw2019CatRp100	-0.001521	% of AOI area classified as open water land cover (NLCD class 11)
Precip8110Cat	-0.001556	PRISM climate data - 30-year normal mean precipitation (mm): Annual period: 1981-2010 within AOI
PctImp2006Ws	-0.001586	Mean imperviousness of anthropogenic surfaces within AOI (NLCD)
ManureCat	-0.001594	Mean rate of manure application to agricultural land from confined animal feeding operations in kg N/ha/yr, within AOI

PctUrbHi2019Cat	-0.001652	% of AOI area classified as developed, high-intensity land use (NLCD class 24)
NABD_DensWs	-0.001661	Density of georeferenced dams within AOI (dams/ square km)
PctImp2019Ws	-0.001693	Mean imperviousness of anthropogenic surfaces within AOI (NLCD)
PctUrbLo2019Cat	-0.001734	% of AOI area classified as developed, low-intensity land use (NLCD class 22)
Precip_Minus_EVTCat	-0.001799	This dataset represents surplus precipitation (mm): precipitation minus potential evaporation described in DOI: 10.1016/j.scitotenv.2020.137661 within individual, local NHDPlusV2 catchments and upstream, contributing watersheds.
OmWs	-0.001820	Mean organic matter content (% by weight) of soils (STATSGO) within AOI
PctAg2006Slp10Ws	-0.001835	Mean % of lithological sulfur (S) content in surface or near surface geology within AOI
K2OWs	-0.001836	Mean % of lithological potassium oxide (K2O) content in surface or near surface geology within AOI
PctUrbMd2019Cat	-0.001852	% of AOI area classified as developed, medium-intensity land use (NLCD class 23)
PctImp2006Cat	-0.001861	Mean imperviousness of anthropogenic surfaces within AOI (NLCD)
PctImp2016Cat	-0.001956	Mean imperviousness of anthropogenic surfaces within AOI (NLCD)
CanalDensWs	-0.001980	Density of NHDPlus line features classified as canal, ditch, or pipeline within the AOI (km/ square km)
InorgNWetDep_2008Cat	-0.002086	Annual gradient map of precipitation-weighted mean deposition for inorganic nitrogen wet deposition from nitrate and ammonium for 2008 in kg of N/ha/yr, within AOI
PctUrbMd2019WsRp100	-0.002287	% of AOI area classified as developed, medium-intensity land use (NLCD class 23)
PctGrs2019CatRp100	-0.002320	% of AOI area classified as grassland/herbaceous land cover (NLCD class 71)
DamDensWs	-0.002323	Density of georeferenced dams within AOI (dams/ square km)
PctBl2019WsRp100	-0.002483	% of AOI area classified as barren land cover (NLCD class 31)
CanalDensCat	-0.002813	Density of NHDPlus line features classified as canal, ditch, or pipeline within the AOI (km/ square km)
MSST_2008	-0.003001	Predicted mean summer stream temperature (July-Aug) for years 2008, 2009, 2013, 2014
PctHay2019Ws	-0.003454	% of AOI area classified as hay land use (NLCD class 81)